Electronic Supplementary Material (ESI) for Organic Chemistry Frontiers.

Supporting Information For

Chemoselective hydroborative reduction of nitro motifs using a transition-metal-free catalyst

Wubing Yao,*[a,b] Jiali Wang,[a,b] Yinpeng Lou,[a] Haijian Wu,[a] Xinxin Qi,[b] Jianguo Yang[a,b] and Aiguo Zhong[a]

[a]School of Pharmaceutical and Materials Engineering, Taizhou University, Jiaojiang 318000, P.R. China

[b]Department of Chemistry, Zhejiang Sci-Tech University, Hangzhou 310018, P.R. China

Corresponding author : Wubing Yao

E-mail: icyyw2010@yeah.net

Table of Contents

1. General considerations.....S3

2. The typical reaction procedures.....S4

3. The mechanism studies.....S5

3.1 The free radical experiment.....S5

3.2 The homogeneous test.....S5

3.3 The kinetic studies.....S6

3.4 The plausible mechanism and DFT calculations.....S13

4. NMR spectra data.....S19

5. References.....S27

6. NMR spectra.....S28

1. General considerations

1.1 Materials

All manipulations were carried out using standard Schlenk, high vacuum, and glovebox techniques. Glassware was dried in a 140 ^{o}C oven over 4 h prior to use. KO*t*Bu (95%), BEt_3 (1M solution in THF) and $B(C_6F_5)_3$ (97%) were purchased from Aladdin and used as received. BPh_3 (96%) and HBpin (97%) were purchased from Alfa and used as received. Flash colum chromatography was performed on silica gel (particle size 300-400 mesh ASTM), purchased from Yantai, China. All solvents, bases and nitro motifs were obtained from commercial sources and dried and degassed according to standard procedures. All heating reactions were performed on the IKA RCT Basic magnetic stirring apparatus with an oil bath.

1.2 Analytical Methods

NMR spectra data were obtained on Avance (III) HD 400 MHz instruments. ^{1}H NMR and ^{13}C NMR spectra were referenced to residual protic solvent peaks or TMS signal (0 ppm). ^{19}F NMR chemical shifts were externally referenced to CCl_3F (0 ppm). Data for ^{1}H NMR are recorded as follows: chemical shift (δ, ppm), multiplicity (s = singlet, d = doublet, t = triplet, m = multiplet or unresolved, br = broad singlet, coupling constant (s) in Hz, integration). Data for ^{13}C NMR are reported in terms of chemical shift (δ, ppm). GC was performed on a Shimadzu GC-2010 plus spectrometer. GC/MS was performed on a Shimadzu GCMS-QP2010 Plus spectrometer.

2. The typical reaction procedures

2.1 Reduction of nitroarenes

In an argon filled glovebox, a 10 mL dried Schlenk tube equipped with a magnetic stir bar was charged with KO*t*Bu (5 mol%), BEt_3 (5 mol%), nitro (0.6 mmol), HBpin (6.0 equiv), THF (2.0 mL). The tube was then sealed with a Teflon plug under an argon atmosphere, and removed from the glovebox. Then, the solution was stirred at 100 ^oC for 24 h. After that, the reaction was quenched by adding 1 M aqueous NaOH (10 mL) at room temperature, and was extracted with Et_2O (3×30 mL). The filtrate was collected and the corresponding reduced amines were concentrated in vacuum. After that, the crude product was purified by silica gel column chromatography using the EtOAc/petroleum ether mixture.

2.2 Reduction of nitro alkanes

In an argon filled glovebox, a 10 mL dried Schlenk tube equipped with a magnetic stir bar was charged with KO*t*Bu (5 mol%), BEt_3 (5 mol%), nitro (0.6 mmol), HBpin (6.0 equiv), THF (2.0 mL). The tube was then sealed with a Teflon plug under an argon atmosphere, and removed from the glovebox. Then, the solution was stirred at 100 ^oC for 24 h. After that, the residue was filtrated though Celite. The filtrate was collected and the corresponding reduced amines were concentrated in vacuum. Consequently, 2.0 mL 1 M aqueous HCl was added to the concentrated amines followed by addition of 10 mL Et_2O, stirring at 25 ^oC for 6 h. The corresponding amine hydrochloride salt was purified by washing with Et_2O. Isolated amine hydrochlorides were characterized through NMR spectroscopy in DMSO-*d6* or D_2O.

3. The mechanism studies

3.1 The free radical experiment

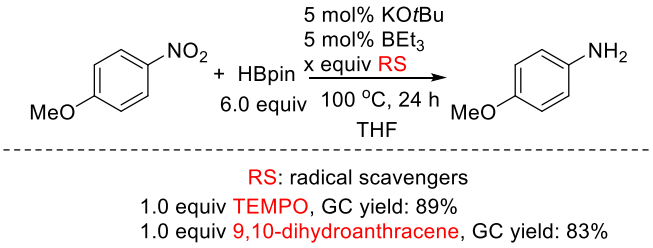

Addition of typical radical scavengers, such as TEMPO and 9, 10-dihydroanthracene, did not obviously effect the reduction transformations, rendering a free radical mechanism unlikely to be operative.

3.2 The homogeneous test

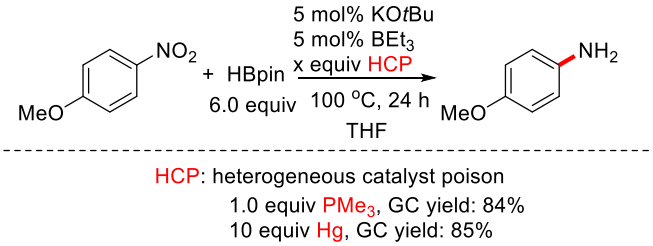

Addition of commonly used heterogeneous catalyst poison PMe_3 or Hg showed no adverse effect on the yield of the product, which indicated that the combined KO*t*Bu/BEt_3 catalyst was likely to be homogeneous under current conditions.

3.3 The kinetic studies

a. General procedure for typical reaction kinetics

For the reaction of 1-methoxy-4-nitrobenzene (0.60 mmol), pinacolborane (3.6 mmol) with KO*t*Bu/BEt$_3$ (0.03 mmol) in 2 ml THF:

In a glovebox, KO*t*Bu /BEt$_3$ (3.36 mg, 0.03 mmol) was added to a Schlenk tube equipped with a magnetic stirring bar and a Teflon cap. Then, a mixture of 1-methoxy-4-nitrobenzene (91.9mg, 0.60 mmol) and pinacolborane (460.7 mg, 3.6 mmol) in 2 mL THF was added. The sealed tube was taken out from the glovebox, and was stirred at 100 ^{o}C taken out at 5, 10, 15, 20, 25, 30, 40, 60, 90, 120, 180 minutes. The sample was analyzed by GC. The percentage yields of the product **2a** were calculated by *p*-xylene as an internal standard, which were then converted to molar concentrations. A duplicate reaction was also run under otherwise identical conditions and an average value was taken for each time point. The yields in molar concentrations are presented in Table S1. The molar concentrations of the product **2a** were plotted against the reaction time to obtain a typical reaction kinetic profile.

Table S1. The molar concentration of product **2a** at different time interval

Time (s)	Yield of **2a** (M)
0	0
300	0.02271
600	0.02765
900	0.03330
1200	0.03715
1500	0.04087
1800	0.04365
2400	0.04769
3600	0.05424
5400	0.05675
7200	0.05906
10800	0.06459

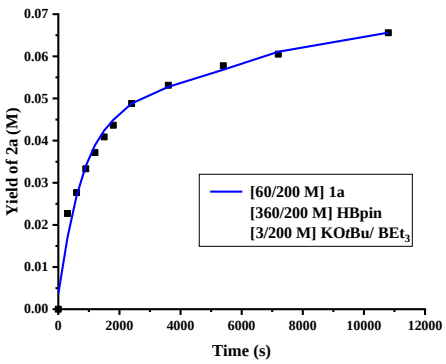

Figure S1. Plot of the rise of product **2a** from the reaction of 1-methoxy-4-nitrobenzene (0.60

mmol), pinacolborane (3.60 mmol) with KO*t*Bu/BEt$_3$ (0.03 mmol) in 2 ml THF. The reaction in different time interval at 100 ^{o}C.

b. General procedure to determine the dependence of reaction rate on the concentration of pinacolborane

For the reaction of 1-methoxy-4-nitrobenzene (0.60 mmol), pinacolborane (3.60 mmol) with KO*t*Bu/BEt$_3$ (0.03 mmol) in 2 ml THF:

In a glovebox, KO*t*Bu/BEt$_3$ (3.36 mg, 0.03 mmol) was added to a Schlenk tube equipped with a magnetic stirring bar and a Teflon cap. Then, a mixture of 1-methoxy-4-nitrobenzene (91.9mg, 0.60 mmol) and pinacolborane (460.7 mg, 3.60 mmol) in 2 mL THF was added. The sealed tube was taken out from the glovebox, and was stirred at 100 ^{o}C taken out at 5, 10, 15, 20 minutes. The sample was analyzed by GC. The percentage yields of the product **2a** were calculated by *p*-xylene as an internal standard, which were then converted to molar concentrations. A duplicate reaction was also run under otherwise identical conditions and an average value was taken for each time point. The yields in molar concentrations are presented in Table S2. The molar concentrations of the product **2a** were plotted against the reaction time to obtain a typical reaction kinetic profile.

For the reaction of 1-methoxy-4-nitrobenzene (0.60 mmol), pinacolborane (3.00 mmol) with KO*t*Bu/BEt$_3$ (0.03 mmol) in 2 ml THF: The procedure for this reaction was the same as above but instead of pinacolborane (3.60 mmol), pinacolborane (3.00 mmol) were added in the reaction.

For the reaction of 1-methoxy-4-nitrobenzene (0.60 mmol), pinacolborane (2.40 mmol) with KO*t*Bu/BEt$_3$ (0.03 mmol) in 2 ml THF: The procedure for this reaction was the same as above but instead of pinacolborane (3.60 mmol), pinacolborane (2.40 mmol) were added in the reaction.

For the reaction of 1-methoxy-4-nitrobenzene (0.60 mmol), pinacolborane (1.80 mmol) with KO*t*Bu/BEt$_3$ (0.03mmol) in 2 ml THF: The procedure for this reaction was the same as above but instead of pinacolborane (3.60 mmol), pinacolborane (1.80 mmol) were added in the reaction.

The percentage yields of the product **2a** were calculated by *p*-xylene as an internal standard, which were then converted to molar concentrations. A duplicate reaction was also run under otherwise identical conditions and an average value was taken for each time point. The molar concentration of product **2a** was plotted against the reaction time and the slope of linear portion of the curve was used to determine the initial rates of the reaction. The table showing molar concentration of product **2a** in different concentration of pinacolborane, graph showing the rate at different concentration of pinacolborane, table with K_{in} in value and the graph showing K_{in} in versus [HBpin] are shown below.

Table S2. The molar concentration of product **2a** in different concentration of pinacolborane at different time interval

Time (s)	HBpin [360/200 M]	HBpin [300/200 M]	HBpin [240/200 M]	HBpin [180/200 M]
300	0.02271	0.02201	0.02021	0.01945
600	0.02765	0.02516	0.02384	0.02139
900	0.03330	0.02895	0.02639	0.02378
1200	0.03715	0.03291	0.02897	0.02535

Table S3. The K_{in} value of product **2a** in different concentration of pinacolborane

HBpin (M)	K_{in} (Ms^{-1})
360/200	1.59232×10^{-5}
300/200	1.21653×10^{-5}
240/200	9.61652×10^{-6}
180/200	6.69135×10^{-6}

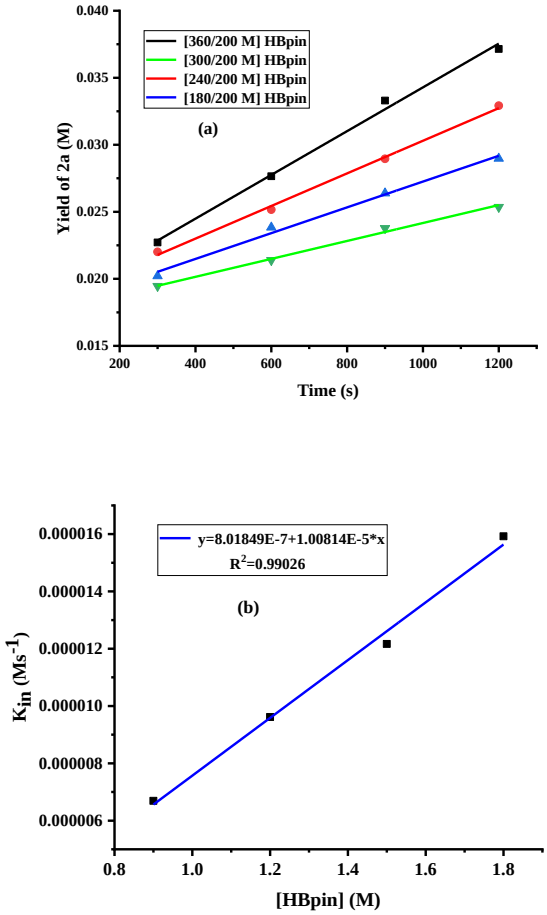

Figure S2. (a) Plot of the rise of product **2a** from the reaction of **1a** (0.6 mmol), KO*t*Bu/BEt_3 (0.03 mmol) with 3.60 mmol, 3.00 mmol, 2.40 mmol and 1.80 mmol of pinacolborane in 2 mL THF at different time. (b) Plot of K_{in} versus [HBpin] from the reaction of **1a** (0.6 mmol), KO*t*Bu/BEt_3 (0.03 mmol) with 3.60 mmol, 3.00 mmol, 2.40 mmol and 1.80 mmol of pinacolborane in 2 mL THF.

c. General procedure to determine the dependence of reaction rate on the concentration of 1a (1-methoxy-4-nitrobenzene)

For the reaction of 1-methoxy-4-nitrobenzene (0.60 mmol), pinacolborane (3.60 mmol) with KO*t*Bu/BEt_3 (0.03 mmol) in 2 ml THF:

In a glovebox, KO*t*Bu/BEt_3 (3.36 mg, 0.03 mmol) was added to a Schlenk tube equipped with a magnetic stirring bar and a Teflon cap. Then, a mixture of 1-methoxy-4-nitrobenzene (91.9mg, 0.60

mmol) and pinacolborane (460.7 mg, 3.6 mmol) in 2 mL THF was added. The sealed tube was taken out from the glovebox, and was stirred at 100 °C taken out at 5, 10, 15, 20 minutes. The sample was analyzed by GC. The percentage yields of the product **2a** were calculated by *p*-xylene as an internal standard, which were then converted to molar concentrations. A duplicate reaction was also run under otherwise identical conditions and an average value was taken for each time point. The yields in molar concentrations are presented in Table S4. The molar concentrations of the product **2a** were plotted against the reaction time to obtain a typical reaction kinetic profile.

For the reaction of 1-methoxy-4-nitrobenzene (0.50 mmol), pinacolborane (3.60 mmol) with KO*t*Bu/BEt$_3$ (0.03 mmol) in 2 ml THF: The procedure for this reaction was the same as above but instead of 1-methoxy-4-nitrobenzene (0.60mmol), 1-methoxy-4-nitrobenzene (0.50 mmol) were added in the reaction.

For the reaction of 1-methoxy-4-nitrobenzene (0.40 mmol), pinacolborane (3.60 mmol) with KO*t*Bu/BEt$_3$ (0.03 mmol) in 2 ml THF: The procedure for this reaction was the same as above but instead of 1-methoxy-4-nitrobenzene(0.60mmol),1-methoxy-4-nitrobenzene (0.40 mmol) were added in the reaction.

For the reaction of 1-methoxy-4-nitrobenzene (0.30 mmol), pinacolborane (3.60 mmol) with KO*t*Bu/BEt$_3$ (0.03 mmol) in 2 ml THF: The procedure for this reaction was the same as above but instead of 1-methoxy-4-nitrobenzene(0.60mmol), 1-methoxy-4-nitrobenzene (0.30 mmol) were added in the reaction.

The percentage yields of the product **2a** were calculated by *p*-xylene as an internal standard, which were then converted to molar concentrations. A duplicate reaction was also run under otherwise identical conditions and an average value was taken for each time point. The molar concentration of product **2a** was plotted against the reaction time and the slope of linear portion of the curve was used to determine the initial rates of the reaction. The table showing molar concentration of product **2a** in different concentration of 1-methoxy-4-nitrobenzene, graph showing the rate at different concentration of 1-methoxy-4-nitrobenzene, table with K_{in} in value and the graph showing K_{in} in versus [1-methoxy-4-nitrobenzene] are shown below.

Table S4. The molar concentration of product **2a** in different concentration of 1-methoxy-4-nitrobenzene (**1a**) at different time interval

Time (s)	**1a** [6/20 M]	**1a** [5/20 M]	**1a** [4/20 M]	**1a** [3/20 M]
300	0.02271	0.02151	0.02006	0.01924
600	0.02765	0.02566	0.02369	0.02125
900	0.03330	0.02875	0.02624	0.02399
1200	0.03715	0.03291	0.02805	0.02457

Table S5. The K_{in} value of product **2a** in different concentration of 1-methoxy-4-nitrobenzene

1a (M)	K_{in} (Ms^{-1})
6/20	1.63233×10^{-5}
5/20	1.24276×10^{-5}
4/20	8.84472×10^{-6}

3/20	6.24529×10^{-6}

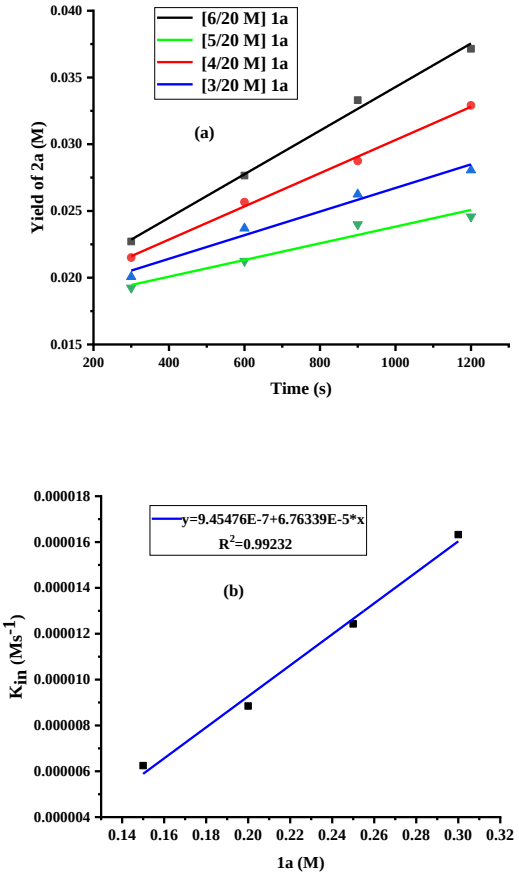

Figure S3. (a) Plot of the rise of product **2a** from the reaction of pinacolborane (3.60 mmol) with KO*t*Bu/BEt$_3$ (0.03 mmol) with 0.30 mmol, 0.40 mmol, 0.50 mmol and 0.60 mmol of 1-methoxy-4-nitrobenzene (**1a**) in 2 mL THF at different time interval. (b) Plot of K_{in} versus [1-methoxy-4-nitrobenzene] from the reaction of pinacolborane (3.60 mmol), KO*t*Bu/BEt$_3$ (0.03 mmol) with 0.30 mmol, 0.40 mmol, 0.50 mmol and 0.60 mmol of 1-methoxy-4-nitrobenzene in 2 mL THF.

d. General procedure to determine the dependence of reaction rate on the concentration of catalyst

For the reaction of 1-methoxy-4-nitrobenzene (0.60 mmol), pinacolborane (3.60 mmol) with KO*t*Bu/BEt$_3$ (0.03 mmol) in 2 ml THF:

In a glovebox, KO*t*Bu/BEt$_3$ (3.36 mg, 0.03 mmol) was added to a Schlenk tube equipped with a magnetic stirring bar and a Teflon cap. Then, a mixture of 1-methoxy-4-nitrobenzene (91.9mg, 0.60 mmol) and pinacolborane (460.7 mg, 3.6 mmol) in 2 mL THF was added. The sealed tube was taken out from the glovebox, and was stirred at 100 ^{o}C taken out at 5, 10, 15, 20 minutes. The sample was analyzed by GC. The percentage yields of the product **2a** were calculated by *p*-xylene as an internal standard, which were then converted to molar concentrations. A duplicate reaction was also run under otherwise identical conditions and an average value was taken for each time point. The yields in molar concentrations are presented in Table S6. The molar concentrations of the product **2a** were plotted against the reaction time to obtain a typical reaction kinetic profile.

For the reaction of 1-methoxy-4-nitrobenzene (0.6 mmol), pinacolborane (3.60 mmol) with KO*t*Bu/BEt$_3$ (0.024 mmol) in 2 ml THF: The procedure for this reaction was the same as above but instead of KO*t*Bu/BEt$_3$ (0.030 mmol), KO*t*Bu/BEt$_3$ (0.024 mmol) were added in the reaction.

For the reaction of 1-methoxy-4-nitrobenzene (0.60mmol), pinacolborane (3.60 mmol) with KO*t*Bu/BEt$_3$ (0.018 mmol) in 2 ml THF: The procedure for this reaction was the same as above but instead of KO*t*Bu /BEt$_3$ (0.030 mmol), KO*t*Bu /BEt$_3$ (0.018 mmol) were added in the reaction.

For the reaction of 1-methoxy-4-nitrobenzene (0.60mmol), pinacolborane (3.60 mmol) with KO*t*Bu/BEt$_3$ (0.012 mmol) in 2 ml THF: The procedure for this reaction was the same as above but instead of KO*t*Bu /BEt$_3$ (0.030 mmol), KO*t*Bu/BEt$_3$ (0.012mol) were added in the reaction.

The percentage yields of the product **2a** were calculated by *p*-xylene as an internal standard, which were then converted to molar concentrations. A duplicate reaction was also run under otherwise identical conditions and an average value was taken for each time point. The molar concentration of product **2a** was plotted against the reaction time and the slope of linear portion of the curve was used to determine the initial rates of the reaction. The table showing molar concentration of product **2a** in different concentration of pinacolborane, graph showing the rate at different concentration of KO*t*Bu/BEt$_3$, table with K_{in} in value and the graph showing K_{in} in versus KO*t*Bu/BEt$_3$ are shown below.

Table S6. The molar concentration of product **2a** in different concentration of KO*t*Bu/BEt$_3$ at different time interval

Time (s)	KO*t*Bu /BEt$_3$ [30/2000M]	KO*t*Bu /BEt$_3$ [24/2000M]	KO*t*Bu /BEt$_3$ [18/2000M]	KO*t*Bu /BEt$_3$ [12/2000 M]
300	0.02271	0.02109	0.01946	0.01846
600	0.02765	0.02551	0.02259	0.0198
900	0.03330	0.02861	0.02585	0.02291
1200	0.03715	0.03303	0.02903	0.02476

Table S7. The K_{in} value of product **2a** in different concentration of KO*t*Bu /BEt$_3$

KO*t*Bu /BEt$_3$ (M)	K_{in} (Ms^{-1})
30/2000	1.63233×10^{-5}
24/2000	1.29766×10^{-5}
18/2000	1.06546×10^{-5}
12/2000	7.33618×10^{-6}

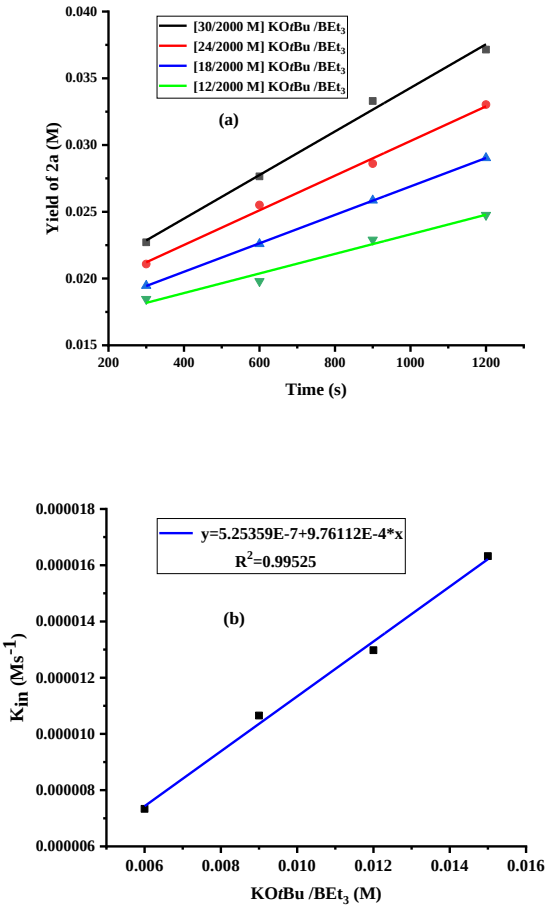

Figure S4. (a) Plot of the rise of product **2a** from the reaction of **1a** (0.6 mmol), pinacolborane (3.6 mmol with 0.012mmol, 0.018mmol, 0.024mmol and 0.030mmol concentration of KO*t*Bu/BEt_3 respectively in different time interval. (b) Plot of K_{in} versus KO*t*Bu/BEt_3 from the reaction of **1a** (0.6 mmol), pinacolborane (3.6 mmol) with 0.012mmol, 0.018mmol, 0.024mmol and 0.030mmol of KO*t*Bu/BEt_3 in 2mL THF.

3.4 The plausible mechanism and DFT calculations

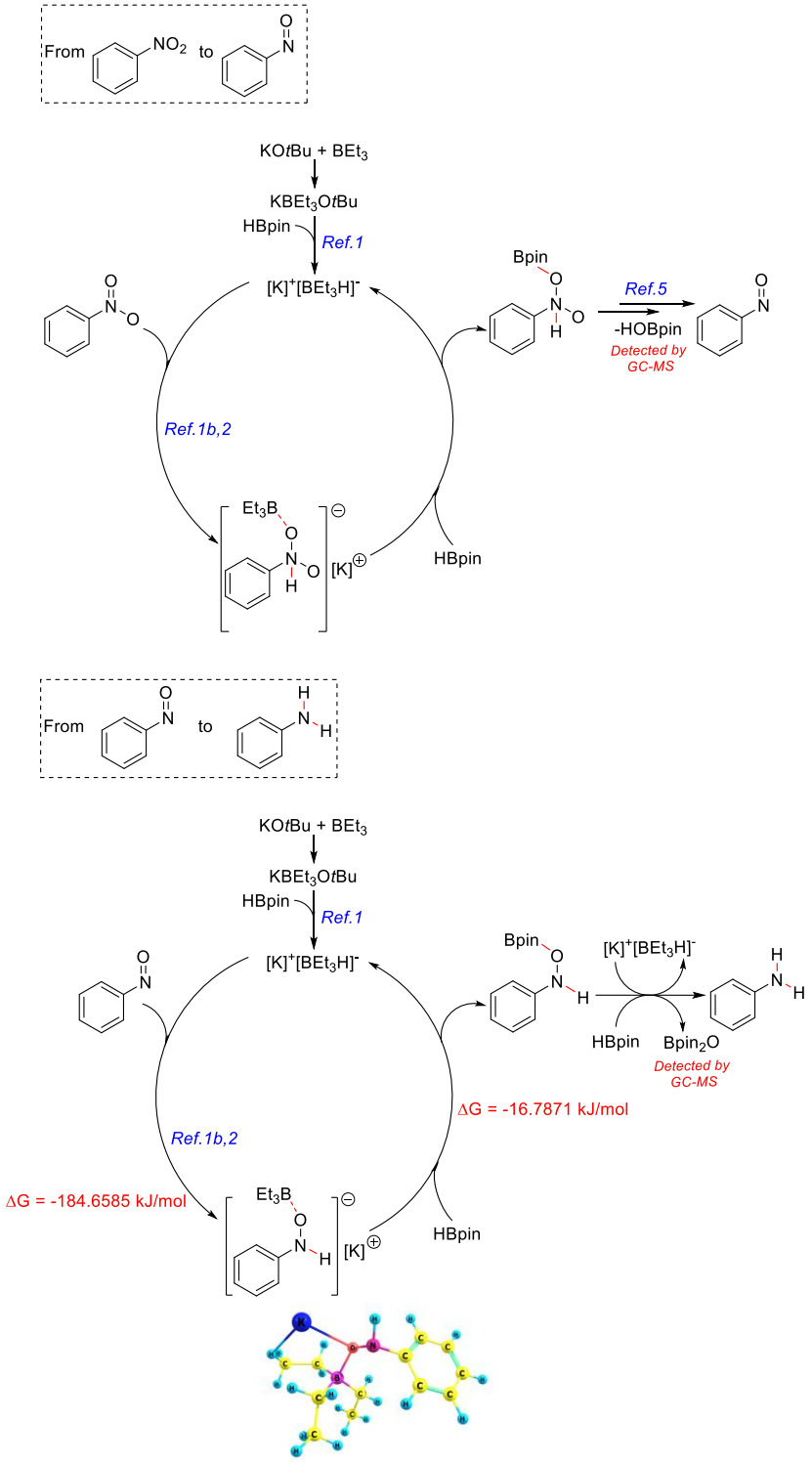

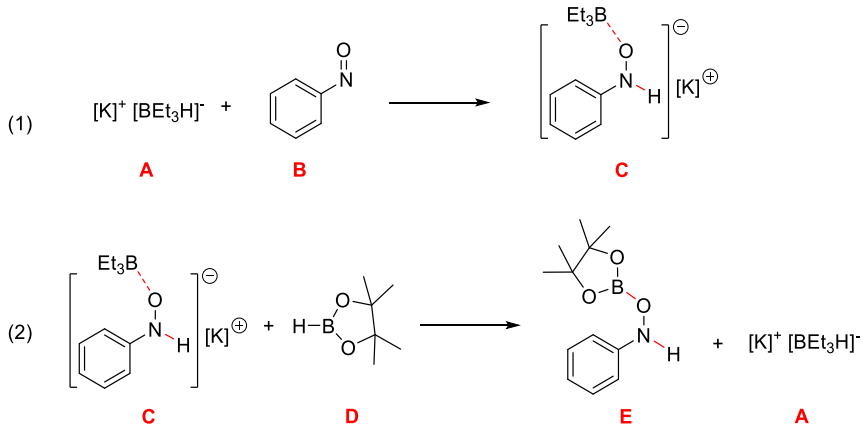

Table S8 The calculated gibbs free energies of reactions by DFT/B3LYP/6-311+G*

Eq (1)	G_A/a.u.	G_B/a.u.	G_C/a.u.		$\Delta G_{eq\ (1)}$ /(a.u.)	$\Delta G_{eq\ (1)}$ /(kcal.mol^{-1})	$\Delta G_{eq\ (1)}$ /(kJ.mol^{-1})
	-863.1434	-361.6306	-1224.8444		-0.0704	-44.1767	-184.6585
Eq (2)	G_C/a.u.	G_D/a.u.	G_E/a.u.	G_A/a.u.	$\Delta G_{eq\ (2)}$ /(a.u.)	$\Delta G_{eq\ (2)}$ /(kcal.mol^{-1})	$\Delta G_{eq\ (2)}$ /(kJ./mol^{-1})
	-1224.8444	-411.9700	-773.6774	-863.1434	-0.0064	-4.0161	-16.7871

(1 a.u. = 627.5095 kcal/mol; 1 kcal/mol = 4.18 kJ/mol)

--- Start of file **A** xyz ---

G_A = -863.1434 a.u.

Center Number	Atomic Number	Atomic Type	Coordinates (Angstroms) X	Y	Z
1	5	0	-0.050941	-0.319707	-0.052913
2	6	0	0.240878	1.156912	0.712674
3	6	0	0.468184	2.328865	-0.255577
4	6	0	-2.714726	-0.000620	-0.259737
5	6	0	-1.577405	-0.929000	0.197926
6	6	0	2.535093	-1.028287	-0.278097
7	6	0	1.134706	-1.459955	0.188271
8	1	0	-0.010025	-0.088217	-1.256860

9	1	0	1.136247	1.128769	1.370176
10	1	0	-0.595208	1.468138	1.375111
11	1	0	0.656296	3.281902	0.256314
12	1	0	-0.400360	2.463644	-0.906128
13	1	0	1.320197	2.126343	-0.910418
14	1	0	-3.710273	-0.446716	-0.141589
15	1	0	-2.591243	0.253730	-1.316442
16	1	0	-2.719189	0.947665	0.291599
17	1	0	-1.839745	-1.257179	1.234172
18	1	0	-1.651895	-1.867947	-0.368790
19	1	0	3.289707	-1.817001	-0.165994
20	1	0	2.900420	-0.152444	0.272044
21	1	0	2.509659	-0.744730	-1.334282
22	1	0	0.845910	-2.356812	-0.377916
23	1	0	1.260792	-1.864247	1.223115
24	19	0	-0.100123	-0.620156	2.798061

--- End of file **A** xyz ---

--- Start of file**B** xyz ---

G_B = -361.6306 a.u.

Center Number	Atomic Number	Atomic Type	Coordinates (Angstroms) X	Y	Z
1	7	0	-0.262946	0.878139	0.024833
2	8	0	-0.413190	2.077454	-0.085531
3	6	0	-1.471902	0.094866	-0.004229
4	6	0	-1.287554	-1.283472	0.123512
5	6	0	-2.394519	-2.127794	0.107368
6	6	0	-3.671380	-1.586109	-0.036030

7	6	0	-3.849505	-0.202407	-0.163732
8	6	0	-2.751743	0.644959	-0.148551
9	1	0	-0.278419	-1.665790	0.233074
10	1	0	-2.265193	-3.200060	0.205654
11	1	0	-4.536222	-2.241432	-0.048999
12	1	0	-4.849070	0.204651	-0.274590
13	1	0	-2.857485	1.719245	-0.245178

--- End of file **B** xyz ---

--- Start of file **C** xyz ---

G_C = -1224.8444 a.u.

Center Number	Atomic Number	Atomic Type	Coordinates (Angstroms) X	Y	Z
1	7	0	-0.660388	-1.692169	0.210566
2	8	0	0.380789	-1.154668	-0.676429
3	6	0	-1.871734	-0.896057	0.245107
4	5	0	1.065112	0.280740	-0.409141
5	6	0	-2.660035	-0.723505	-0.895962
6	6	0	-3.847493	-0.002381	-0.823331
7	6	0	-4.254874	0.555034	0.390016
8	6	0	-3.471058	0.382966	1.528657
9	6	0	-2.281870	-0.342770	1.455666
10	6	0	2.463747	0.052658	-1.261068
11	6	0	1.349017	0.494651	1.222946
12	6	0	0.079295	1.408471	-1.081650
13	6	0	0.682907	2.740559	-1.563980
14	1	0	-2.323760	-1.138367	-1.840833
15	1	0	-4.454386	0.130098	-1.713504
16	1	0	-5.179358	1.120963	0.445379
17	1	0	-3.783279	0.813023	2.475068
18	1	0	-1.666653	-0.485474	2.337011
19	1	0	2.238016	0.065969	-2.336705
20	1	0	0.595616	-0.048109	1.815927
21	1	0	-0.380433	0.927448	-1.956409
22	1	0	1.438862	2.585659	-2.340761
23	1	0	1.161465	3.306877	-0.759210
24	1	0	-0.910011	-2.528395	-0.314560

25	1	0	2.327916	0.068482	1.528773
26	1	0	-0.765999	1.642219	-0.418962
27	6	0	1.359772	1.942605	1.742551
28	1	0	0.411082	2.443718	1.534957
29	1	0	1.525249	1.993711	2.825849
30	1	0	2.146605	2.535339	1.268877
31	6	0	3.628069	1.021474	-0.987525
32	1	0	4.508656	0.793776	-1.600831
33	1	0	3.354593	2.057970	-1.195856
34	1	0	3.953042	0.987649	0.059074
35	1	0	2.855368	-0.973264	-1.100225
36	1	0	-0.082730	3.395582	-1.998223
37	19	0	1.844327	-2.340642	0.957024

--- End of file **C** xyz ---

--- Start of file **D** xyz ---

G_D = -411.9700 a.u.

Center Number	Atomic Number	Atomic Type	Coordinates (Angstroms) X	Y	Z
1	8	0	0.360880	1.085024	1.183550
2	6	0	0.042888	0.789243	-0.213561
3	6	0	-0.042888	-0.789243	-0.213561
4	8	0	-0.360880	-1.085024	1.183550
5	5	0	0.000000	0.000000	1.930062
6	6	0	1.140299	1.379576	-1.091806
7	6	0	-1.294160	1.475976	-0.510164
8	6	0	1.294160	-1.475976	-0.510164
9	6	0	-1.140299	-1.379576	-1.091806
10	1	0	0.000000	0.000000	3.117021
11	1	0	0.972679	1.135849	-2.144928
12	1	0	2.128688	1.019975	-0.806883
13	1	0	1.140828	2.467571	-0.996426
14	1	0	-1.590997	1.349035	-1.554167
15	1	0	-1.197016	2.545236	-0.311158
16	1	0	-2.095535	1.091396	0.124233

17	1	0	1.197016	-2.545236	-0.311158
18	1	0	2.095535	-1.091396	0.124233
19	1	0	1.590997	-1.349035	-1.554167
20	1	0	-1.140828	-2.467571	-0.996426
21	1	0	-0.972679	-1.135849	-2.144928
22	1	0	-2.128688	-1.019975	-0.806883

--- End of file **D** xyz ---

--- Start of file **E** xyz ---

G_E = -773.6774 a.u.

Center Number	Atomic Number	Atomic Type	Coordinates (Angstroms) X	Y	Z
1	6	0	-4.470437	-1.250381	0.543850
2	6	0	-3.166425	-1.157061	0.059699
3	6	0	-2.684083	0.074365	-0.391794
4	6	0	-3.517938	1.201273	-0.356156
5	6	0	-4.816626	1.092009	0.126889
6	6	0	-5.303560	-0.134743	0.581316
7	1	0	-4.834750	-2.210887	0.895058
8	1	0	-2.522180	-2.025684	0.032251
9	1	0	-3.149370	2.158571	-0.714952
10	1	0	-5.450708	1.972799	0.150817
11	1	0	-6.317095	-0.216780	0.959069
12	7	0	-1.404843	0.218127	-0.976629
13	1	0	-0.966182	1.100689	-0.725631
14	8	0	-0.521234	-0.835826	-0.576679
15	5	0	0.750569	-0.459077	-0.266810
16	6	0	2.978028	-0.641677	0.125613
17	6	0	2.511675	0.856330	0.332552
18	8	0	1.709682	-1.364396	0.094859
19	8	0	1.181317	0.847478	-0.279032
20	6	0	3.360414	1.903676	-0.377242
21	1	0	2.944822	2.898095	-0.199295
22	1	0	4.385505	1.897989	0.003992
23	1	0	3.391202	1.741695	-1.454335
24	6	0	2.318992	1.234872	1.803538

25	1	0	1.817901	2.203552	1.861155
26	1	0	1.699921	0.505668	2.330555
27	1	0	3.274478	1.315876	2.326996
28	6	0	3.827546	-1.212426	1.254878
29	1	0	4.763065	-0.655811	1.361572
30	1	0	3.301367	-1.193099	2.208919
31	1	0	4.080139	-2.251775	1.034353
32	6	0	3.658963	-0.882619	-1.224971
33	1	0	4.650001	-0.424383	-1.266191
34	1	0	3.773989	-1.957578	-1.377389
35	1	0	3.063991	-0.491451	-2.053222

--- End of file **E** xyz ---

4. NMR spectra data

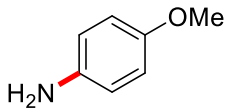

4-Methoxyaniline (2a), white solid, 0.062 g, 84%. ^{1}H NMR (400 MHz, $CDCl_3$, 20 ^{o}C) δ 6.78-6.72 (m, 2H), 6.68-6.61 (m, 2H), 3.75 (s, 3H), 3.41 (s, 2H). ^{13}C {^{1}H} NMR (101 MHz, $CDCl_3$, 20 ^{o}C) δ 152.9, 140.1, 116.5, 114.9, 55.8. These spectroscopic data correspond to reported data.[4]

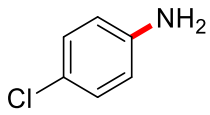

4-Chloroaniline (2c), white solid, 0.056 g, 73%. ^{1}H NMR (400 MHz, $CDCl_3$, 20 ^{o}C) δ 7.14-7.05 (m, 2H), 6.68-6.54 (m, 2H), 3.60 (s, 2H). ^{13}C{^{1}H} NMR (101 MHz, $CDCl_3$, 20 ^{o}C) δ 145.1, 129.2, 123.2, 116.3. These spectroscopic data correspond to reported data.[5]

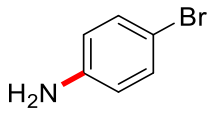

4-Bromoaniline (2d), gray solid, 0.076 g, 74%. ^{1}H NMR (400 MHz, $CDCl_3$, 20 ^{o}C) δ 7.22 (d, *J* = 8.6 Hz, 2H), 6.54 (d, *J* = 8.6 Hz, 2H), 3.65 (s, 2H). ^{13}C {^{1}H} NMR (101 MHz, $CDCl_3$, 20 ^{o}C) δ 145.5, 132.0, 116.8, 110.2. These spectroscopic data correspond to reported data.[4]

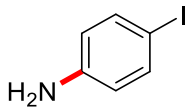

4-Iodoaniline (2e), grayish-brown solid, 0.088 g, 67%. ^{1}H NMR (400 MHz, $CDCl_3$, 20 ^{o}C) δ 7.41 (t, *J* = 5.7 Hz, 2H), 6.47 (t, *J* = 5.7 Hz, 2H), 3.62 (s, 2H). ^{13}C {^{1}H} NMR (101 MHz, $CDCl_3$, 20 ^{o}C) δ 146.2, 138.0, 117.4, 79.5. These spectroscopic data correspond to reported data.[4]

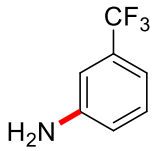

3-(Trifluoromethyl)aniline (2f), colorless oil, 0.068 g, 70%. ^{1}H NMR (400 MHz, $CDCl_3$, 20 ^{o}C) δ 7.22 (dd, *J* = 10.5 Hz, *J* = 5.3 Hz, 1H), 6.98 (d, *J* = 7.7 Hz, 1H), 6.87 (s, 1H), 6.79 (dd, *J* = 8.0 Hz, *J* = 2.2 Hz, 1H), 3.80 (s, 2H). ^{13}C {^{1}H} NMR (101 MHz, $CDCl_3$, 20 ^{o}C) δ 146.9, 131.7 (q, *J* = 31.8 Hz), 129.9, 124.4 (q, *J* = 272.2 Hz), 118.1 (d, *J* = 1.2 Hz), 115.1 (q, *J* = 4.0 Hz), 111.4 (q, *J* = 3.9 Hz). ^{19}F NMR (377 MHz, $CDCl_3$, 20 ^{o}C) δ -62.91. These spectroscopic data correspond to reported data.[4]

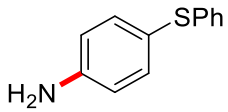

4-(Phenylthio)aniline (2g), yellow solid, 0.078 g, 65%. ^{1}H NMR (400 MHz, $CDCl_3$, 20 ^{o}C) δ 7.36-7.29 (m, 2H), 7.24-7.18 (m, 2H), 7.16-7.06 (m, 3H), 6.72-6.63 (m, 2H), 3.81 (s, 2H). ^{13}C {^{1}H} NMR (101 MHz, $CDCl_3$, 20 ^{o}C) δ 147.2, 139.8, 136.3, 128.9, 127.4, 125.4, 120.6, 116.0. These spectroscopic data correspond to reported data.[6]

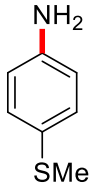

4-(Methylthio)aniline (2h), colorless oil, 0.046 g, 55%. ^{1}H NMR (400 MHz, $CDCl_3$, 20 ^{o}C) δ 7.18 (d, *J* = 8.1 Hz, 2H), 6.63 (d, *J* = 8.1 Hz, 2H), 3.67 (s, 2H), 2.41 (s, 3H). ^{13}C {^{1}H} NMR (101 MHz, $CDCl_3$, 20 ^{o}C) δ 145.2, 131.1, 115.8, 18.9. These spectroscopic data correspond to reported data.[5]

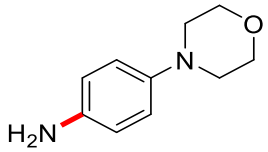

4-Morpholinoaniline (2i), white solid, 0.079 g, 74%. ^{1}H NMR (400 MHz, $CDCl_3$, 20

°C) δ 6.79 (d, *J* = 8.7 Hz, 2H), 6.66 (d, *J* = 8.7 Hz, 2H), 3.91-3.79 (m, 4H), 3.41 (s, 2H), 3.08-2.94 (m, 4H). ^{13}C {^{1}H} NMR (101 MHz, $CDCl_3$, 20 °C) δ 144.5, 140.4, 118.3, 116.3, 67.2, 51.2.These spectroscopic data correspond to reported data.[5]

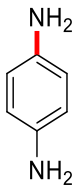

***p*-Phenylenediamine (2j)**, white solid, 0.042 g, 65%. ^{1}H NMR (400 MHz, $CDCl_3$, 20 °C) δ 6.56 (s, 4H), 3.32 (s, 4H). ^{13}C {^{1}H} NMR (101 MHz, $CDCl_3$, 20 °C) δ 138.7, 116.8 . These spectroscopic data correspond to reported data.[4]

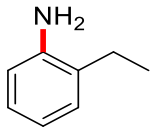

2-Ethylaniline (2k), yellow oil, 0.058 g, 80%. ^{1}H NMR (400 MHz, $CDCl_3$, 20 °C) δ 7.12 (dd, *J* = 17.3 Hz, *J* = 7.8 Hz, 2H), 6.82 (t, *J* = 7.4 Hz, 1H), 6.73 (d, *J* = 7.8 Hz, 1H), 3.65 (s, 2H), 2.57 (q, *J* = 7.5 Hz, 2H), 1.32 (t, *J* = 7.5 Hz, 3H). ^{13}C {^{1}H} NMR (101 MHz, $CDCl_3$, 20 °C) δ 144.1, 128.4, 128.1, 126.9, 118.9, 115.4, 24.1, 13.1. These spectroscopic data correspond to reported data.[4]

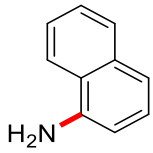

1-Naphthylamine (2l), white solid, 0.069 g, 80%. ^{1}H NMR (400 MHz, $CDCl_3$, 20 °C) δ 7.84 (ddd, *J* = 5.5 Hz, *J* = 3.1 Hz, *J* =1.4 Hz, 2H), 7.56-7.44 (m, 2H), 7.34 (qd, *J* = 8.1 Hz, *J* = 7.0 Hz, 2H), 6.80 (dd, *J* = 6.9 Hz, *J* =1.5 Hz, 1H), 4.15 (s, 2H). ^{13}C {^{1}H} NMR (101 MHz, $CDCl_3$, 20 °C) δ 142.2, 134.5, 128.6, 126.4, 125.9, 125.0, 123.8, 120.9, 119.1, 109.8. These spectroscopic data correspond to reported data.[4]

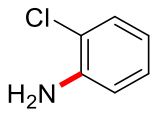

2-Chloroaniline (2m), yellow oil, 0.058 g, 76%. ^{1}H NMR (400 MHz, $CDCl_3$, 20 °C) δ 7.22 (dd, *J* = 8.0 Hz, *J* = 1.2 Hz, 1H), 7.07-6.98 (m, 1H), 6.72 (dd, *J* = 8.0 Hz, *J* = 1.3 Hz, 1H), 6.69-6.62 (m, 1H), 4.00 (s, 2H). ^{13}C {^{1}H} NMR (101 MHz, $CDCl_3$, 20 °C) δ 143.0, 129.5, 127.7, 119.3, 119.1, 116.0. These spectroscopic data correspond to reported data.[7]

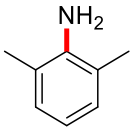

2, 6-Dimethylaniline (2n), yellow oil, 0.063 g, 87%. ^{1}H NMR (400 MHz, $CDCl_3$, 20 ^{o}C) δ 7.02 (d, *J* = 7.5 Hz, 2H), 6.72 (t, *J* = 7.5 Hz, 1H), 3.62 (s, 2H), 2.25 (s, 6H). ^{13}C {^{1}H} NMR (101 MHz, $CDCl_3$, 20 ^{o}C) δ 142.8, 128.3, 121.7, 118.0, 17.7. These spectroscopic data correspond to reported data.[4]

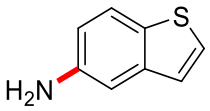

Benzo[b]thiophen-5-amine (2o), white solid, 0.064 g, 71%. ^{1}H NMR (400 MHz, $CDCl_3$, 20 ^{o}C) δ 7.64 (d, *J* = 8.5 Hz, 1H), 7.38 (d, *J* = 5.4 Hz, 1H), 7.15 (d, *J* = 5.4 Hz, 1H), 7.10 (s, 1H), 6.82-6.73 (m, 1H). ^{13}C {^{1}H} NMR (101 MHz, $CDCl_3$, 20 ^{o}C) δ 143.6, 140.9, 130.5, 127.2, 123.1, 123.0, 115.0, 108.4. These spectroscopic data correspond to reported data.[5]

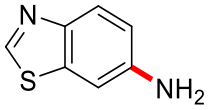

Benzo[d]thiazol-6-amine (2p), white solid, 0.055 g, 61%. ^{1}H NMR (400 MHz, DMSO-d_6, 20 ^{o}C) δ 8.87 (s, 1H), 7.72 (d, *J* = 8.7 Hz, 1H), 7.13 (d, *J* = 1.7 Hz, 1H), 6.81 (dd, *J* = 8.7 Hz, *J* =1.9 Hz, 1H), 5.41 (s, 2H). ^{13}C{^{1}H} NMR (101 MHz, DMSO-d_6, 20 ^{o}C) δ 149.1, 147.3, 144.8, 135.2, 123.1, 114.9, 103.8. These spectroscopic data correspond to reported data.[5]

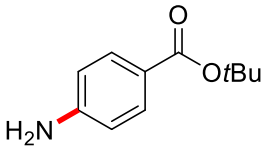

***t*-Butyl-4-aminobenzoate (2q)**, white solid, 0.11 g, 99%. ^{1}H NMR (400 MHz, $CDCl_3$, 20 ^{o}C) δ 7.80 (d, *J* = 8.6 Hz, 2H), 6.66-6.57 (m, 2H), 4.02 (s, 2H), 1.56 (s, 9H). ^{13}C {^{1}H} NMR (101 MHz, $CDCl_3$, 20 ^{o}C) δ 166.1, 150.5, 131.5, 121.8, 113.8, 80.2, 28.4. These spectroscopic data correspond to reported data.[8]

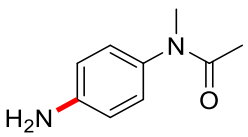

N-(4-aminophenyl)-N-methylacetamide (2r), yellow solid, 0.060 g, 61%. ^{1}H NMR (400 MHz, $CDCl_3$, 20 ^{o}C) δ 6.92 (d, *J* = 8.5 Hz, 2H), 6.66 (d, *J* = 8.5 Hz, 2H), 3.83 (s, 2H), 3.18 (s, 3H), 1.83 (s, 3H). ^{13}C {^{1}H} NMR (101 MHz, $CDCl_3$, 20 ^{o}C) δ 171.4, 146.1,

135.5, 128.0, 115.7, 37.4, 29.8, 22.4. These spectroscopic data correspond to reported data.[9]

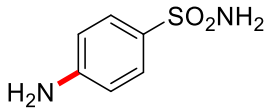

4-Aminobenzenesulfonamide (2s), white solid, 0.083 g, 80%. ^{1}H NMR (400 MHz, DMSO-d_6, 20 ^{o}C) δ 7.45 (d, J = 8.6 Hz, 2H), 6.88 (s, 2H), 6.58 (d, J = 8.6 Hz, 2H), 5.80 (s, 2H). ^{13}C{^{1}H} NMR (101 MHz, DMSO-d_6, 20 ^{o}C) δ 151.9, 130.0, 127.4, 112.4. These spectroscopic data correspond to reported data.[10]

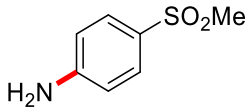

4-(Methylsulfonyl)aniline (2t), yellow solid, 0.077 g, 75%. ^{1}H NMR (400 MHz, DMSO-d_6, 20 ^{o}C) δ 7.50 (d, J = 8.7 Hz, 2H), 6.64 (d, J = 8.7 Hz, 2H), 6.09 (s, 2H), 3.02 (s, 3H). ^{13}C{^{1}H} NMR (101 MHz, DMSO-d_6, 20 ^{o}C) δ 153.5, 128.8, 125.8, 112.7, 44.5. These spectroscopic data correspond to reported data.[11]

Ethylamine hydrochloride (5a), white solid, 0.039 g, 80%. ^{1}H NMR (400 MHz, DMSO-d_6, 20 ^{o}C) δ 7.84 (s, 3H), 2.77 (dd, J = 14.0 Hz, J = 6.9 Hz, 2H), 1.15 (t, J = 7.1 Hz, 3H). ^{13}C{^{1}H} NMR (101 MHz, DMSO-d_6, 20 ^{o}C) δ 34.0, 12.5. These spectroscopic data correspond to reported data.[12]

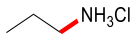

***n*-Propylamine hydrochloride (5b)**, white solid, 0.051 g, 88%. ^{1}H NMR (400 MHz, D_2O, 20 ^{o}C) δ 2.96 (t, J = 7.4 Hz, 2H), 1.67 (dq, J = 14.7 Hz, J = 7.3 Hz, 2H), 0.97 (t, J = 7.4 Hz, 3H). ^{13}C {^{1}H} NMR (101 MHz, D_2O, 20 ^{o}C) δ 41.1, 20.2, 10.1. These spectroscopic data correspond to reported data.[12]

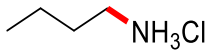

***n*-Butylamine hydrochloride (5c)**, white solid, 0.059 g, 90%. ^{1}H NMR (400 MHz, DMSO-d_6, 20 ^{o}C) δ 7.99 (s, 3H), 2.73 (t, J = 7.5 Hz, 2H), 1.59-1.46 (m, 2H), 1.31 (dq, J = 14.5 Hz, J = 7.1 Hz, 2H), 0.86 (t, J = 7.2 Hz, 3H). ^{13}C{^{1}H} NMR (101 MHz, DMSO-d_6, 20 ^{o}C) δ 38.4, 29.0, 19.2, 13.5. These spectroscopic data correspond to reported data.[12]

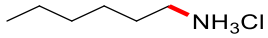

Hexylamine hydrochloride (5d), white solid, 0.077 g, 93%. ^{1}H NMR (400 MHz, DMSO-d_6, 20 ^{o}C) δ 8.22 (s, 3H), 2.69 (t, J = 7.5 Hz, 2H), 1.63-1.46 (m, 2H), 1.28 (dd, J = 14.5 Hz, J = 7.7 Hz, 6H), 0.85 (t, J = 6.7 Hz, 3H). ^{13}C{^{1}H} NMR (101 MHz, DMSO-d_6, 20 ^{o}C) δ 30.8, 26.8, 25.6, 22.0, 13.9. These spectroscopic data correspond to reported

data.[12]

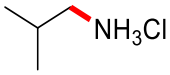

Isobutylamine hydrochloride (5e), white solid, 0.055 g, 83%. ^{1}H NMR (400 MHz, DMSO-d_6, 20 ºC) δ 8.11 (s, 3H), 2.59 (s, 2H), 1.93-1.83 (m, 1H), 0.91 (d, J = 6.7 Hz, 6H). ^{13}C{^{1}H} NMR (101 MHz, DMSO-d_6, 20 ºC) δ 45.6, 26.3, 19.8. These spectroscopic data correspond to reported data.[12]

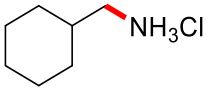

Cyclohexanemethylamine hydrochloride (5f), white solid, 0.079 g, 88%. ^{1}H NMR (400 MHz, DMSO-d_6, 20 ºC) δ 8.08 (s, 3H), 2.60 (s, 2H), 1.70 (dd, J = 24.2 Hz, J = 12.6 Hz, 4H), 1.65-1.47 (m, 2H), 1.24-1.05 (m, 3H), 1.02-0.74 (m, 2H). ^{13}C{^{1}H} NMR (101 MHz, DMSO-d_6, 20 ºC) δ 44.3, 35.4, 29.8, 25.6, 25.0. These spectroscopic data correspond to reported data.[12]

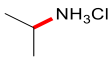

***i*-Propylamine hydrochloride (5g)**, white solid, 0.056 g, 97%. ^{1}H NMR (400 MHz, D_2O, 20 ºC) δ 3.49 (s, 1H), 1.30 (s, 6H). ^{13}C {^{1}H} NMR (101 MHz, D_2O, 20 ºC) δ 44.0, 19.8. These spectroscopic data correspond to reported data.[5]

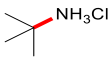

***t*-Butylamine hydrochloride (5h)**, white solid, 0.059 g, 89%. ^{1}H NMR (400 MHz, D_2O, 20 ºC) δ 1.38(s, 9 H). ^{13}C {^{1}H} NMR (101 MHz, D_2O, 20 ºC) δ 52.0, 26.6. These spectroscopic data correspond to reported data.[5]

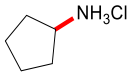

Cyclopentylamine hydrochloride (5i), white solid, 0.064 g, 87%. ^{1}H NMR (400 MHz, D_2O, 20 ºC) δ 3.66 (s, 1H), 2.06 (s, 2H), 1.69 (d, J = 43.7 Hz, 6H). ^{13}C {^{1}H} NMR (101 MHz, D_2O, 20 ºC) δ 52.2, 30.6, 23.5. These spectroscopic data correspond to reported data.[5]

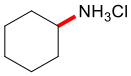

Cyclohexylamine hydrochloride (5j), white solid, 0.073 g, 90%. ^{1}H NMR (400 MHz, D_2O, 20 ºC) δ 3.16 (td, J = 10.6 Hz, J = 5.2 Hz, 1H), 2.00 (d, J = 7.5 Hz, 2H), 1.81 (d, J = 4.9 Hz, 2H), 1.66 (d, J = 12.2 Hz, 1H), 1.44-1.26 (m, 4H), 1.25-1.10 (m, 1H). ^{13}C {^{1}H} NMR (101 MHz, D_2O, 20 ºC) δ 50.4, 30.3, 24.3, 23.8. These spectroscopic data correspond to reported data.[5]

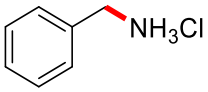

Benzylamine hydrochloride (5k), white solid, 0.085 g, 99%. ^{1}H NMR (400 MHz, D_2O, 20 ^{o}C) δ 7.54-7.42 (m, 5H), 4.19 (s, 2H). ^{13}C{^{1}H} NMR (101 MHz, D_2O, 20 ^{o}C) δ 132.6, 129.2, 128.8, 43.1. These spectroscopic data correspond to reported data.[13]

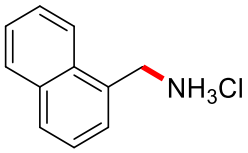

Naphthalen-1-ylmethanamine hydrochloride (5l), white solid, 0.092 g, 79%. ^{1}H NMR (400 MHz, DMSO-d_6, 20 ^{o}C) δ 8.52 (s, 3H), 8.15 (d, J = 8.2 Hz, 1H), 8.00 (t, J = 9.1 Hz, 2H), 7.69-7.51 (m, 4H), 4.52 (d, J = 5.6 Hz, 2H). ^{13}C{^{1}H} NMR (101 MHz, DMSO-d_6, 20 ^{o}C) δ 133.2, 130.7, 130.2, 128.9, 128.7, 127.3, 126.8, 126.2, 125.4, 123.5. These spectroscopic data correspond to reported data.[12]

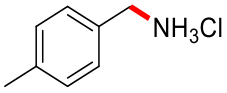

4-Methylbenzylamine hydrochloride (5m), white solid, 0.093 g, 98%. ^{1}H NMR (400 MHz, DMSO-d_6, 20 ^{o}C) δ 8.38 (s, 3H), 7.37 (d, J = 8.0 Hz, 2H), 7.22 (d, J = 7.8 Hz, 2H), 3.95 (q, J = 5.7 Hz, 2H), 2.31 (s, 3H). ^{13}C{^{1}H} NMR (101 MHz, DMSO-d_6, 20 ^{o}C) δ 137.8, 131.0, 129.1, 128.9, 41.9, 20.7. These spectroscopic data correspond to reported data.[13]

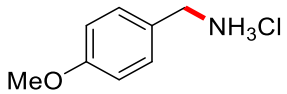

4-Methoxybenzylamine hydrochloride (5n), white solid, 0.10g, 99%. ^{1}H NMR (400 MHz, DMSO-d_6, 20 ^{o}C) δ 8.29 (s, 3H), 7.41 (d, J = 8.6 Hz, 2H), 6.97 (d, J = 8.6 Hz, 2H), 3.93 (q, J = 5.7 Hz, 2H), 3.76 (s, 3H). ^{13}C{^{1}H} NMR (101 MHz, DMSO-d_6, 20 ^{o}C) δ 159.4, 130.5, 125.9, 113.9, 55.2, 41.7. These spectroscopic data correspond to reported data.[13]

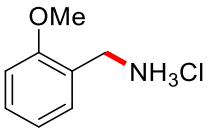

***o*-Anisidine hydrochloride (5o)**, white solid, 0.085 g, 82%. ^{1}H NMR (400 MHz, DMSO-d_6, 20 ^{o}C) δ 8.33 (s, 3H), 7.39 (dd, J = 11.6 Hz, J = 7.6 Hz, 2H), 7.07 (d, J = 8.2 Hz, 1H), 6.98 (t, J = 7.4 Hz, 1H), 3.95 (q, J = 5.6 Hz, 2H), 3.83 (s, 3H). ^{13}C{^{1}H} NMR (101 MHz, DMSO-d_6, 20 ^{o}C) δ 157.2, 130.3 (d, J = 3.8 Hz), 121.7, 120.3, 110.9, 55.5, 37.6. These spectroscopic data correspond to reported data.[12]

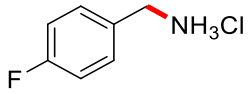

4-Fluorobenzylamine hydrochloride (5p), white solid, 0.084 g, 87%. ^{1}H NMR (400 MHz, DMSO-d_6, 20 ^{o}C) δ 8.52 (s, 3H), 7.56 (dd, J = 8.3 Hz, J = 5.7 Hz, 2H), 7.25 (t, J = 8.9 Hz, 2H), 4.00 (s, 2H). ^{19}F NMR (377 MHz, DMSO-d_6, 20 ^{o}C) δ -113.69. ^{13}C{^{1}H} NMR (101 MHz, DMSO-d_6, 20 ^{o}C) δ 163.3, 160.8, 131.3 (d, J = 8.4 Hz), 130.4 (d, J = 3.1 Hz), 115.4, 115.2, 41.4. These spectroscopic data correspond to reported data.[12]

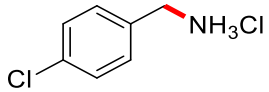

4-Chlorobenzylamine hydrochloride (5q), white solid, 0.085 g, 80%. ^{1}H NMR (400 MHz, DMSO-d_6, 20 ^{o}C) δ 8.60 (s, 3H), 7.55 (d, J = 7.9 Hz, 2H), 7.47 (d, J = 7.9 Hz, 2H), 4.00 (s, 2H). ^{13}C{^{1}H} NMR (101 MHz, DMSO-d_6, 20 ^{o}C) δ 133.2, 133.1, 131.0, 128.5, 41.4. These spectroscopic data correspond to reported data.[12]

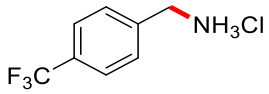

[4-(Trifluoromethyl)phenyl]methanamine hydrochloride (5r), white solid, 0.10 g, 79%. ^{1}H NMR (400 MHz, DMSO-d_6, 20 ^{o}C) δ 8.89 (s, 3H), 7.75 (q, J = 8.2 Hz, 4H), 4.10 (s, 2H). ^{13}C{^{1}H} NMR (101 MHz, DMSO-d_6, 20 ^{o}C) δ 138.9, 130.0, 129.0 (q, J = 31.8 Hz), 125.4 (d, J = 3.7 Hz), 124.3 (d, J = 273.7 Hz), 41.7. ^{19}F NMR (377 MHz, DMSO-d_6, 20 ^{o}C) δ -61.17. These spectroscopic data correspond to reported data.[13]

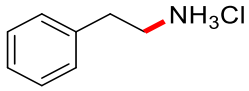

2-Phenylethylamine hydrochloride (5s), white solid, 0.069 g, 73%. ^{1}H NMR (400 MHz, D_2O, 20 ^{o}C) δ 7.38 (dt, J = 15.0 Hz, J = 7.1 Hz, 5H), 3.27 (t, J = 7.2 Hz, 2H), 3.05- 2.96 (m, 2H). ^{13}C {^{1}H} NMR (101 MHz, D_2O, 20 ^{o}C) δ 136.6, 129.0, 128.9, 127.3, 40.6, 32.7. These spectroscopic data correspond to reported data.[12]

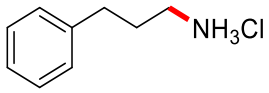

Phenylethylamine hydrochloride (5t), white solid, 0.087 g, 84%. ^{1}H NMR (400 MHz, DMSO-d_6, 20 ^{o}C) δ 8.03 (s, 3H), 7.30 (t, J = 7.4 Hz, 2H), 7.25-7.13 (m, 2H), 2.76 (dd, J = 13.4 Hz, J = 6.4 Hz, 2H), 2.64 (t, J = 7.7 Hz, 2H), 1.93-1.72 (m, 2H). ^{13}C{^{1}H} NMR (101 MHz, DMSO-d_6, 20 ^{o}C) δ 140.9, 128.4, 128.2, 126.0, 38.3, 31.8, 28.7. These spectroscopic data correspond to reported data.[12]

5. References

[1] (*a*) D. Peng, M. Zhang and Z. Huang, *Chem. Eur. J*., 2015, **21**, 14737; (*b*) W. Yao, J. Wang, A. Zhong, J. Li and J. Yang, *Org. Lett*., 2020, **22**, 8086.

[2] (a) M. G. Manas, L. S. Sharninghausen, D. Balcells and R. H. Crabtree, *New J. Chem*., 2014, **38**, 1694; (b) D. Bedi, A. Brar and M. Findlater, *Green Chem*., 2020, **22**, 1125.

[3] (*a*) J. Xiao, Y. He, F. Ye and S. Zhu, *Chem*, 2018, **4**, 1645; (*b*) S. Park, I. S. Lee and J. Park, *Org. Biomol. Chem*., 2013, **11**, 395.

[4] V. Zubar, A. Dewanji and M. Rueping, *Org. Lett*., 2021, **23**, 2742.

[5] L. Zhao, C. Hu, X. Cong, G. Deng, L. L. Liu, M. Luo and X. Zeng, *J. Am. Chem. Soc*., 2021, **143**, 1618.

[6] A. C. Jones, W. I. Nicholson, H. R. Smallman and D. L. Browne, *Org. Lett*., 2020, **22**, 8746.

[7] H. R. Dasgupta, S. Mukherjee and P. Ghosh, *Tetrahedron Lett*., 2019, **60**, 151028.

[8] N. R. Lee, A. A. Bikovtseva, M. Cortes-Clerget, F. Gallou and B. H. Lipshutz, *Org. Lett*., 2017, **19**, 6518.

[9] H.-G. Cheng, M. Pu, G. Kundu and F. Schoenebeck, *Org. Lett*., 2020, **22**, 4581.

[10] G. Fernández, J. Sort and R. Pleixats, *ChemistrySelect*, 2018, **3**, 8597.

[11] D. Han, S. Li, S. Xia, M. Su and J. Jin, *Chem. Eur. J*. 2020, **26**, 12349.

[12] C. Bäumler, C. Bauer and R. Kempe, *ChemSusChem*, 2020, **13**, 3110.

[13] M. Bhunia, S. R. Sahoo, A. Das, J. Ahmed, S. P. and S. K. Mandal, *Chem. Sci*., 2020, **11**, 1848.

6. NMR spectra

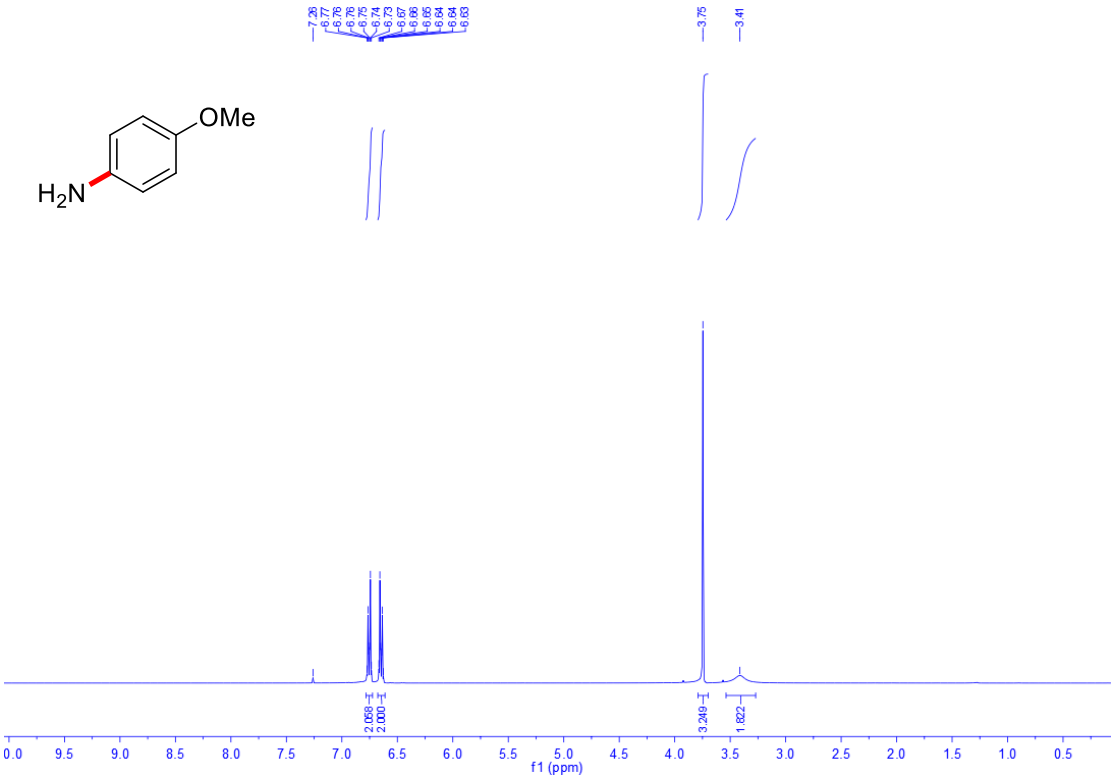

Figure S5. ^{1}H NMR (400 MHz, $CDCl_3$, 20 °C) of **2a**

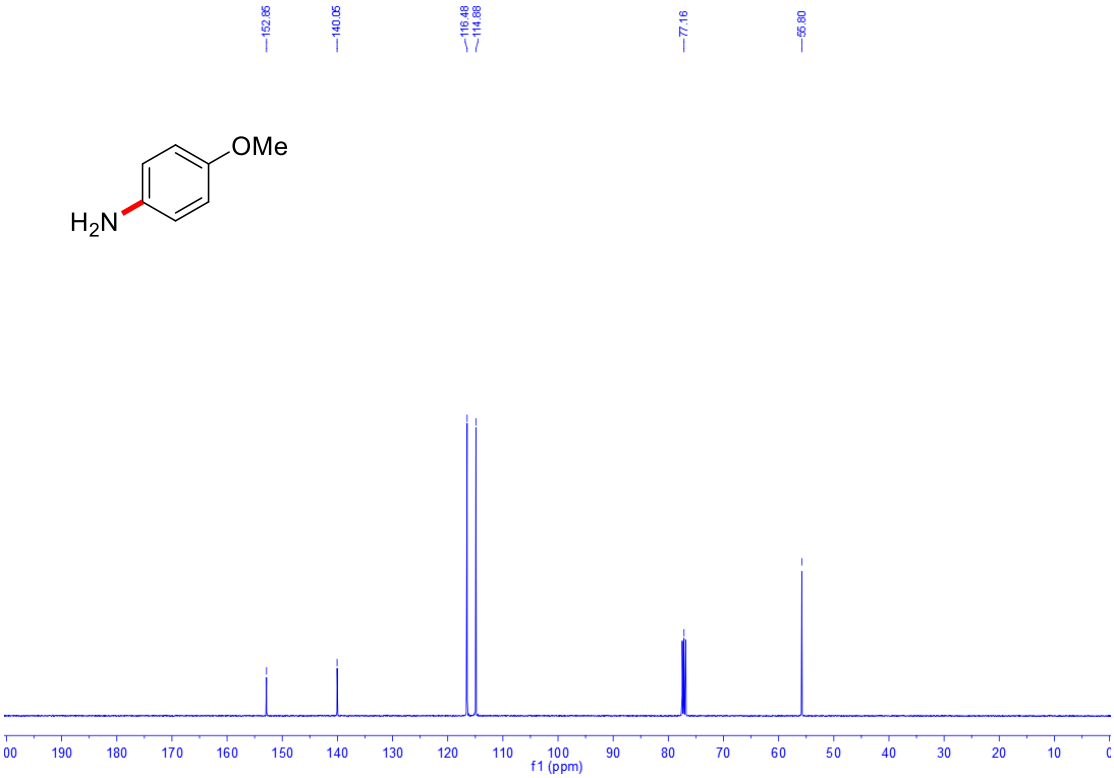

Figure S6. $^{13}C\{^{1}H\}$ (101 MHz, $CDCl_3$, 20 °C) of **2a**

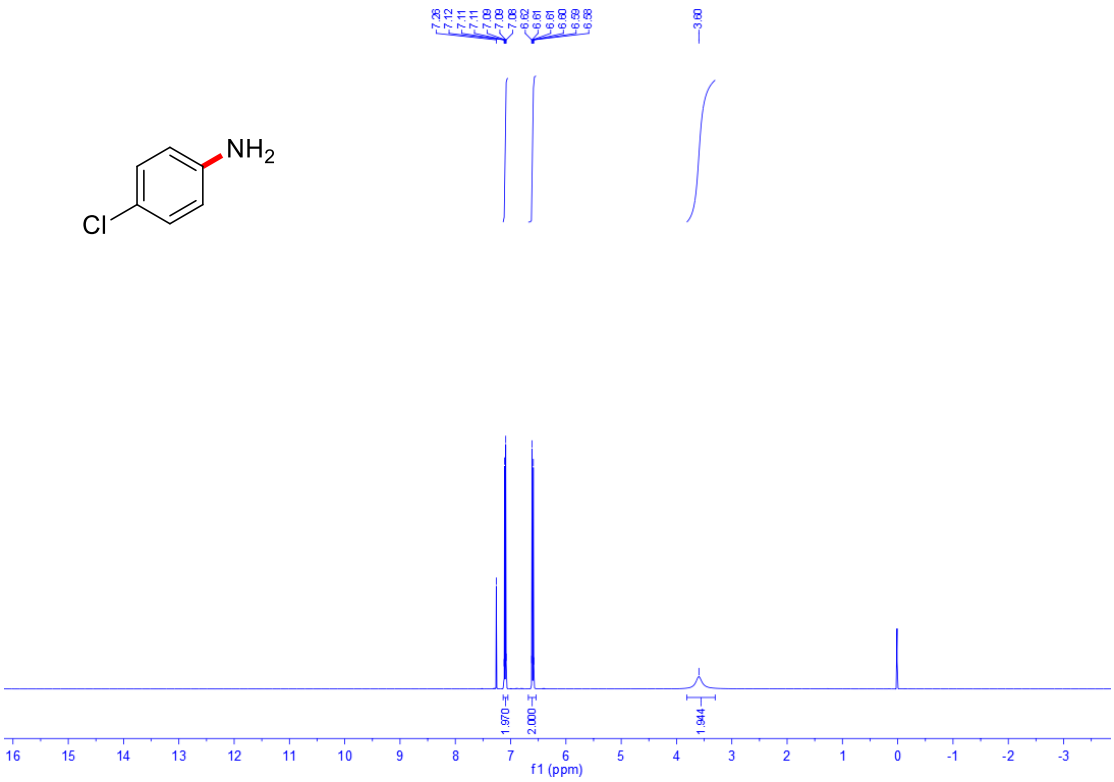

Figure S7. ^{1}H NMR (400 MHz, $CDCl_3$, 20 °C) of **2c**

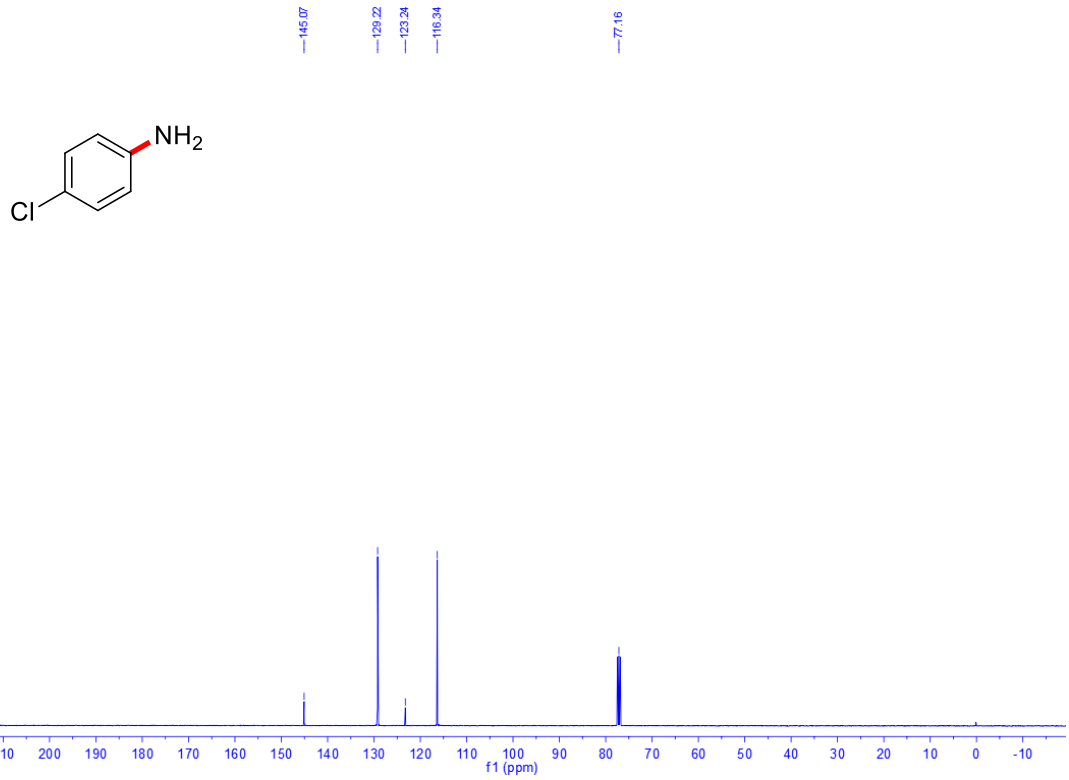

Figure S8. ^{13}C{^{1}H} (101 MHz, $CDCl_3$, 20 °C) of **2c**

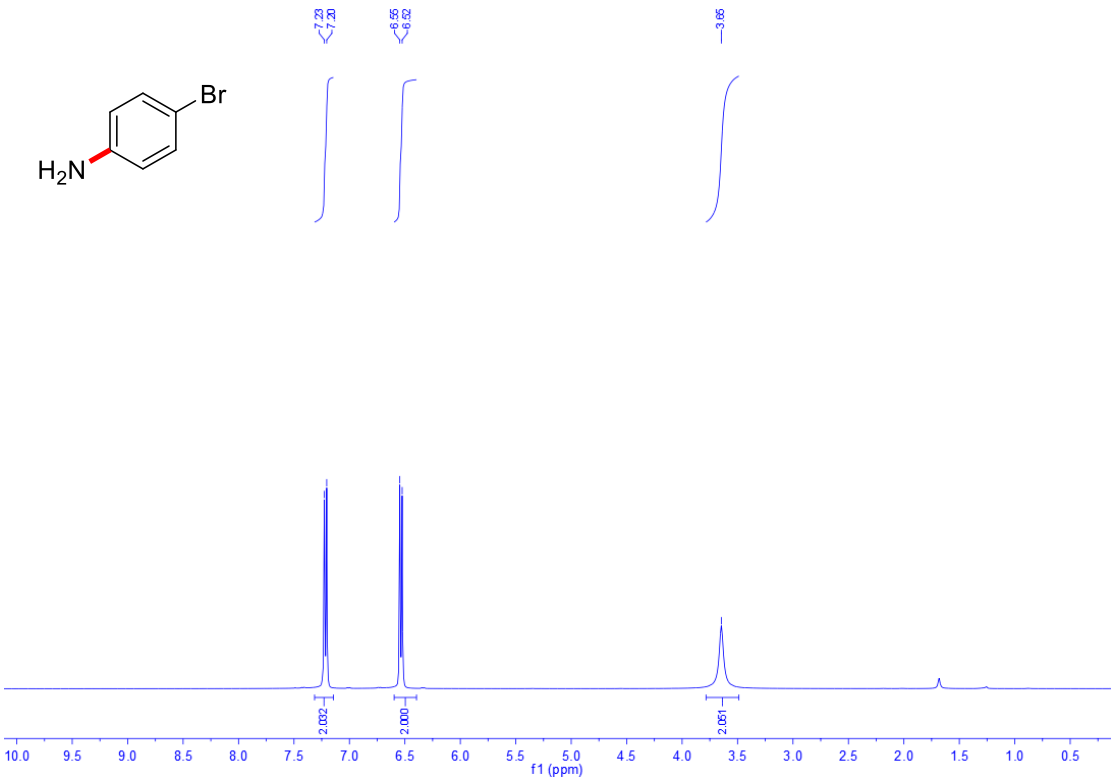

Figure S9. ^{1}H NMR (400 MHz, $CDCl_3$, 20 °C) of **2d**

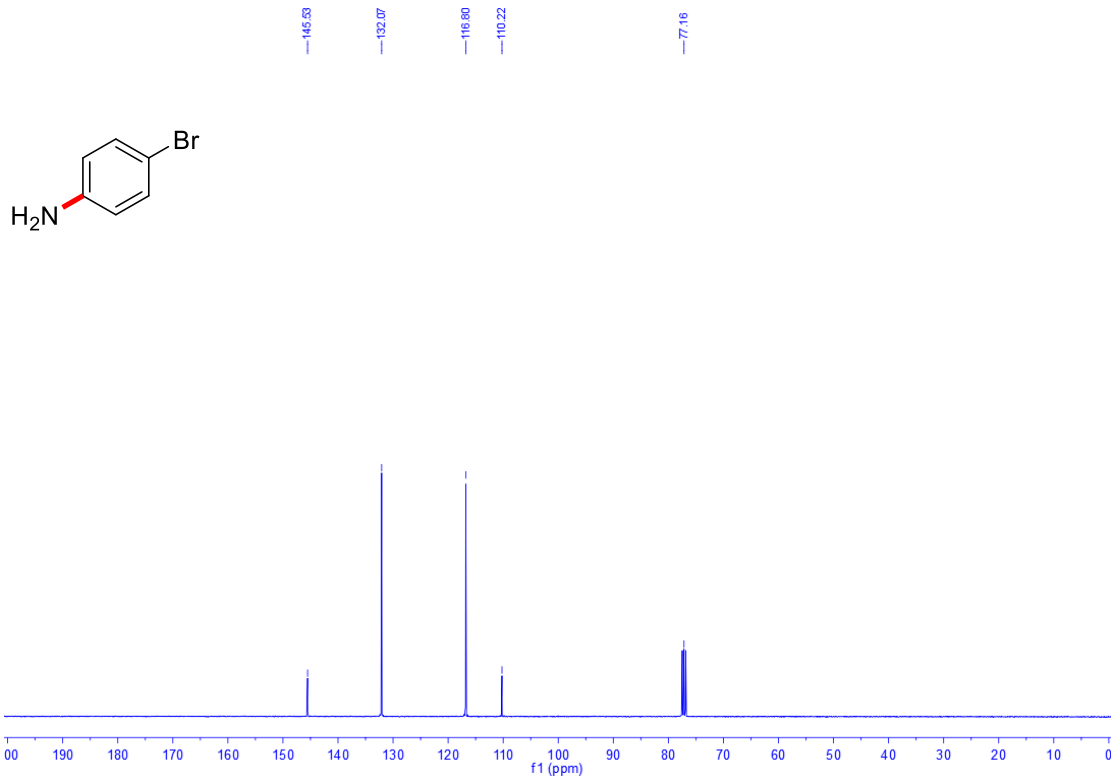

Figure S10. ^{13}C{^{1}H} (101 MHz, $CDCl_3$, 20 °C) of **2d**

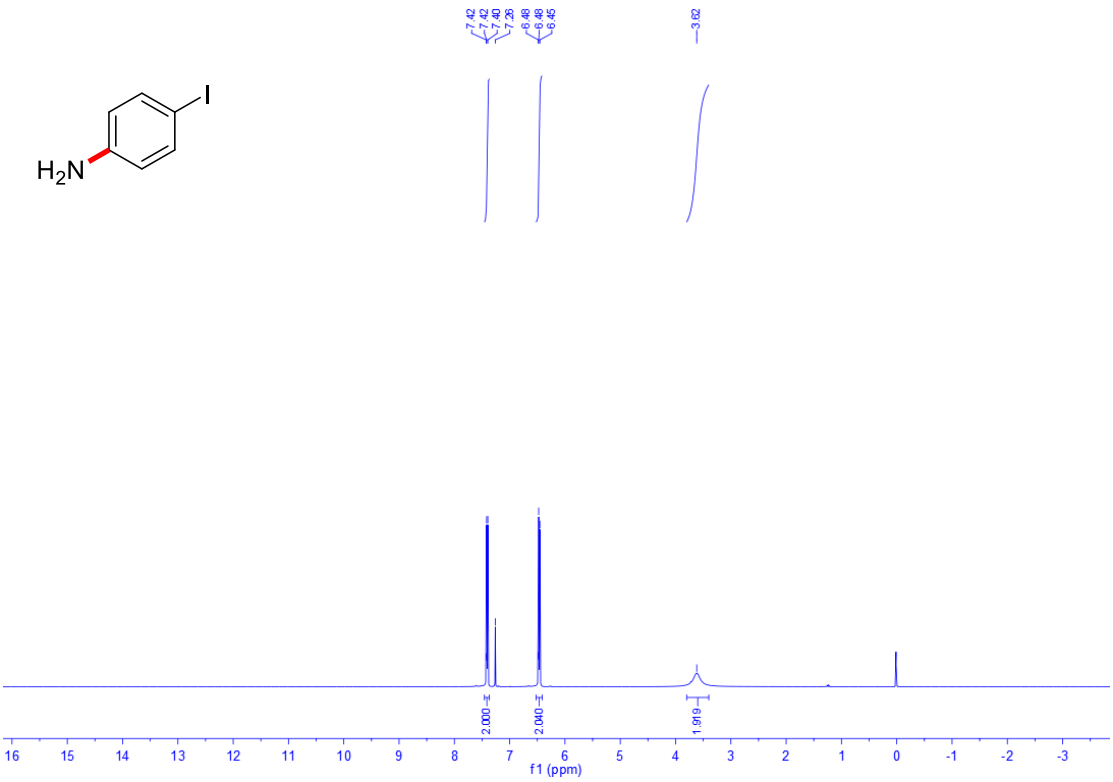

Figure S11. ^{1}H NMR (400 MHz, $CDCl_3$, 20 °C) of **2e**

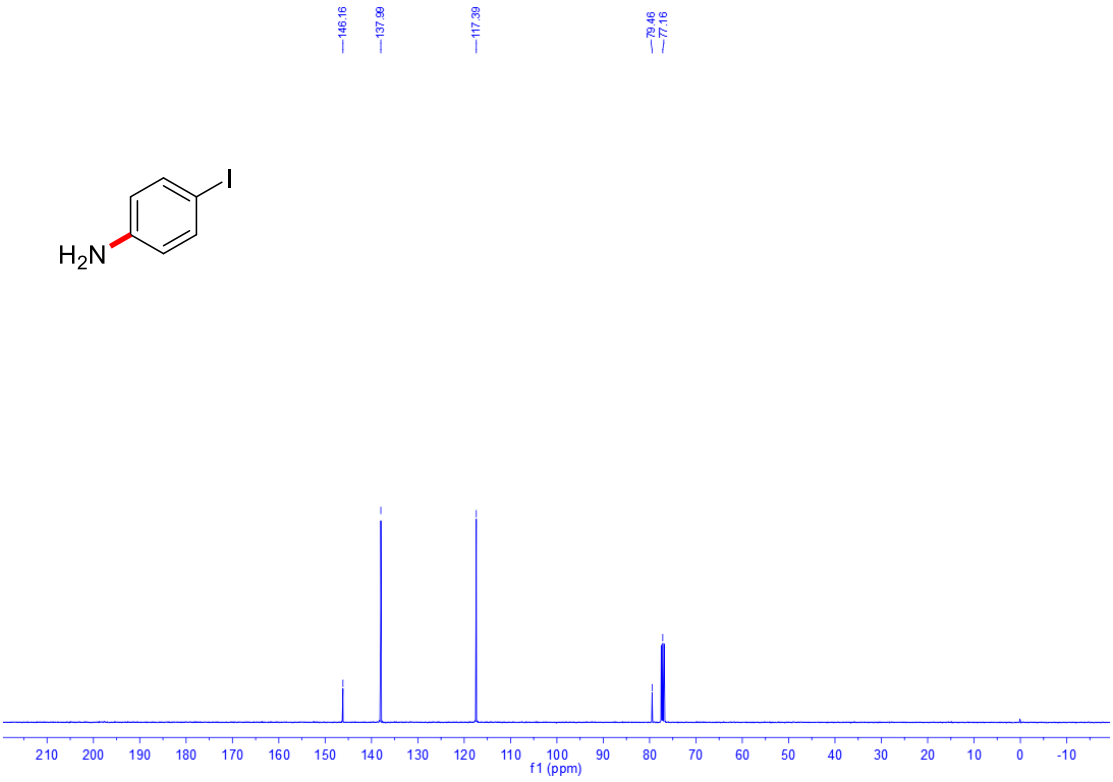

Figure S12. $^{13}C\{^{1}H\}$ (101 MHz, $CDCl_3$, 20 °C) of **2e**

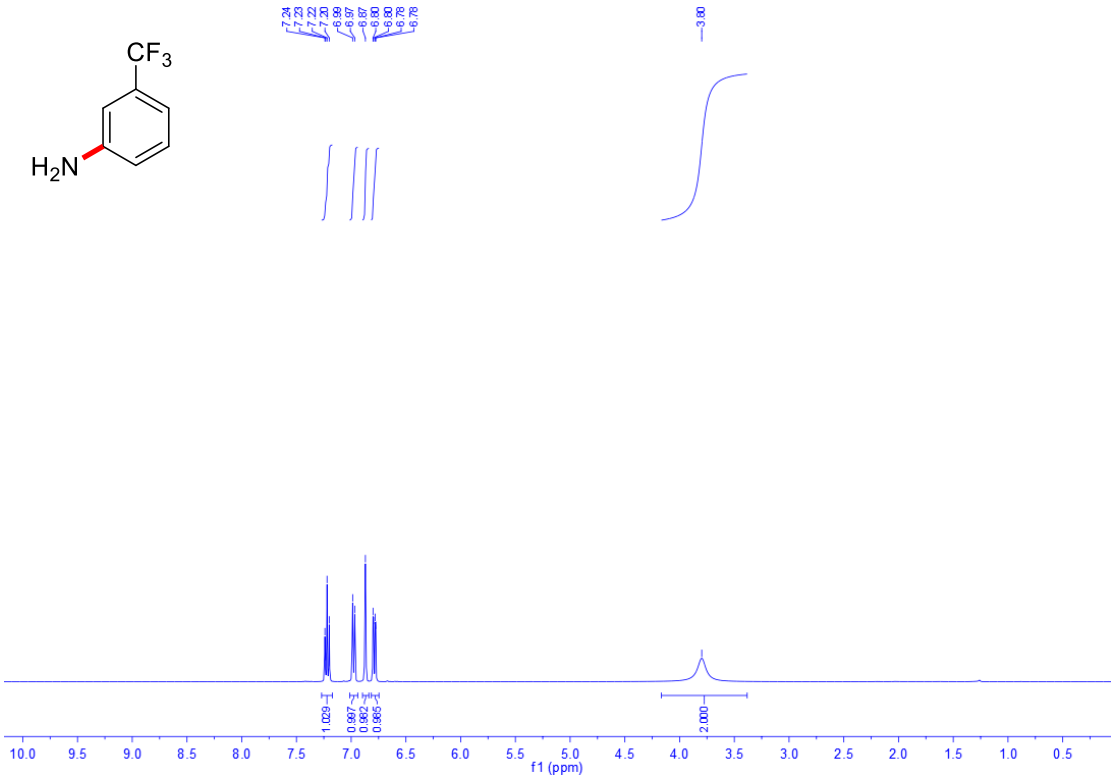

Figure S13. ^{1}H NMR (400 MHz, $CDCl_3$, 20 ^{o}C) of **2f**

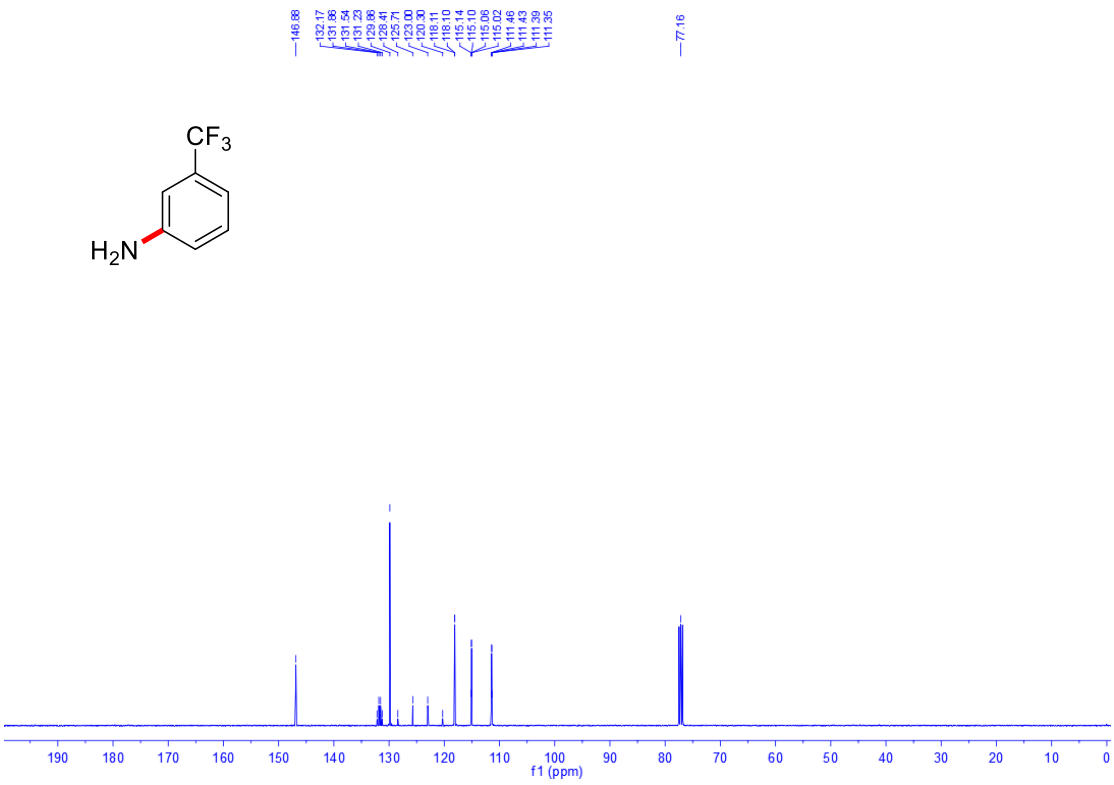

Figure S14. ^{13}C{^{1}H} (101 MHz, $CDCl_3$, 20 ^{o}C) of **2f**

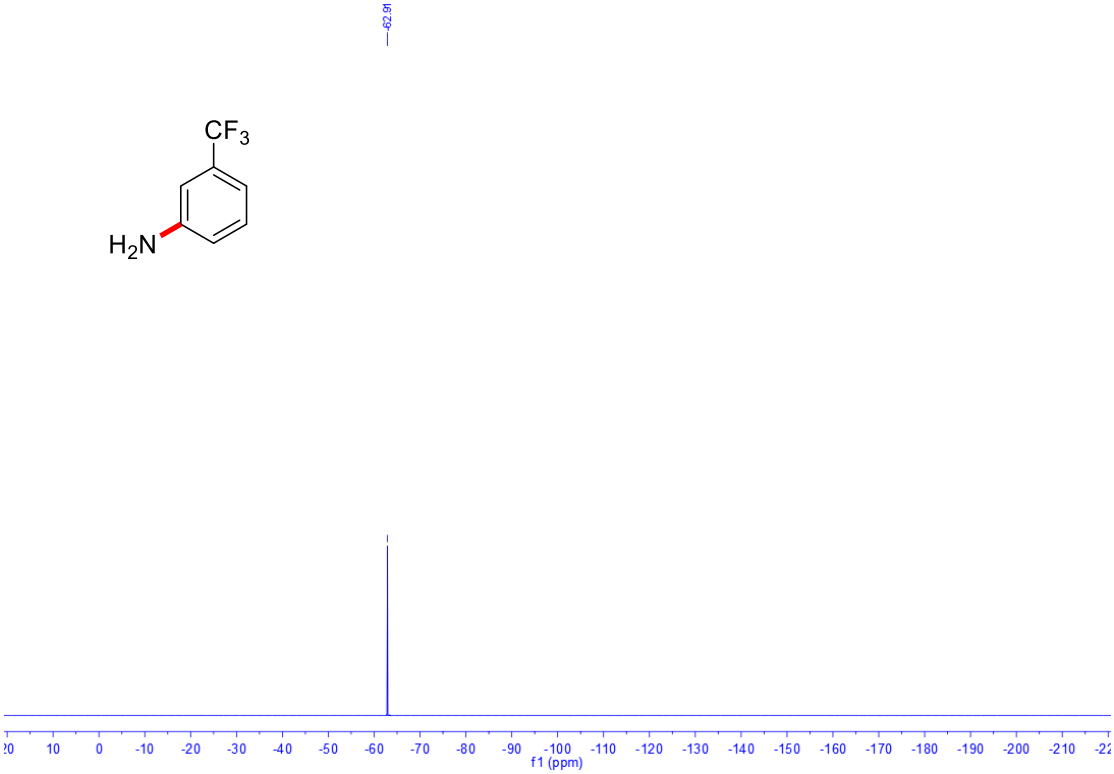

Figure S15. ^{19}F NMR (377 MHz, $CDCl_3$, 20 °C) of **2f**

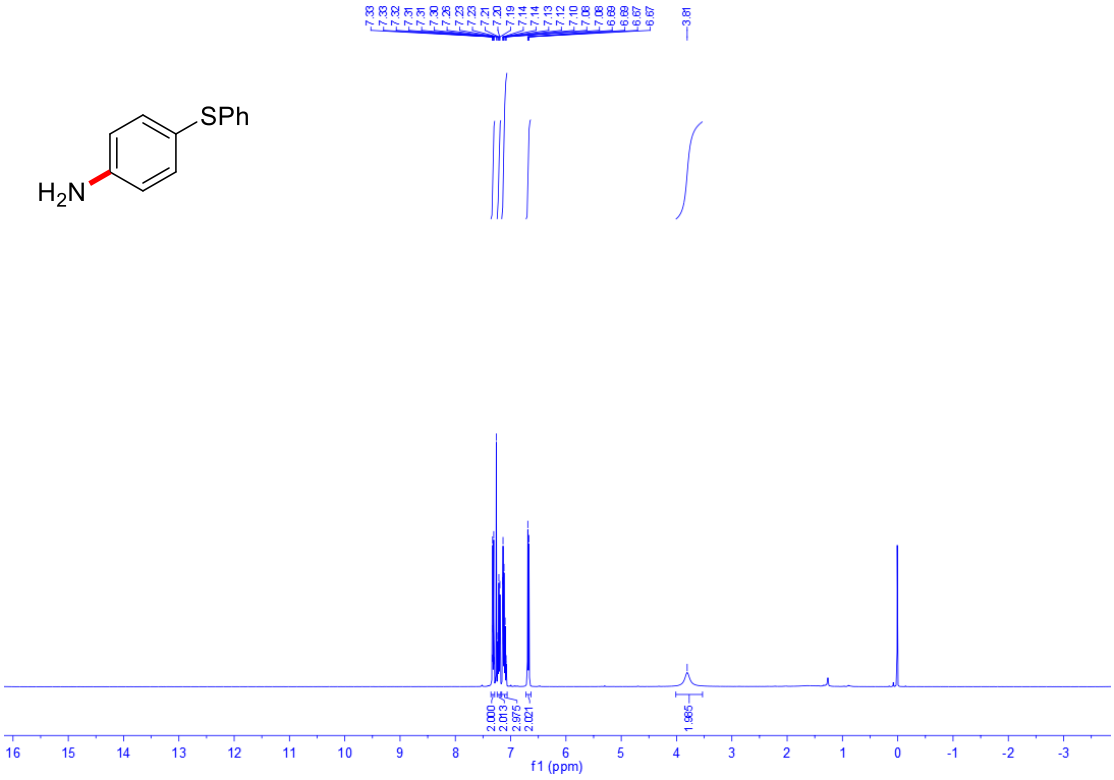

Figure S16. ^{1}H NMR (400 MHz, $CDCl_3$, 20 °C) of **2g**

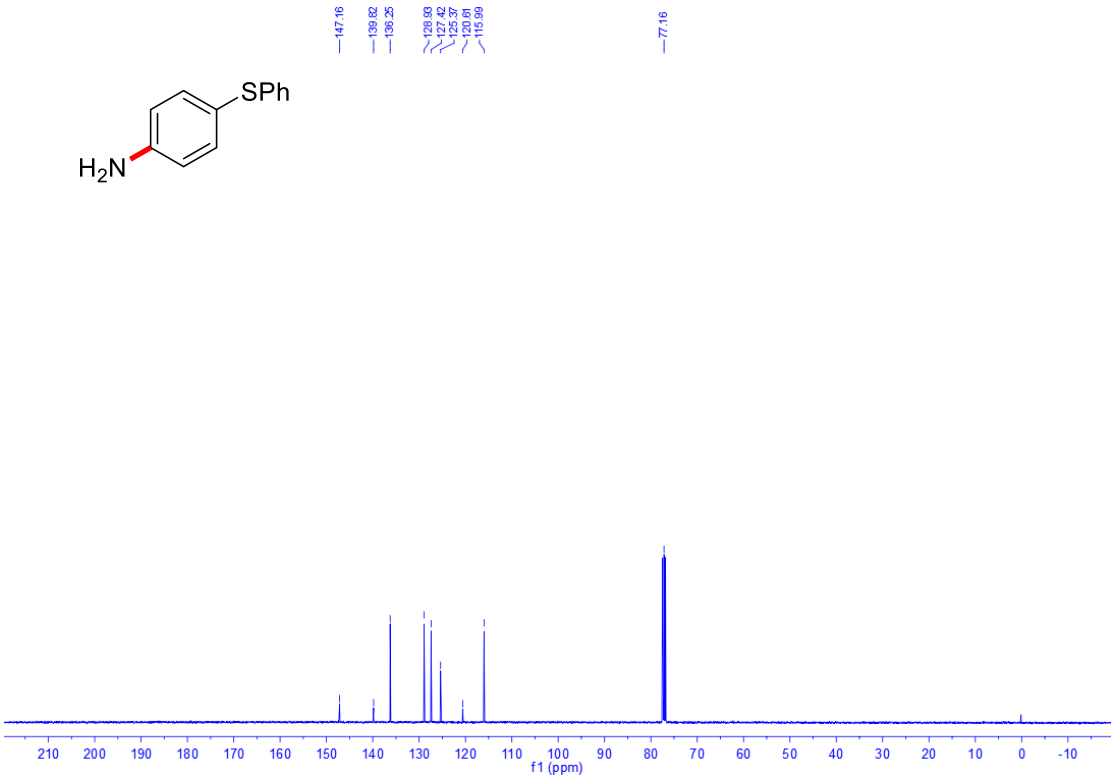

Figure S17. $^{13}C\{^{1}H\}$ (101 MHz, $CDCl_3$, 20 °C) of **2g**

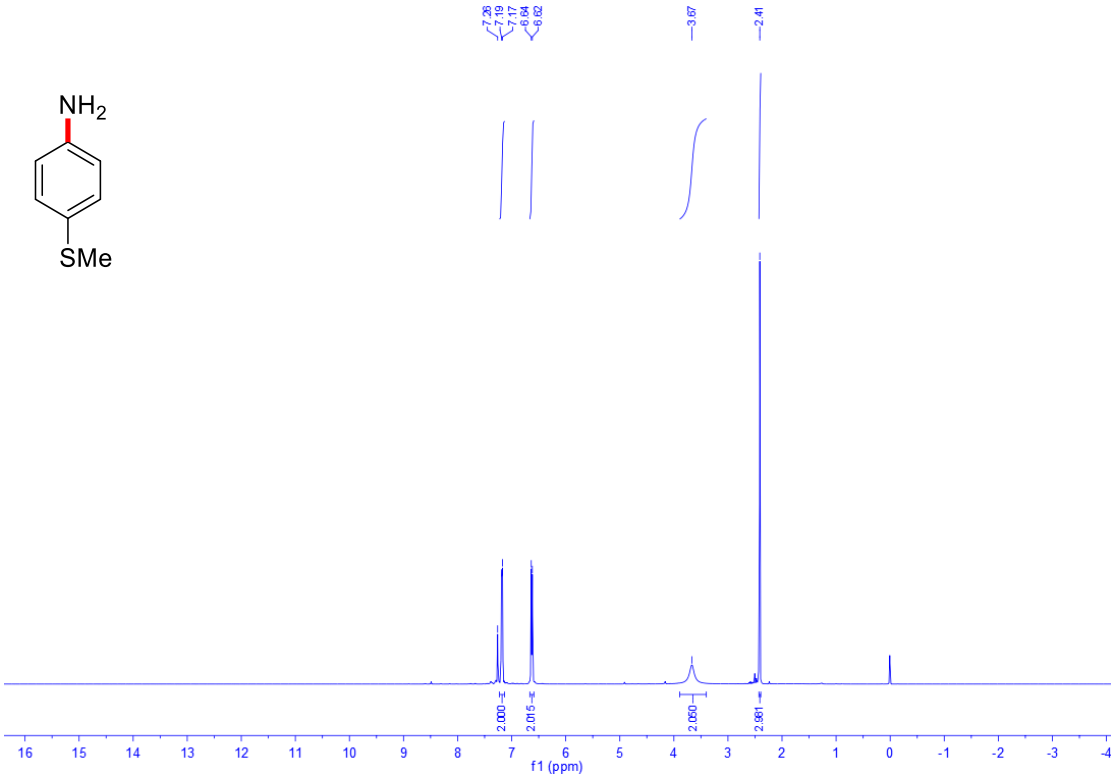

Figure S18. ^{1}H NMR (400 MHz, $CDCl_3$, 20 °C) of **2h**

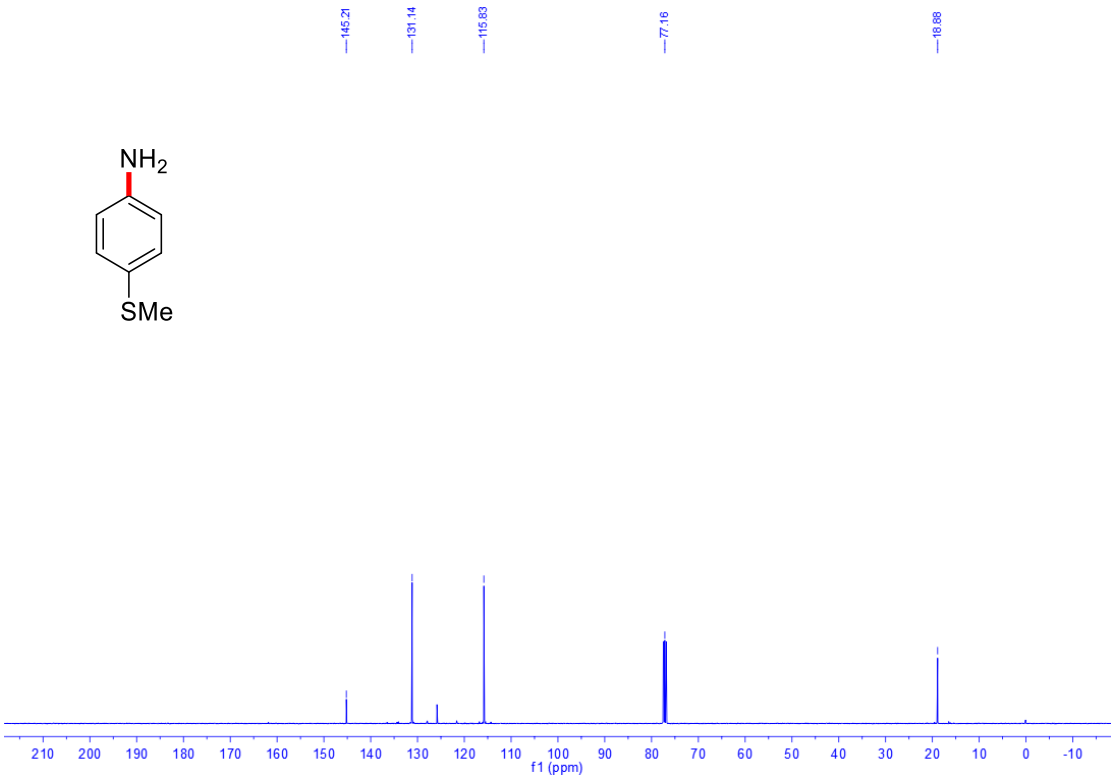

Figure S19. $^{13}C\{^{1}H\}$ (101 MHz, $CDCl_3$, 20 °C) of **2h**

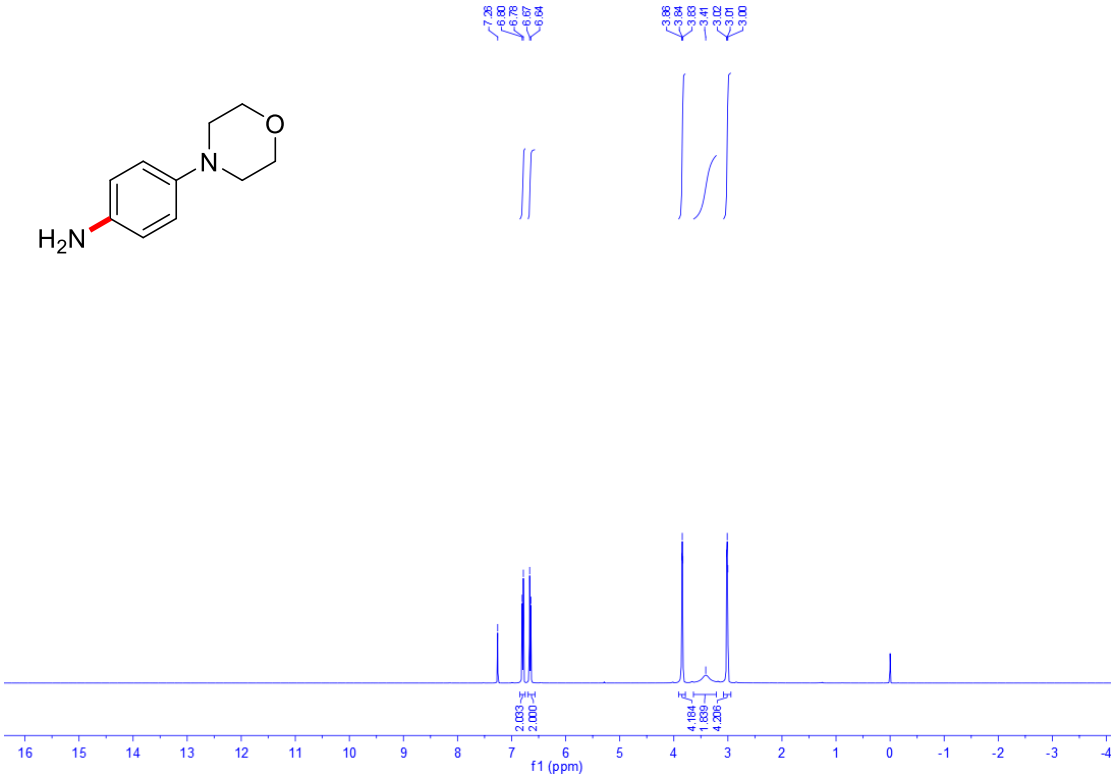

Figure S20. ^{1}H NMR (400 MHz, $CDCl_3$, 20 °C) of **2i**

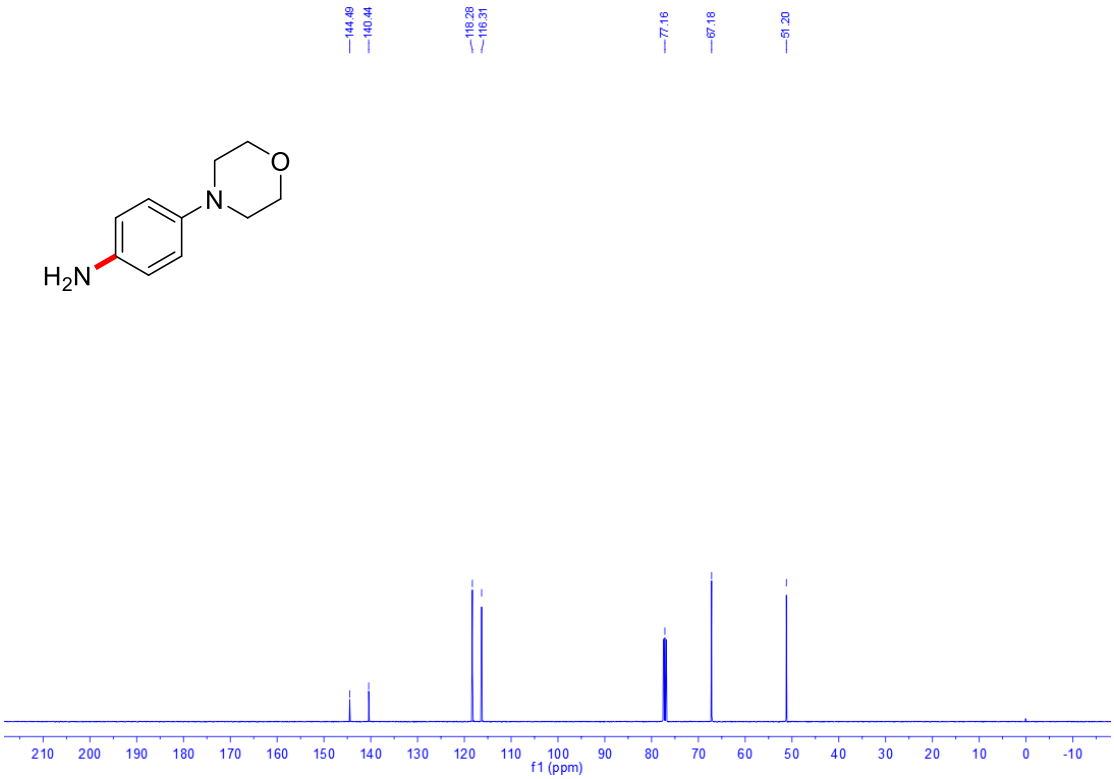

Figure S21. $^{13}C\{^{1}H\}$ (101 MHz, $CDCl_3$, 20 °C) of **2i**

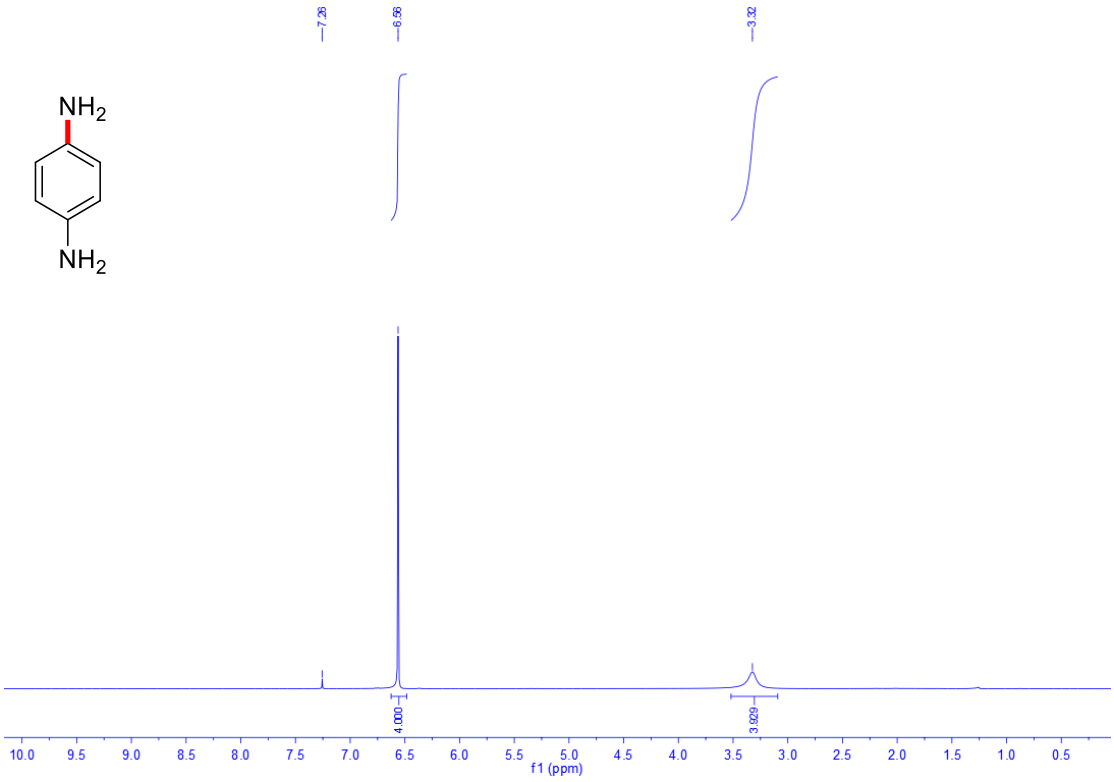

Figure S22. ^{1}H NMR (400 MHz, $CDCl_3$, 20 °C) of **2j**

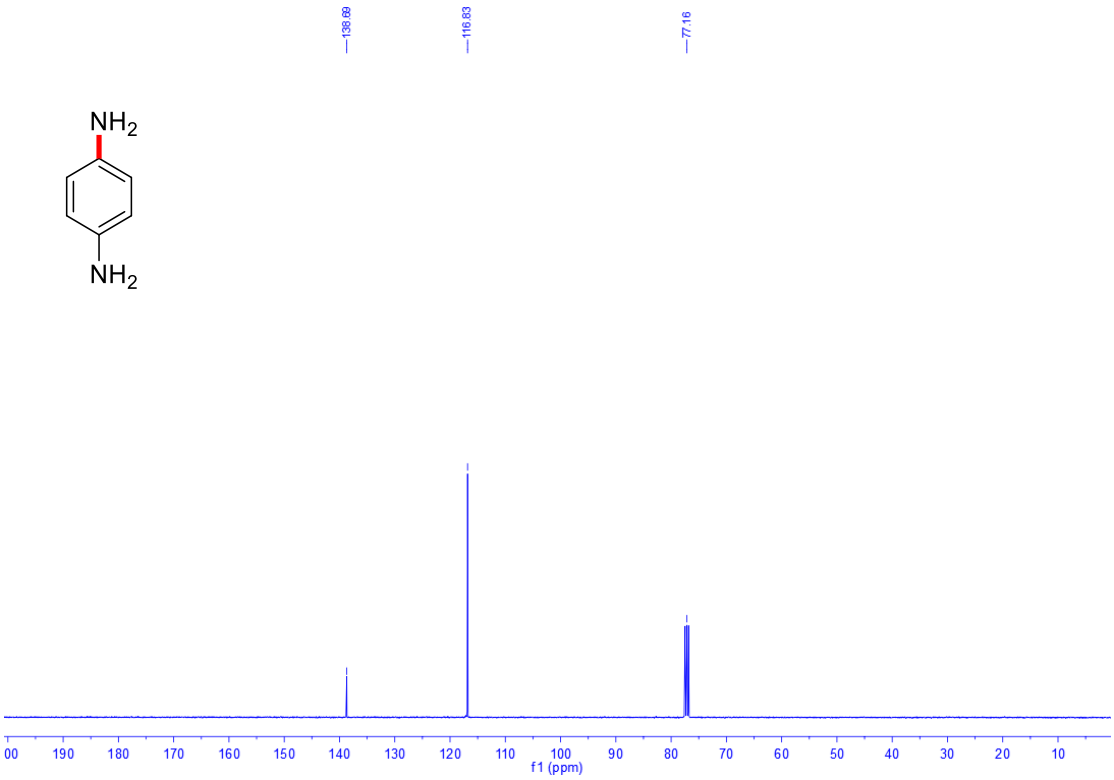

Figure S23. $^{13}C\{^{1}H\}$ (101 MHz, $CDCl_3$, 20 °C) of **2j**

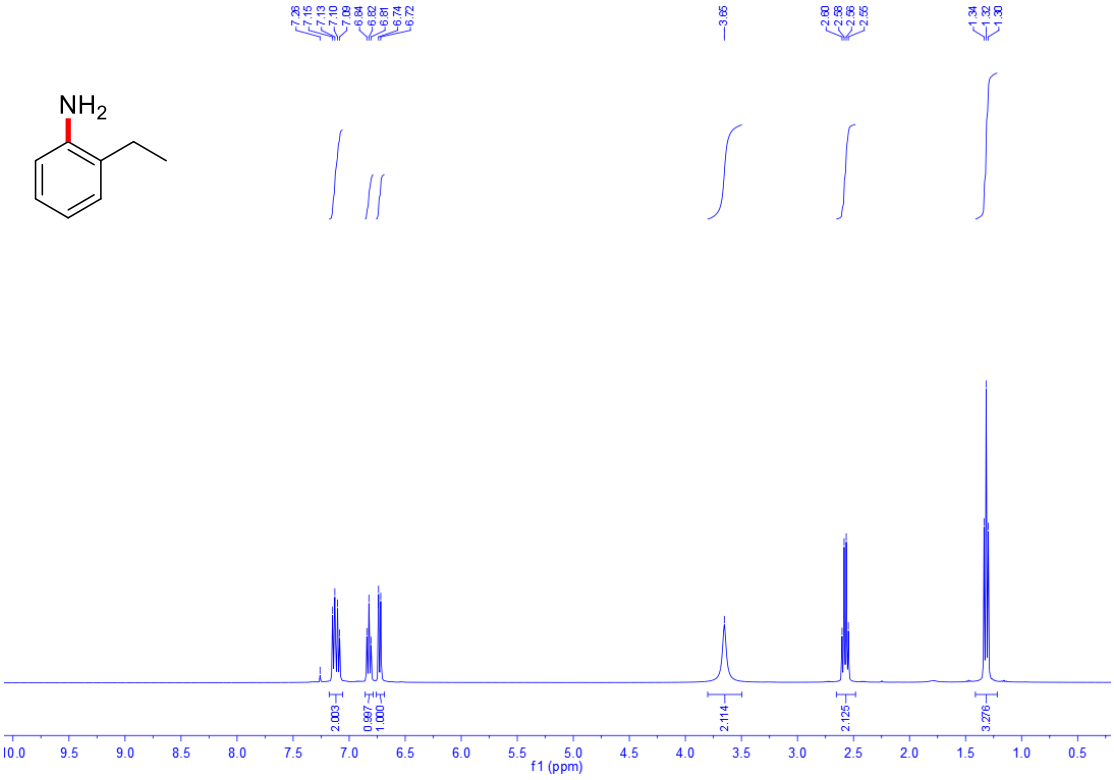

Figure S24. ^{1}H NMR (400 MHz, $CDCl_3$, 20 °C) of **2k**

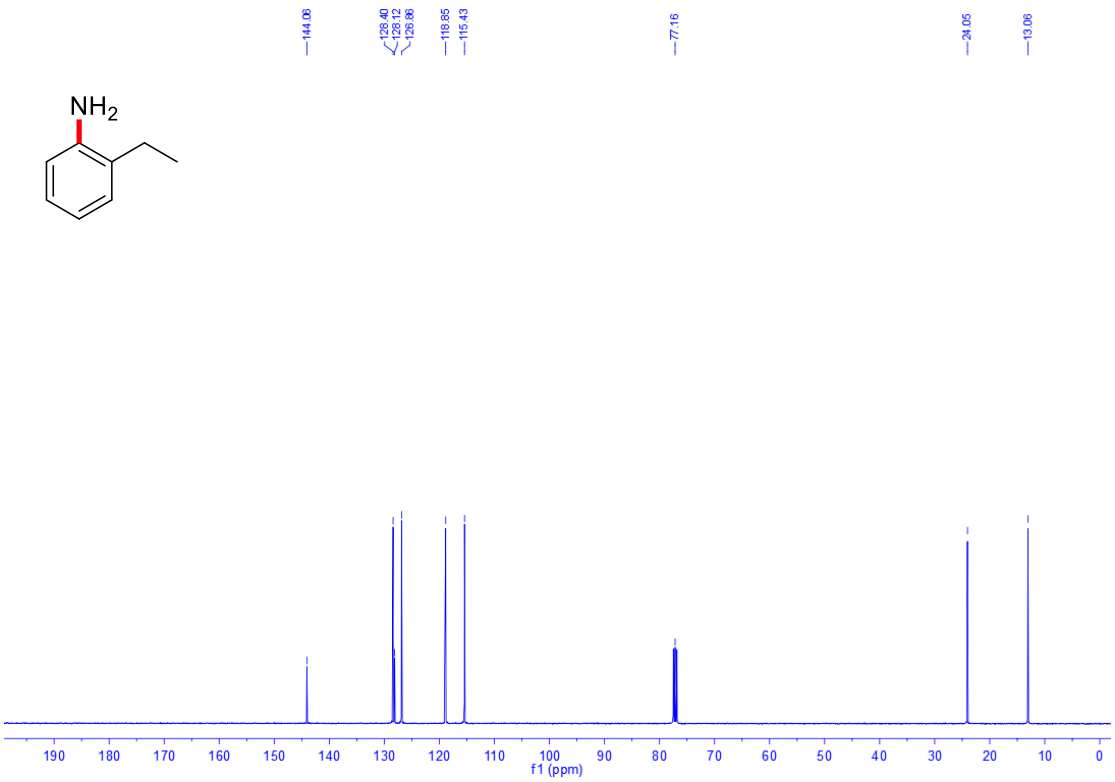

Figure S25. $^{13}C\{^{1}H\}$ (101 MHz, $CDCl_3$, 20 °C) of **2k**

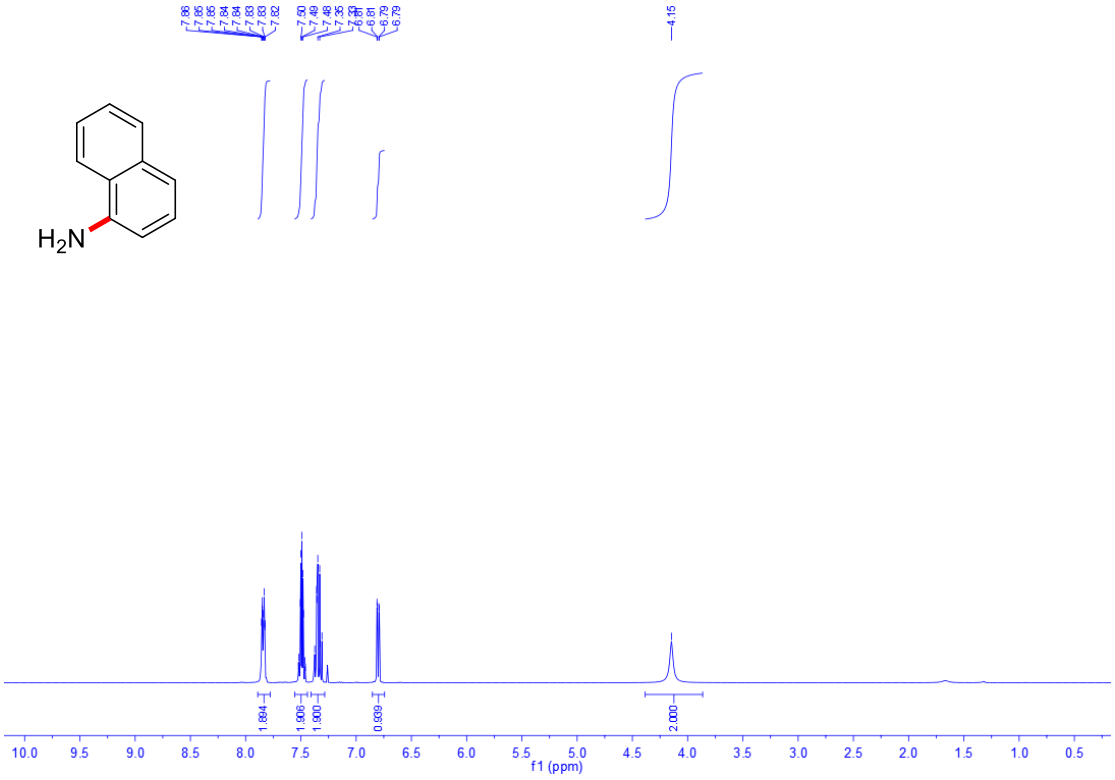

Figure S26. ^{1}H NMR (400 MHz, $CDCl_3$, 20 °C) of **2l**

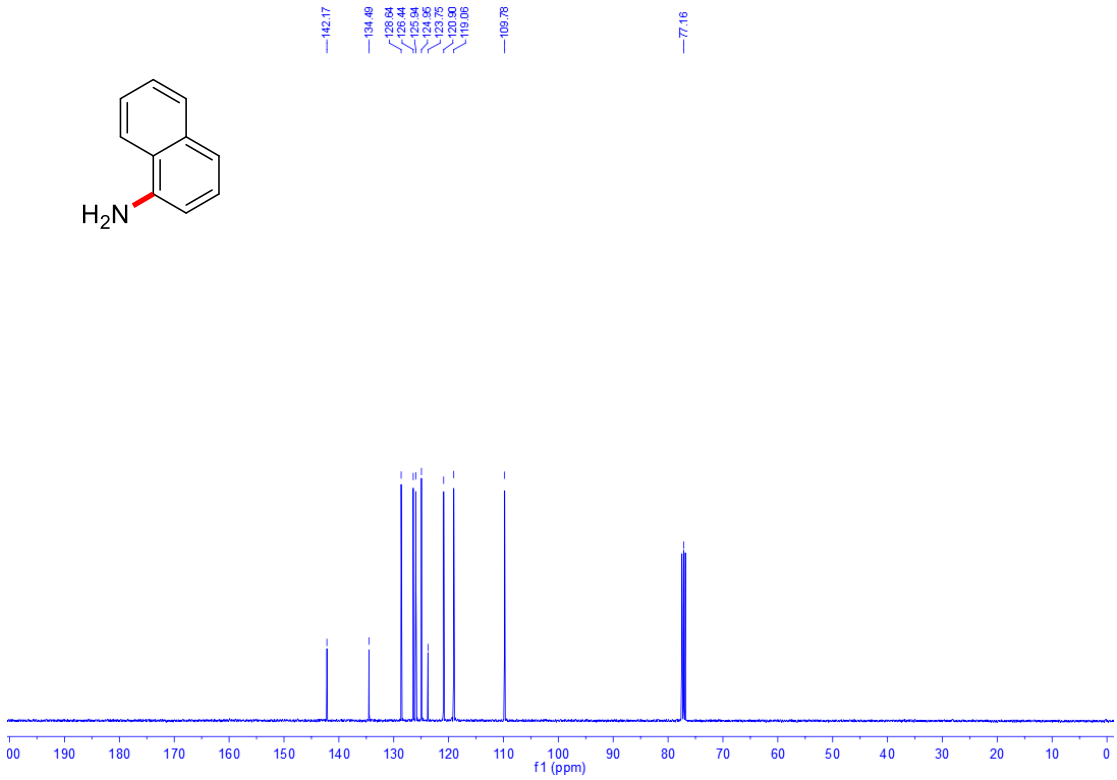

Figure S27. $^{13}C\{^{1}H\}$ (101 MHz, $CDCl_3$, 20 °C) of **2l**

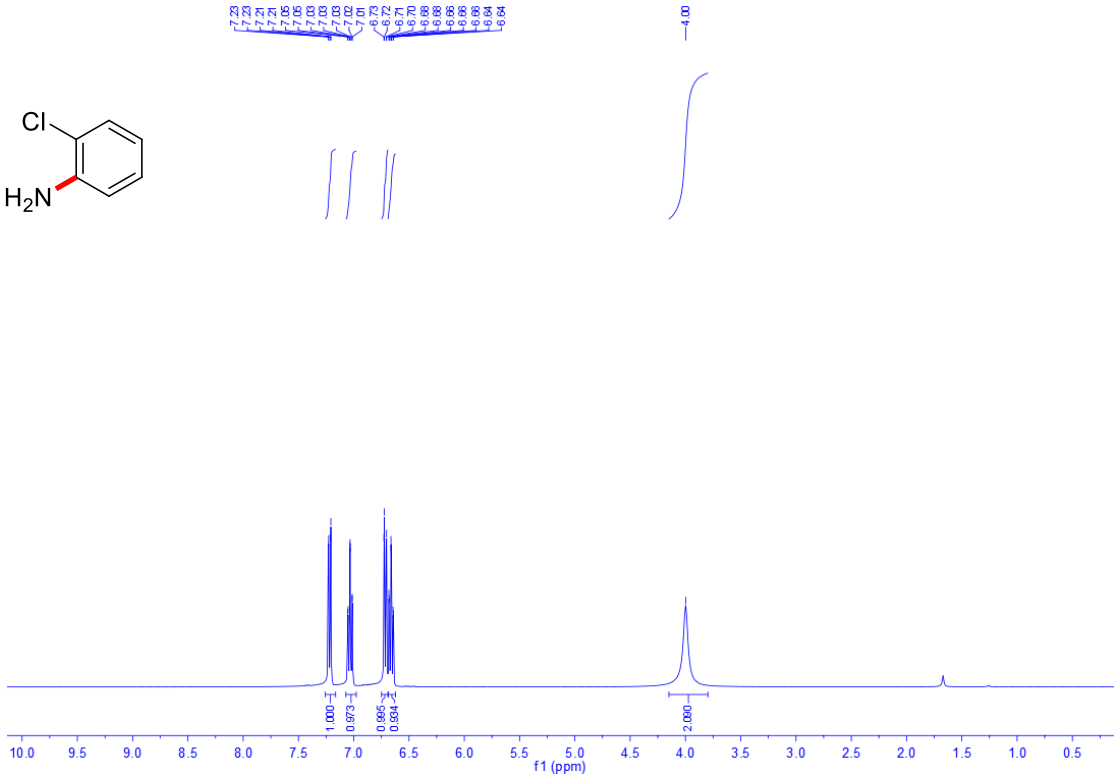

Figure S28. ^{1}H NMR (400 MHz, $CDCl_3$, 20 °C) of **2m**

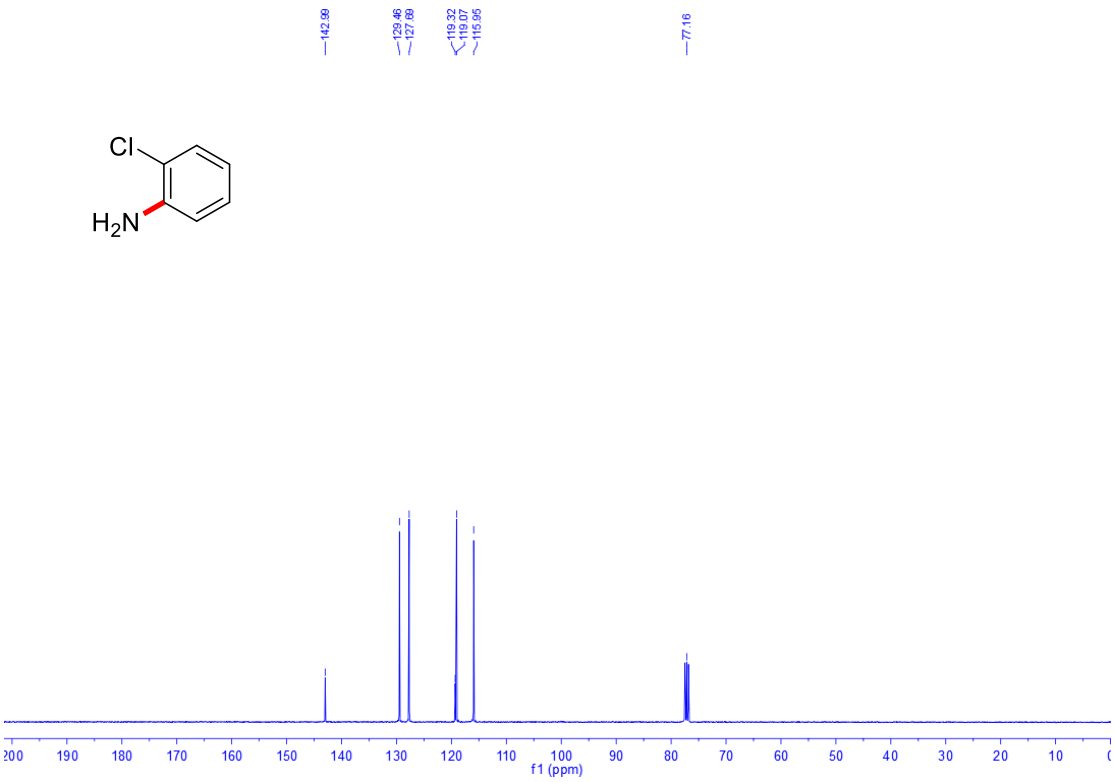

Figure S29. $^{13}C\{^{1}H\}$ (101 MHz, $CDCl_3$, 20 °C) of **2m**

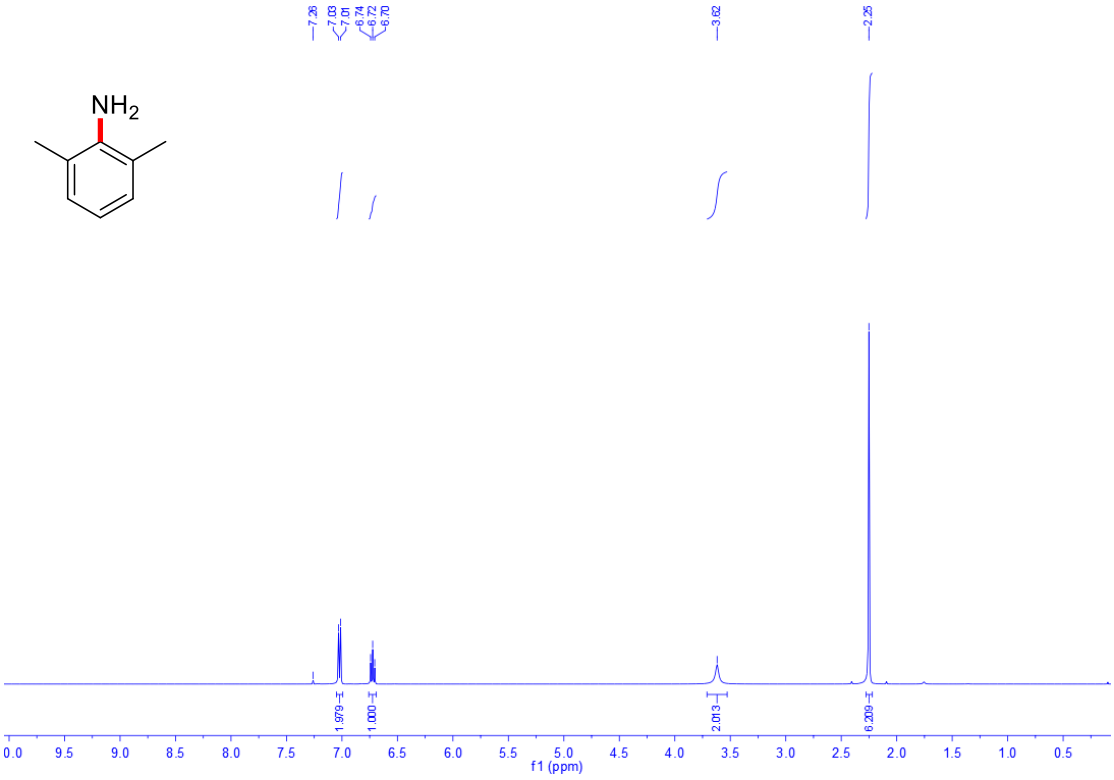

Figure S30. ^{1}H NMR (400 MHz, $CDCl_3$, 20 °C) of **2n**

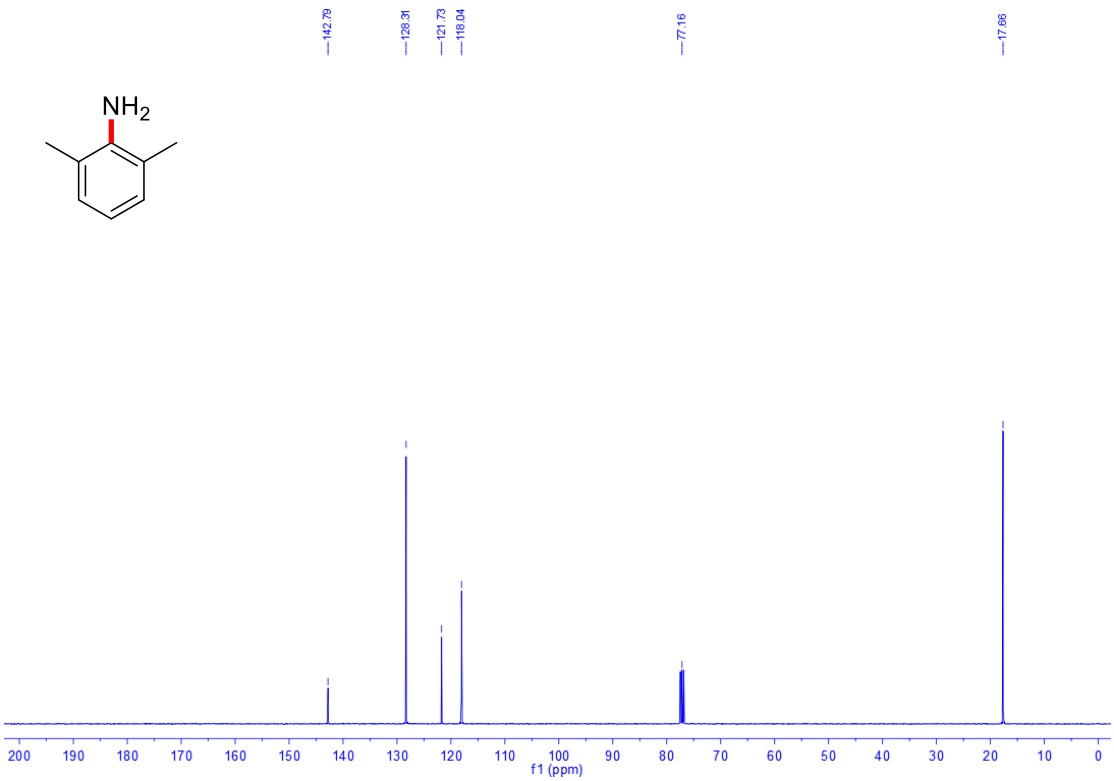

Figure S31. $^{13}C\{^{1}H\}$ (101 MHz, $CDCl_3$, 20 °C) of **2n**

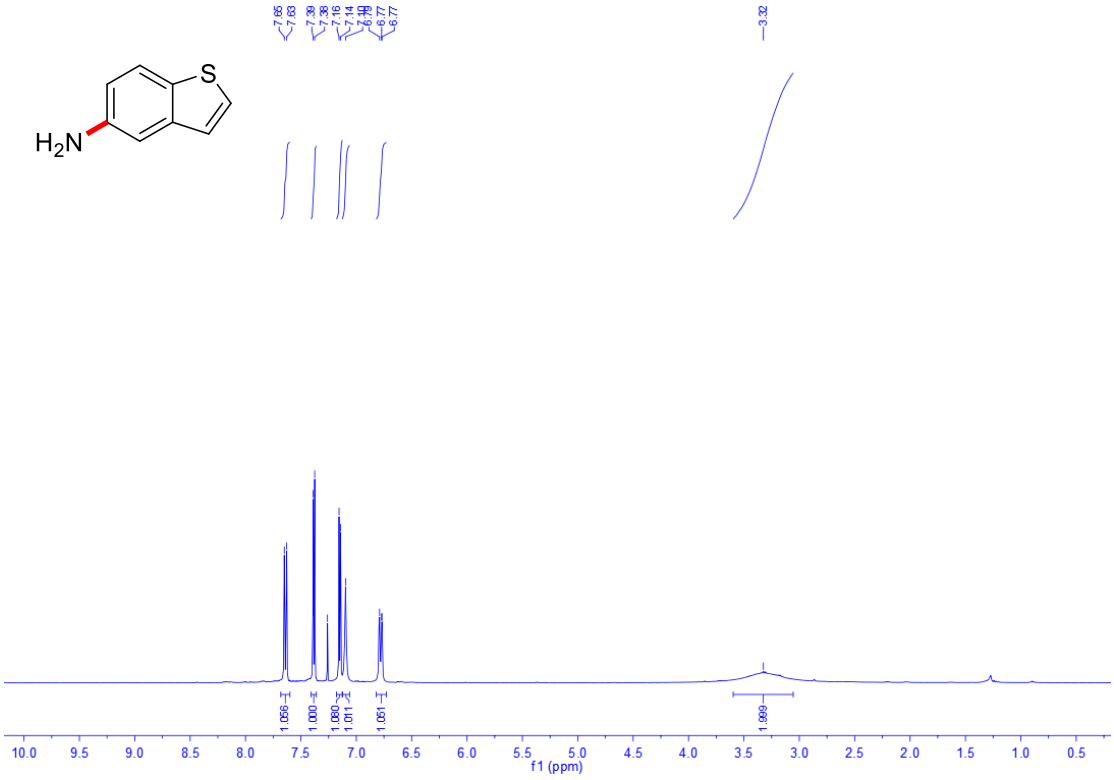

Figure S32. ^{1}H NMR (400 MHz, $CDCl_3$, 20 °C) of **2o**

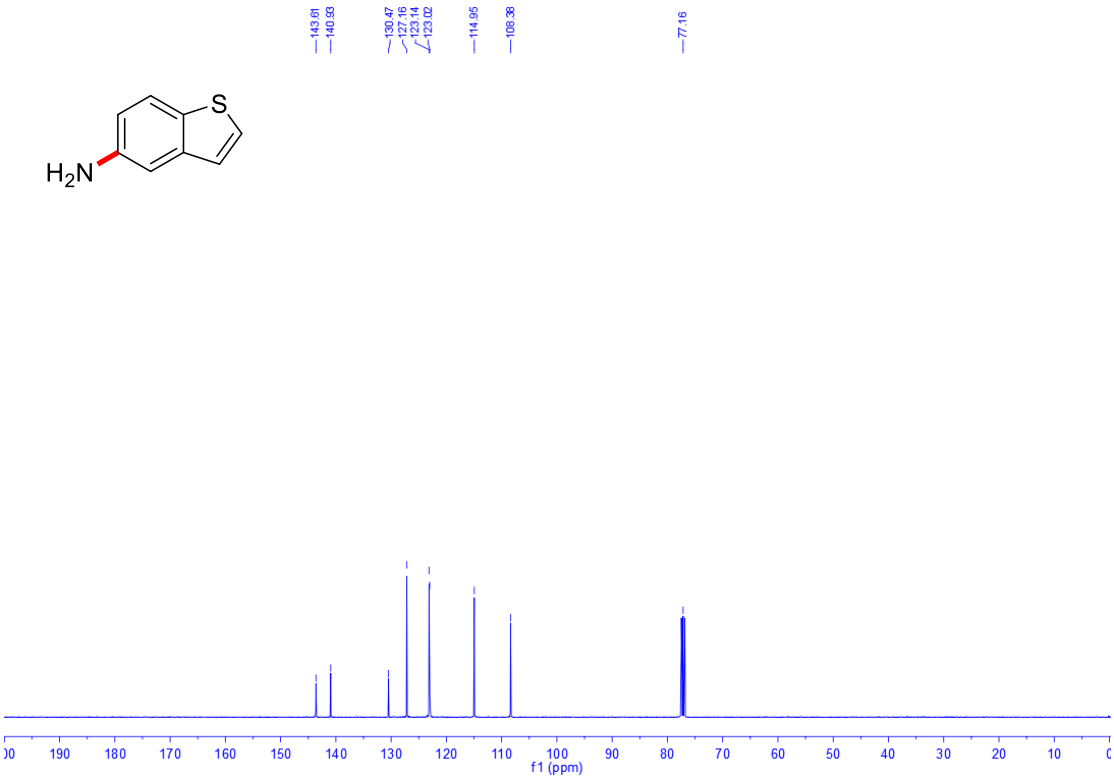

Figure S33. $^{13}C\{^{1}H\}$ (101 MHz, $CDCl_3$, 20 °C) of **2o**

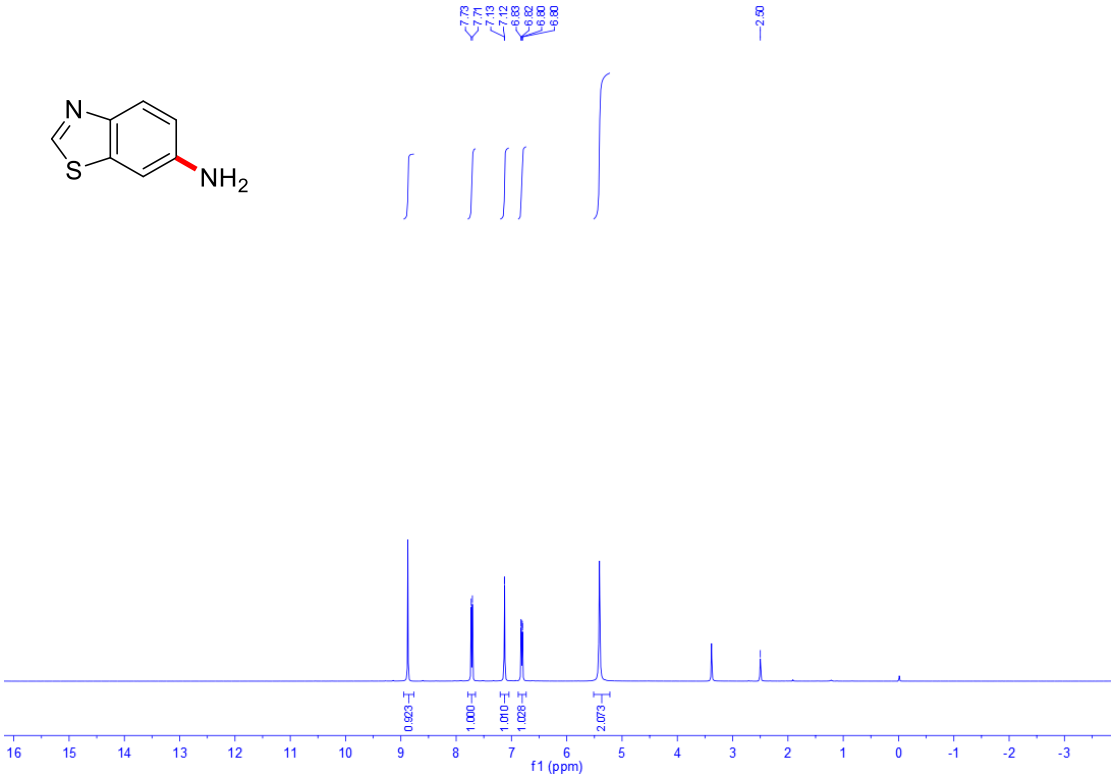

Figure S34. ^{1}H NMR (400 MHz, DMSO-d_6, 20 °C) of **2p**

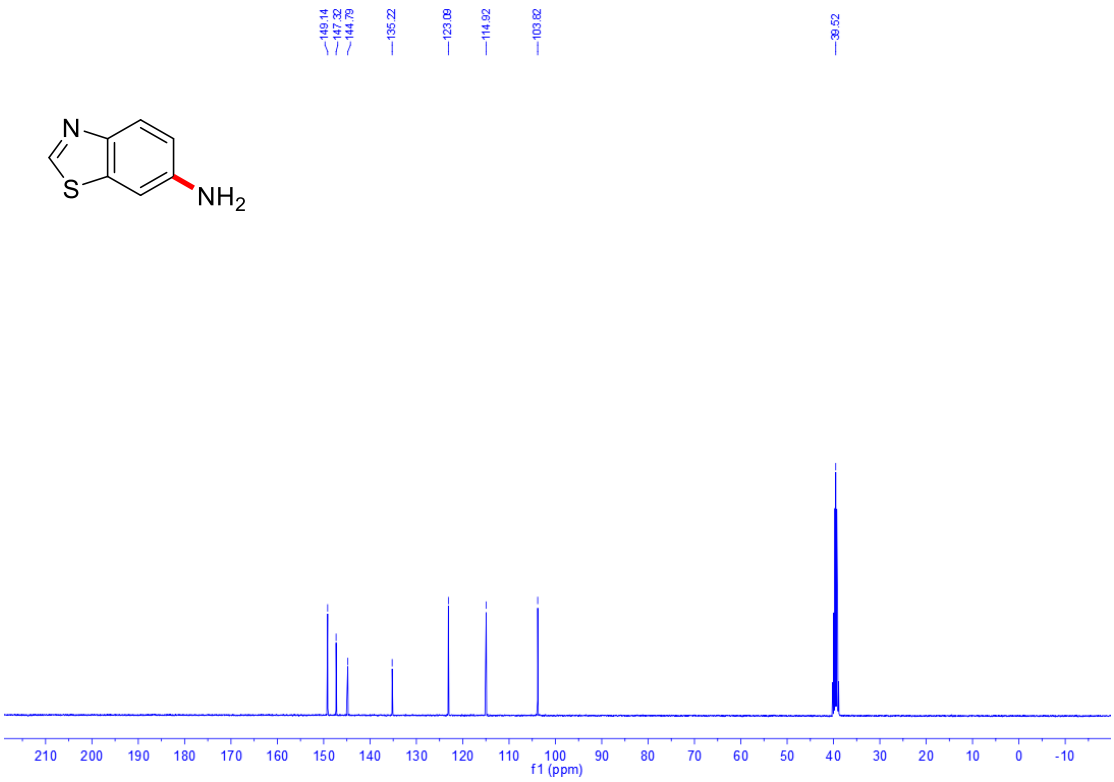

Figure S35. $^{13}C\{^{1}H\}$ (101 MHz, DMSO-d_6, 20 °C) of **2p**

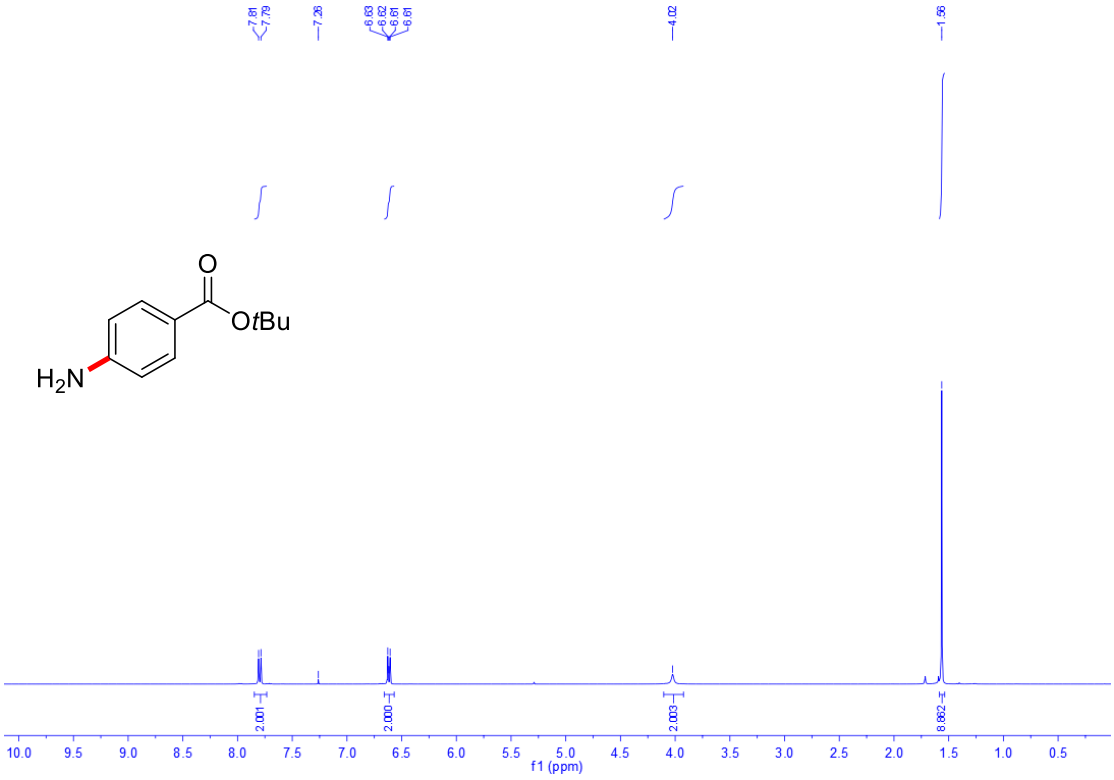

Figure S36. ^{1}H NMR (400 MHz, $CDCl_3$, 20 °C) of **2q**

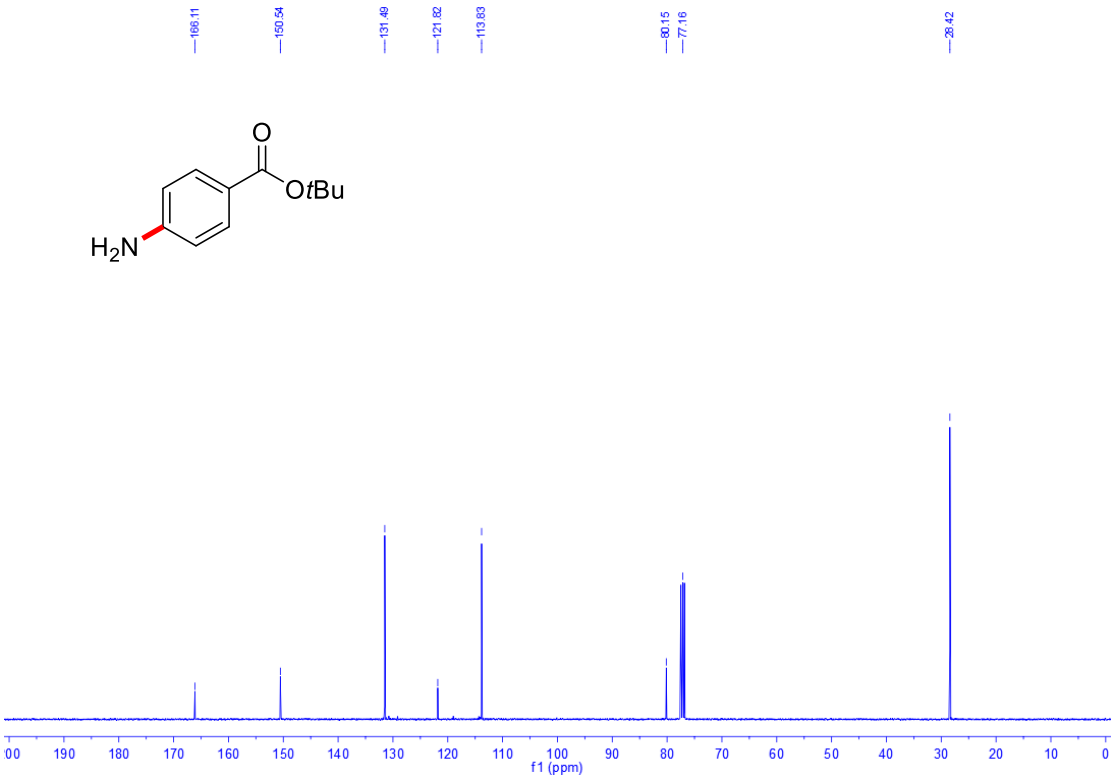

Figure S37. $^{13}C\{^{1}H\}$ (101 MHz, $CDCl_3$, 20 °C) of **2q**

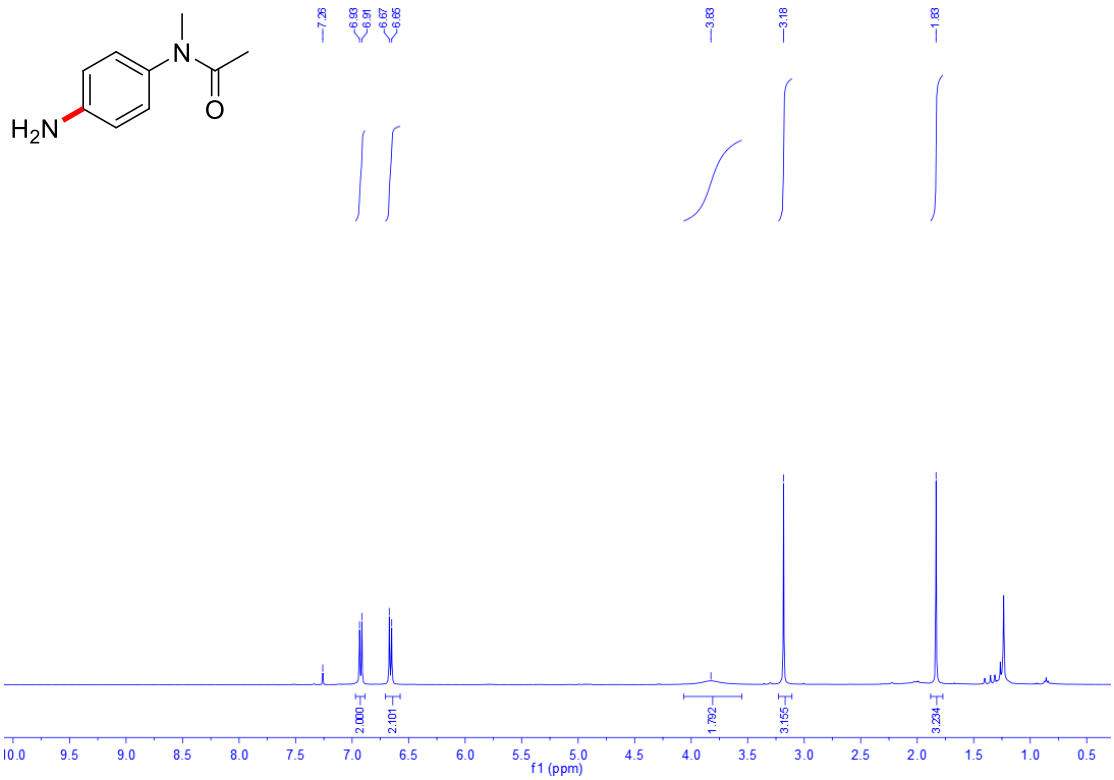

Figure S38. ^{1}H NMR (400 MHz, $CDCl_3$, 20 °C) of **2r**

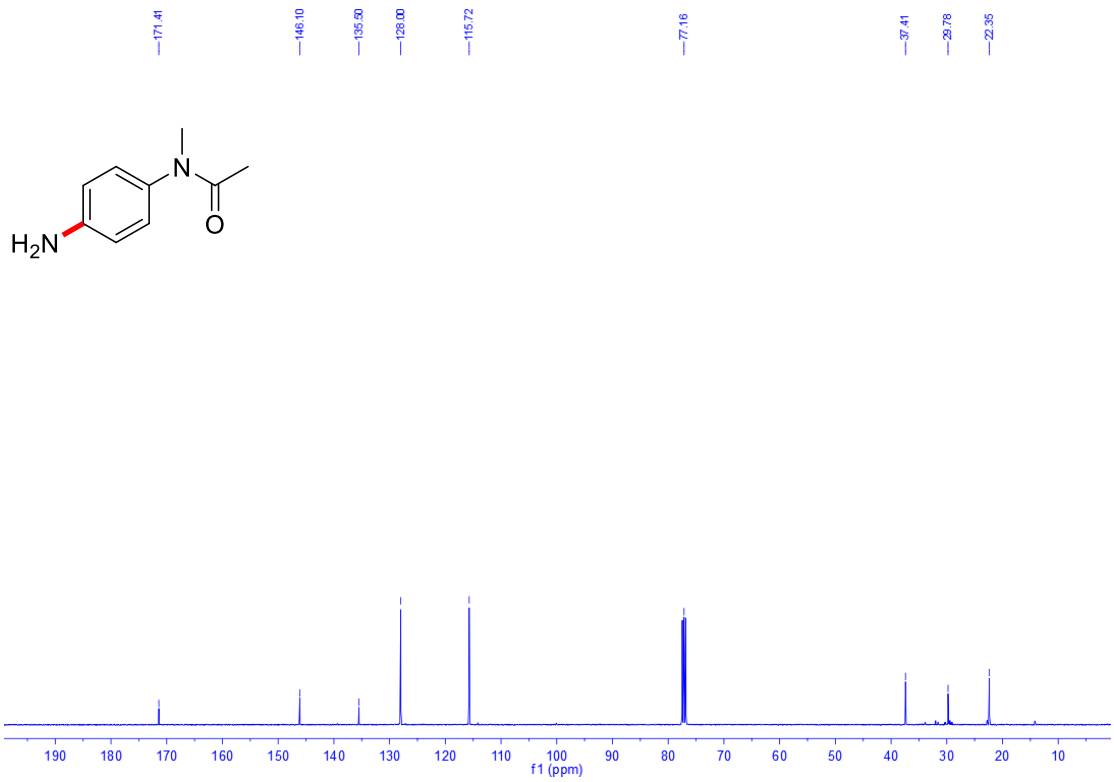

Figure S39. $^{13}C\{^{1}H\}$ (101 MHz, $CDCl_3$, 20 °C) of **2r**

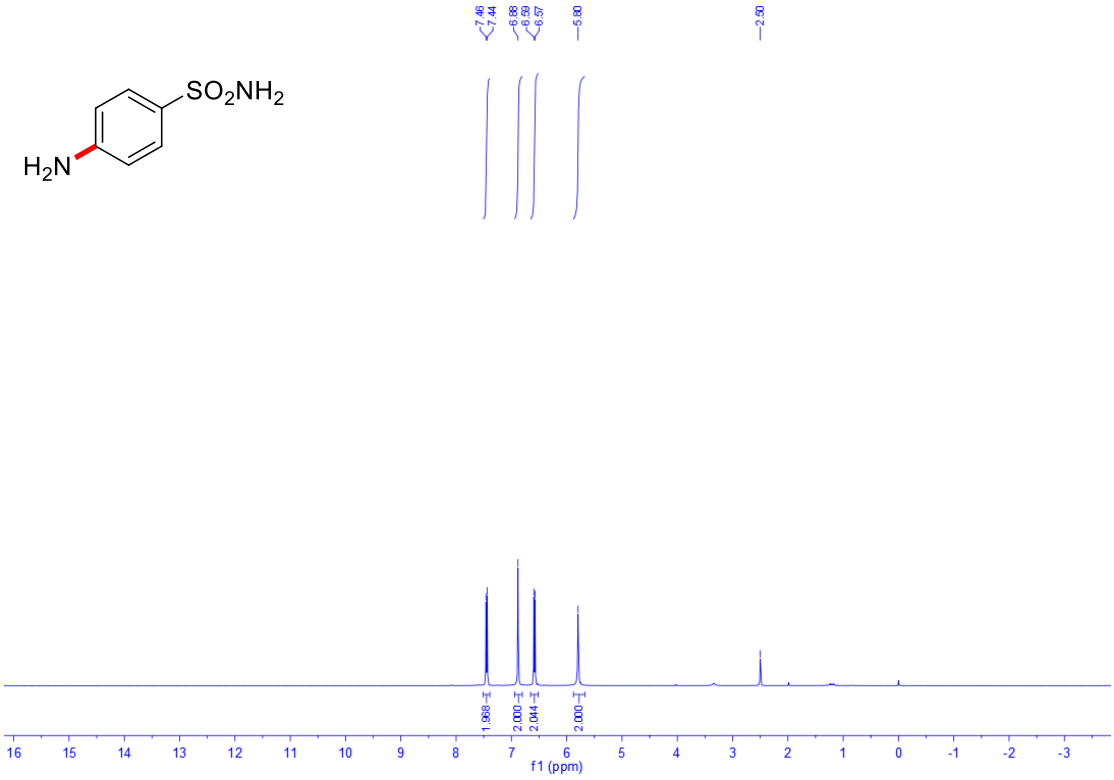

Figure S40. ^{1}H NMR (400 MHz, DMSO-d_6, 20 °C) of **2s**

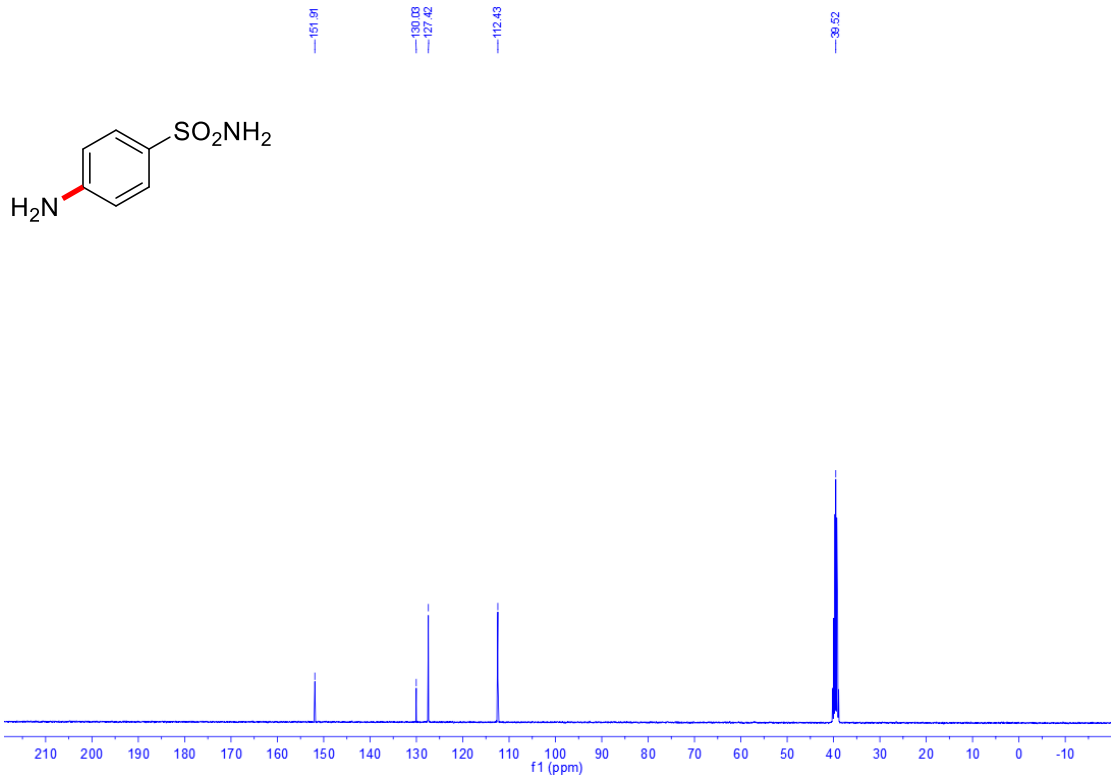

Figure S41. $^{13}C\{^{1}H\}$ (101 MHz, DMSO-d_6, 20 °C) of **2s**

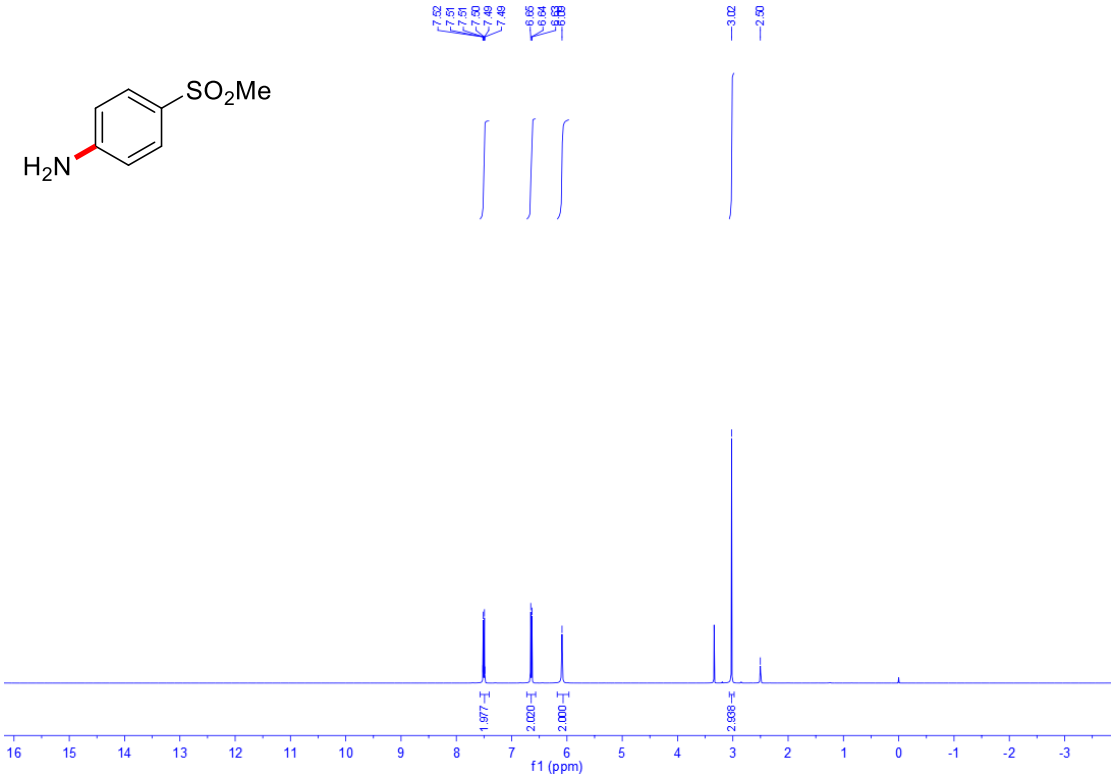

Figure S42. ^{1}H NMR (400 MHz, DMSO-d_6, 20 °C) of **2t**

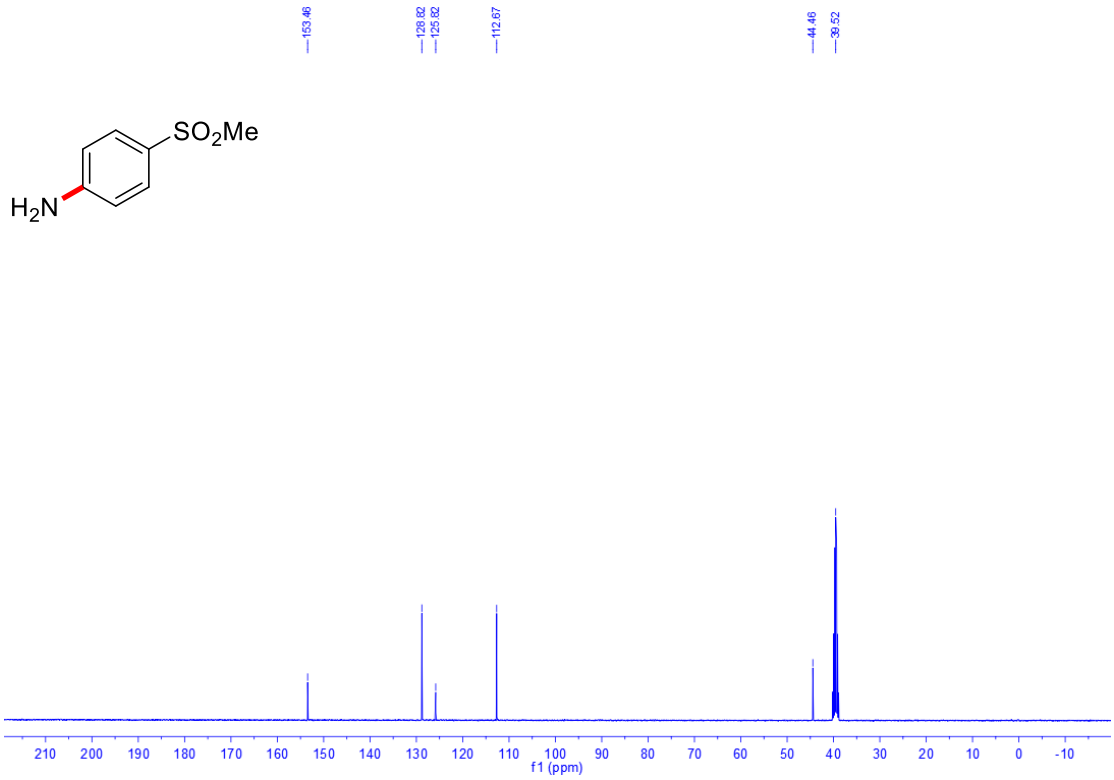

Figure S43. $^{13}C\{^{1}H\}$ (101 MHz, DMSO-d_6, 20 °C) of **2t**

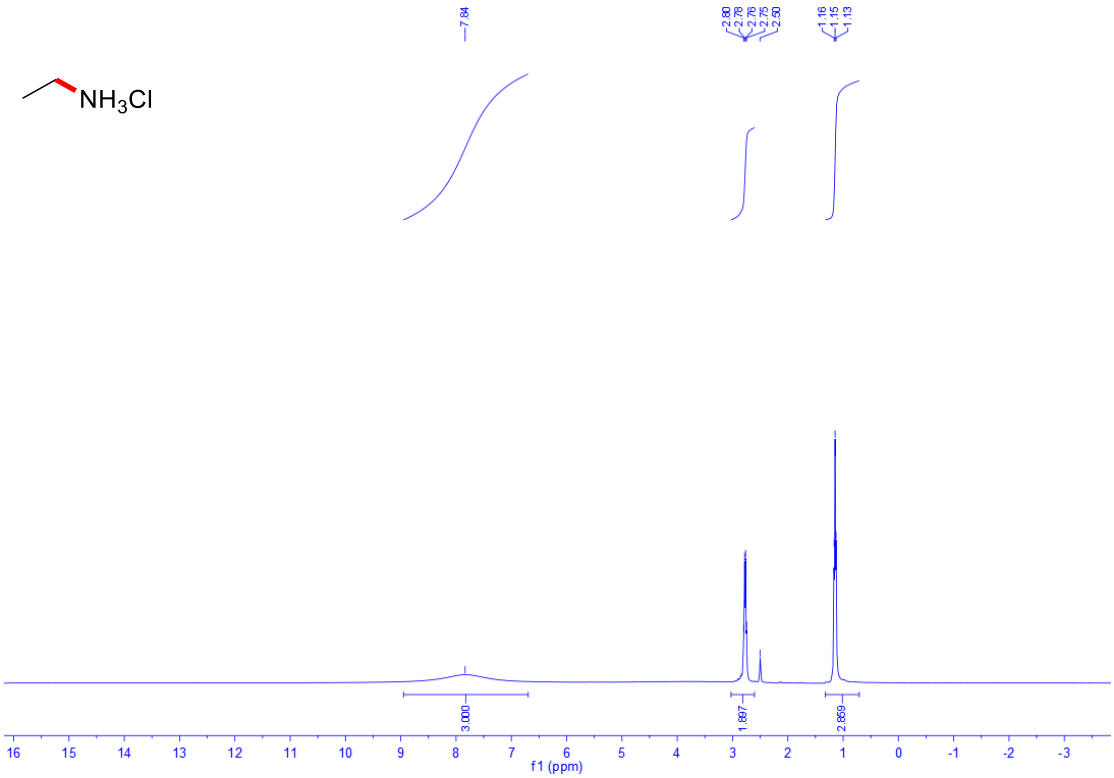

Figure S44. ^{1}H NMR (400 MHz, DMSO-d_6, 20 °C) of **5a**

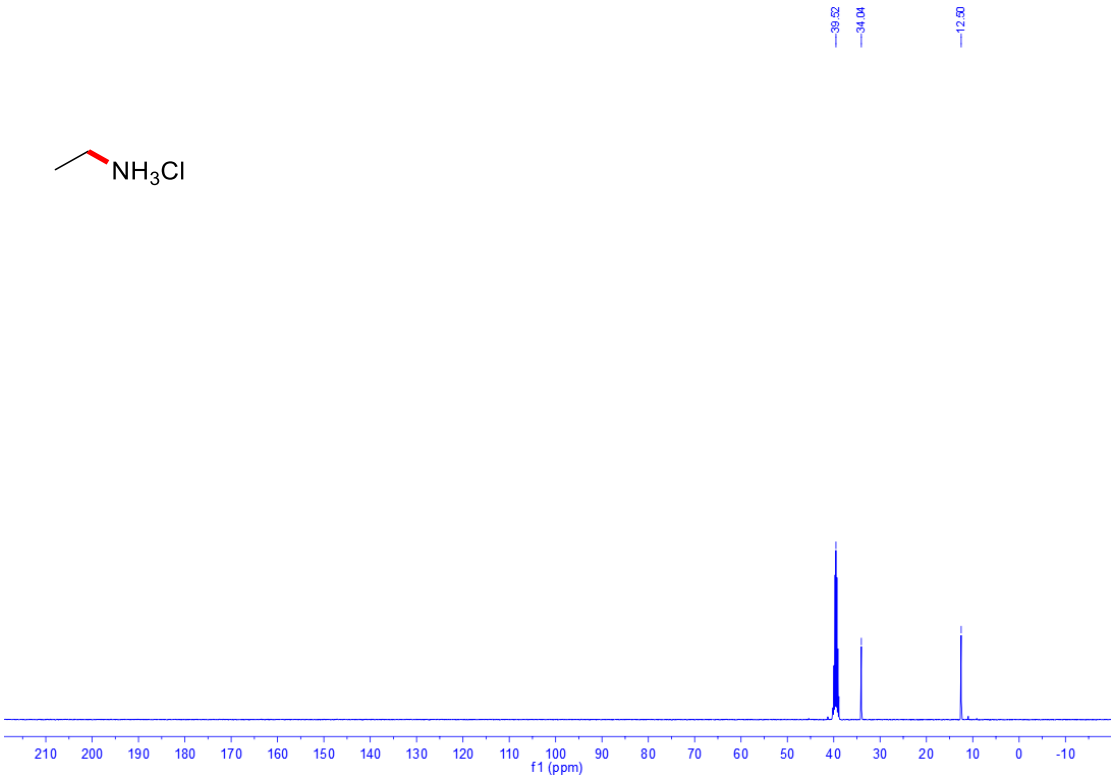

Figure S45. $^{13}C\{^{1}H\}$ (101 MHz, DMSO-d_6, 20 ºC) of **5a**

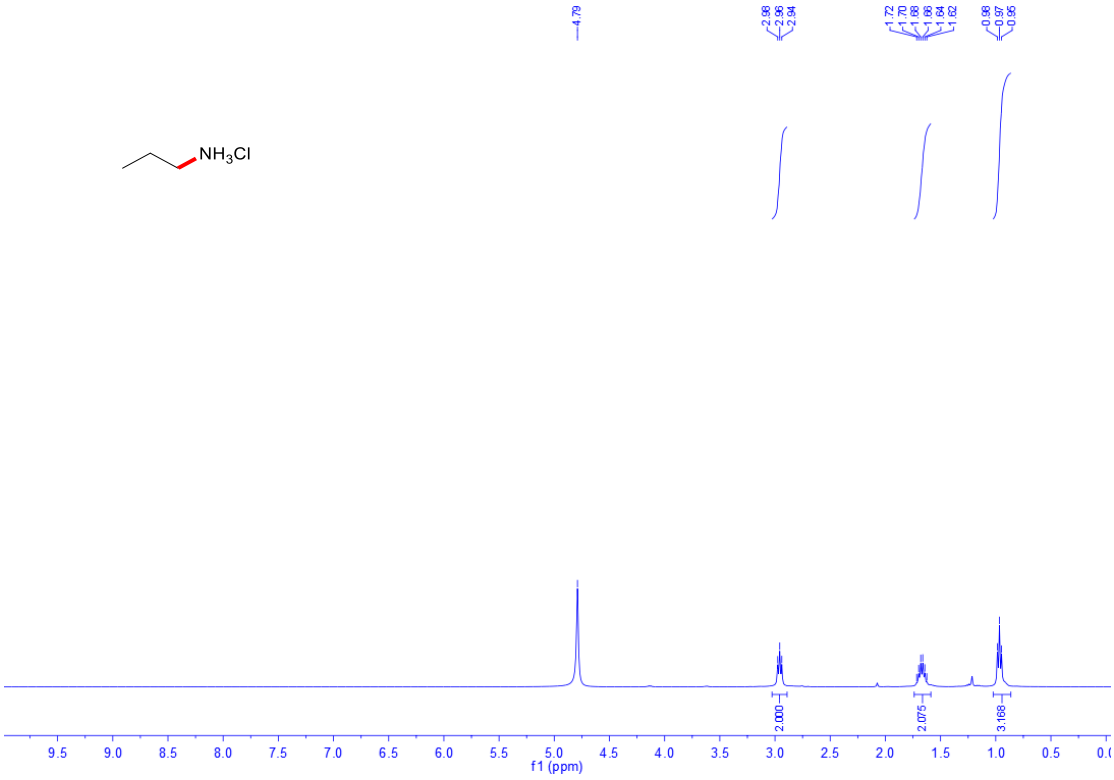

Figure S46. ^{1}H NMR (400 MHz, D_2O, 20 ºC) of **5b**

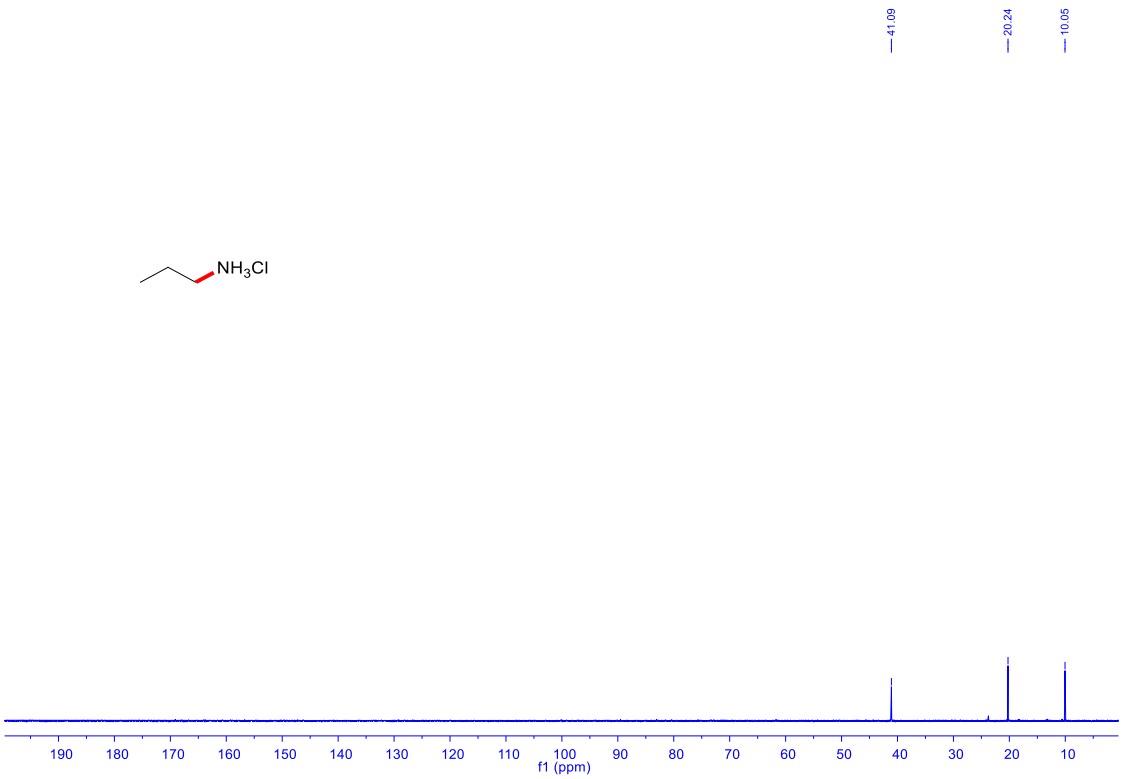

Figure S47. $^{13}C\{^{1}H\}$ (101 MHz, D_2O, 20 °C) of **5b**

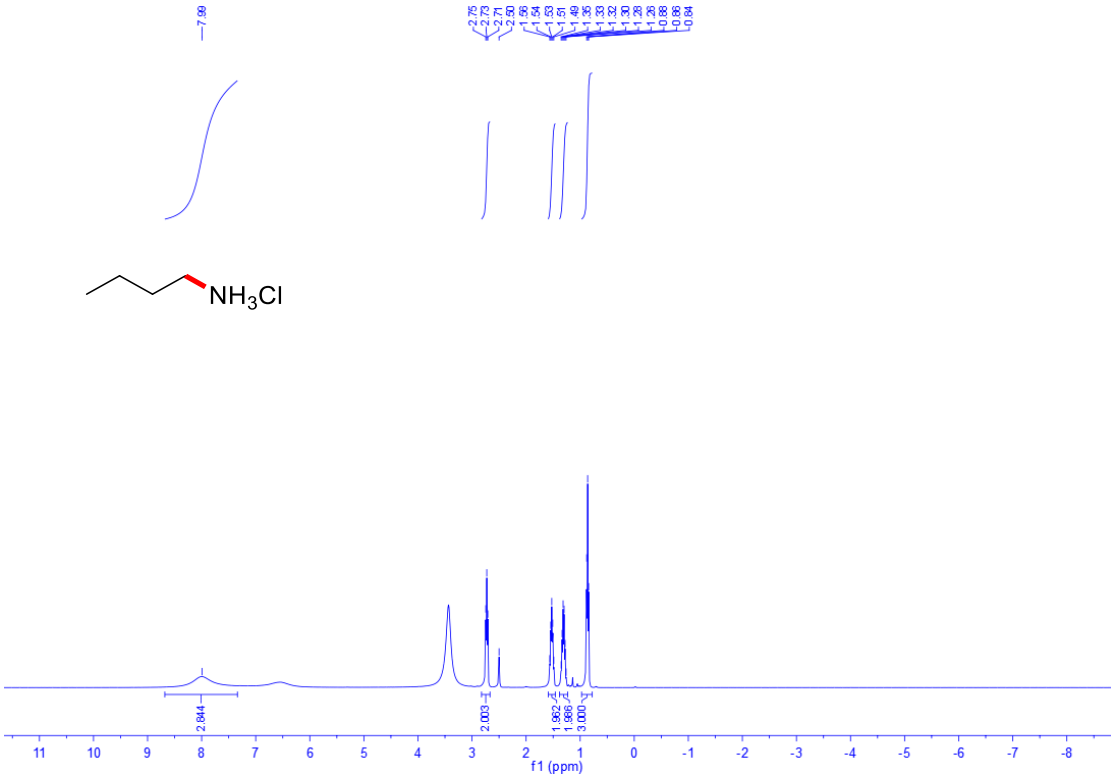

Figure S48. ^{1}H NMR (400 MHz, DMSO-d_6, 20 °C) of **5c**

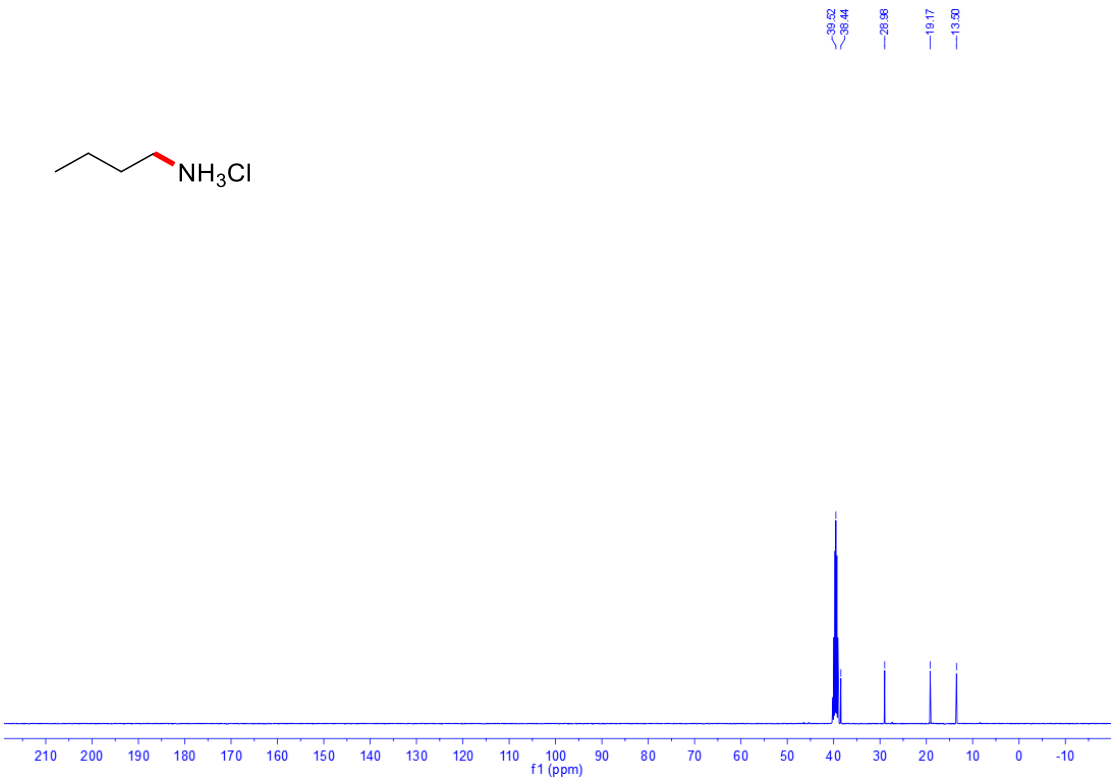

Figure S49. $^{13}C\{^{1}H\}$ (101 MHz, DMSO-d_6, 20 ºC) of **5c**

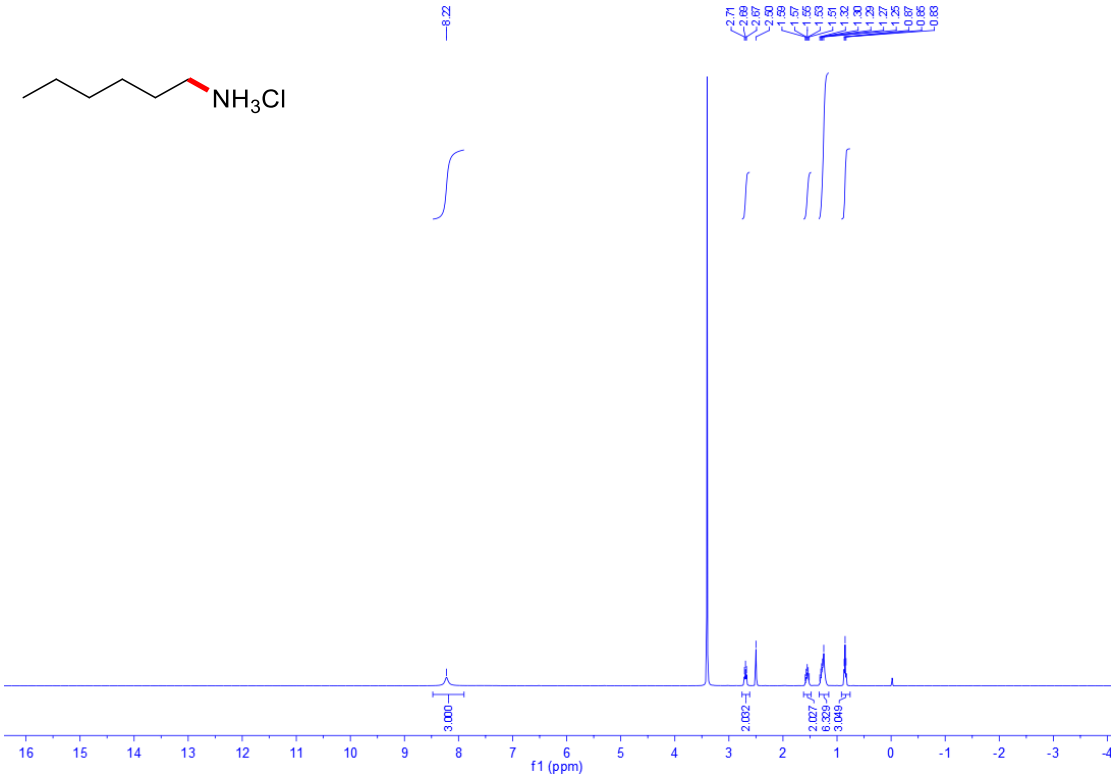

Figure S50. ^{1}H NMR (400 MHz, DMSO-d_6, 20 ºC) of **5d**

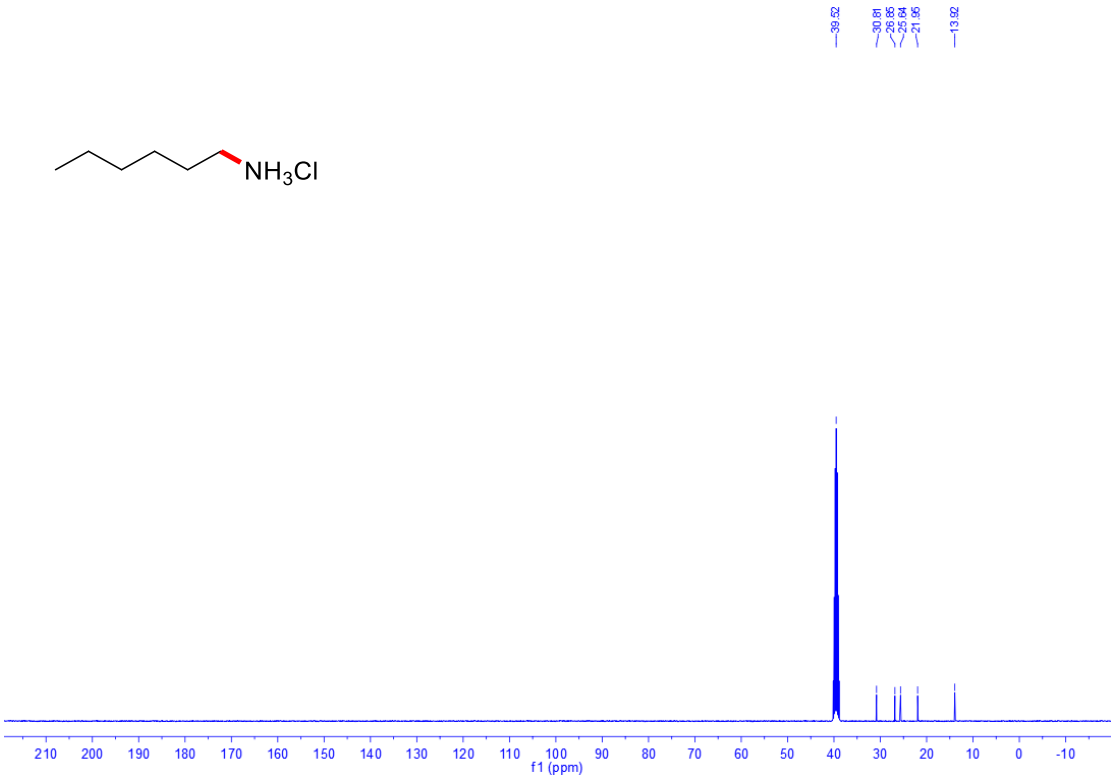

Figure S51. $^{13}C\{^{1}H\}$ (101 MHz, DMSO-d_6, 20 ºC) of **5d**

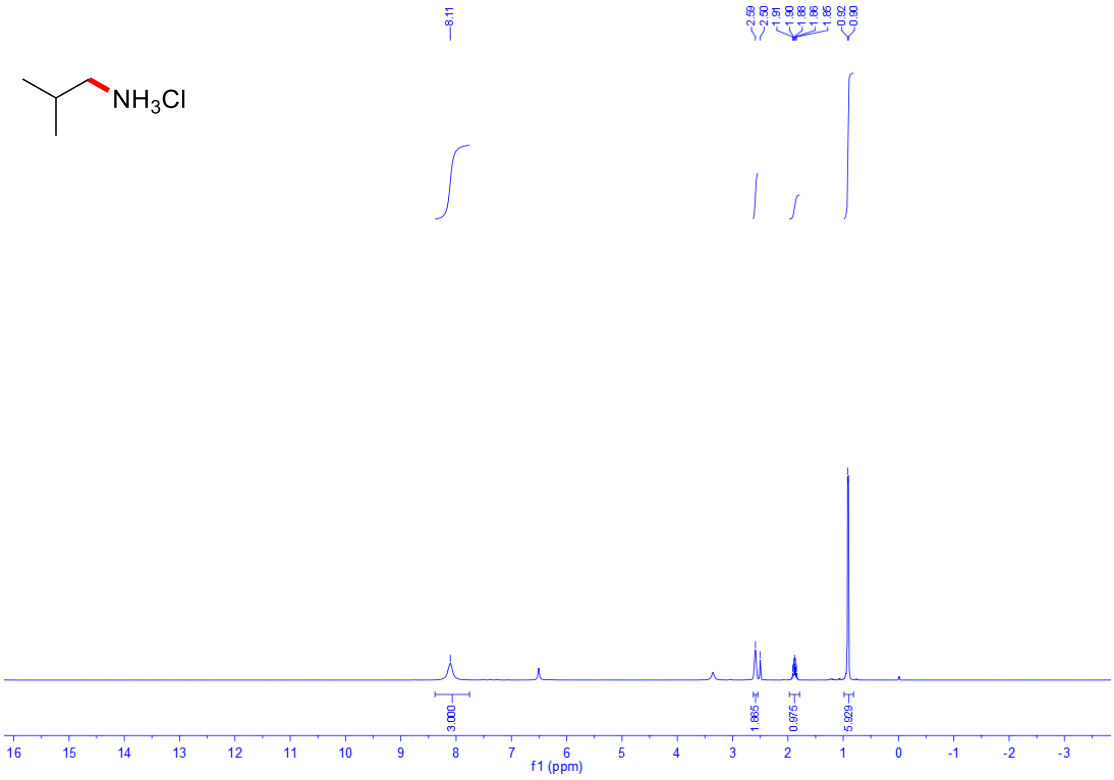

Figure S52. ^{1}H NMR (400 MHz, DMSO-d_6, 20 ºC) of **5e**

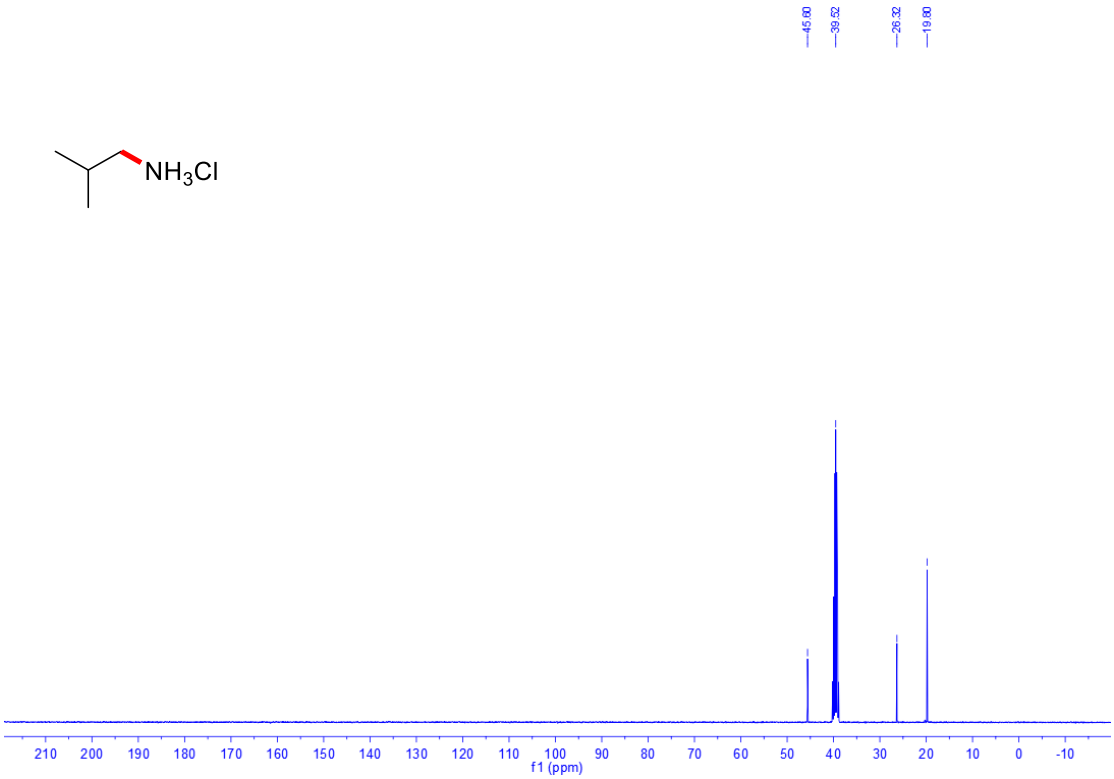

Figure S53. $^{13}C\{^{1}H\}$ (101 MHz, DMSO-d_6, 20 ºC) of **5e**

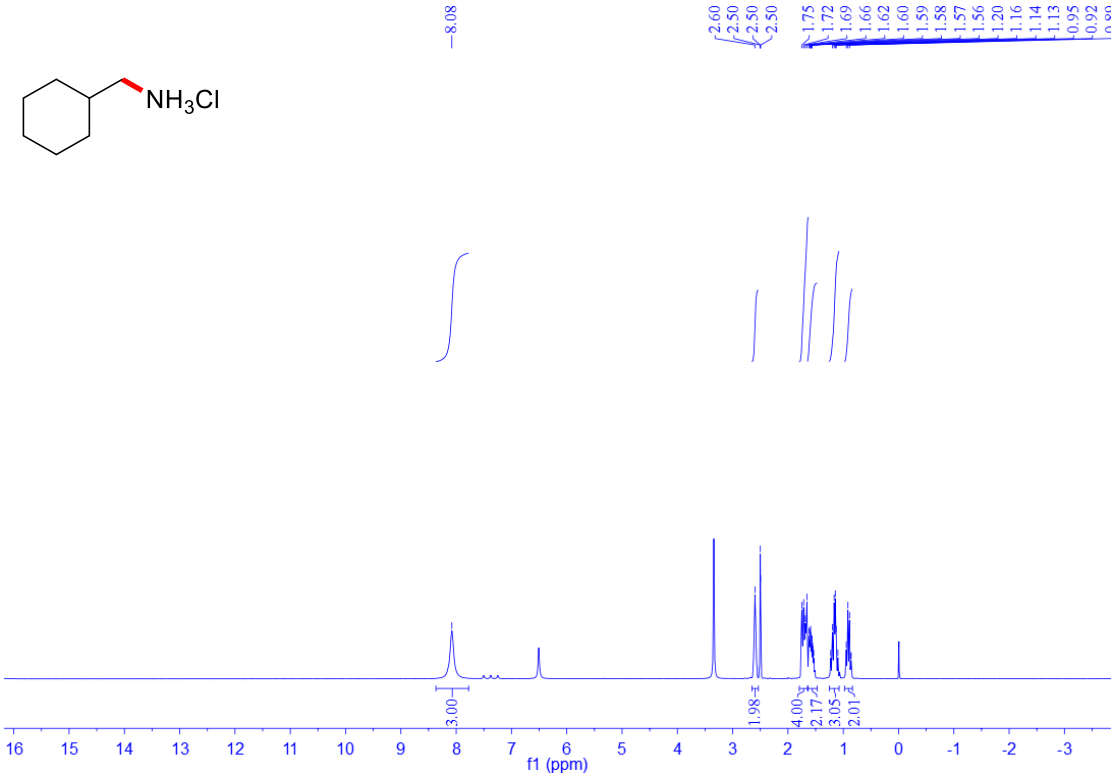

Figure S54. ^{1}H NMR (400 MHz, DMSO-d_6, 20 ºC) of **5f**

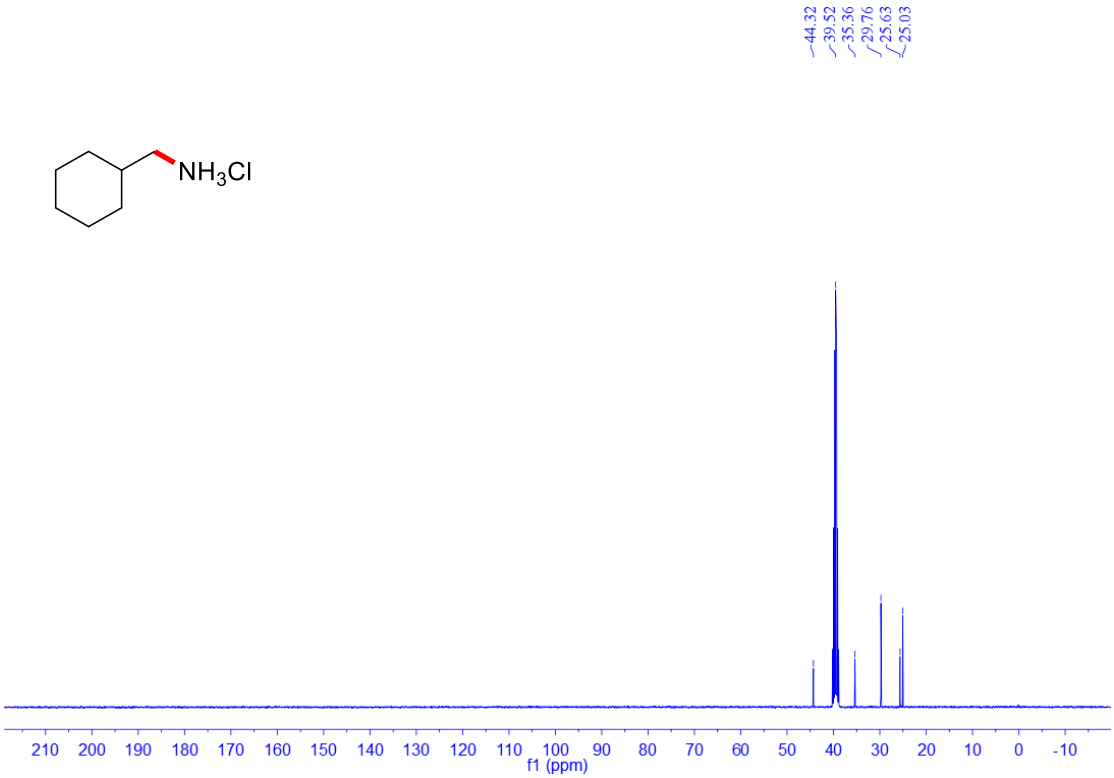

Figure S55. $^{13}C\{^{1}H\}$ (101 MHz, DMSO-d_6, 20 °C) of **5f**

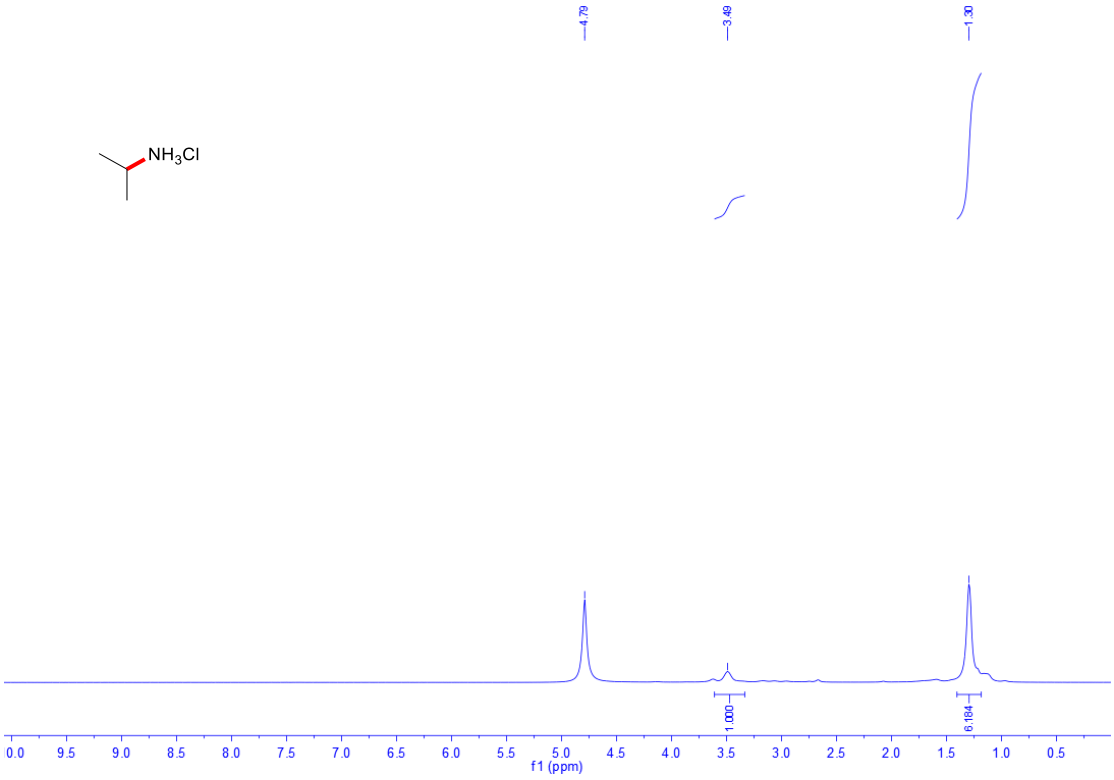

Figure S56. ^{1}H NMR (400 MHz, D_2O, 20 °C) of **5g**

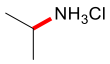

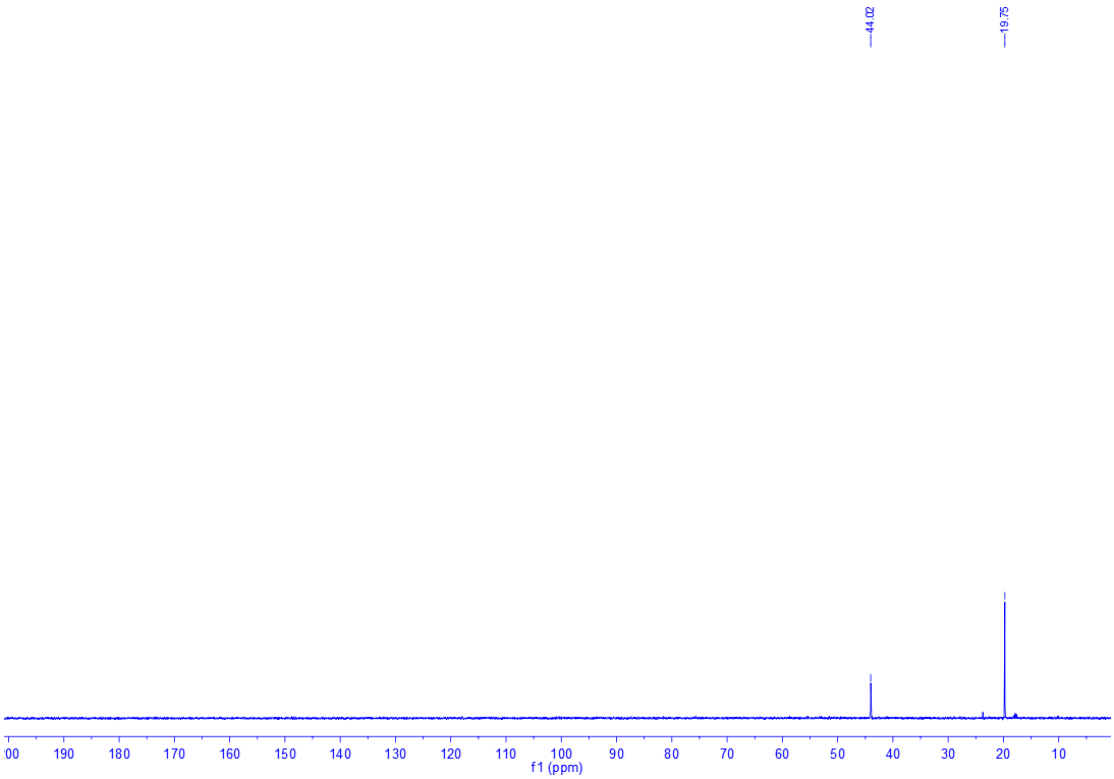

Figure S57. $^{13}C\{^{1}H\}$ (101 MHz, D_2O, 20 °C) of **5g**

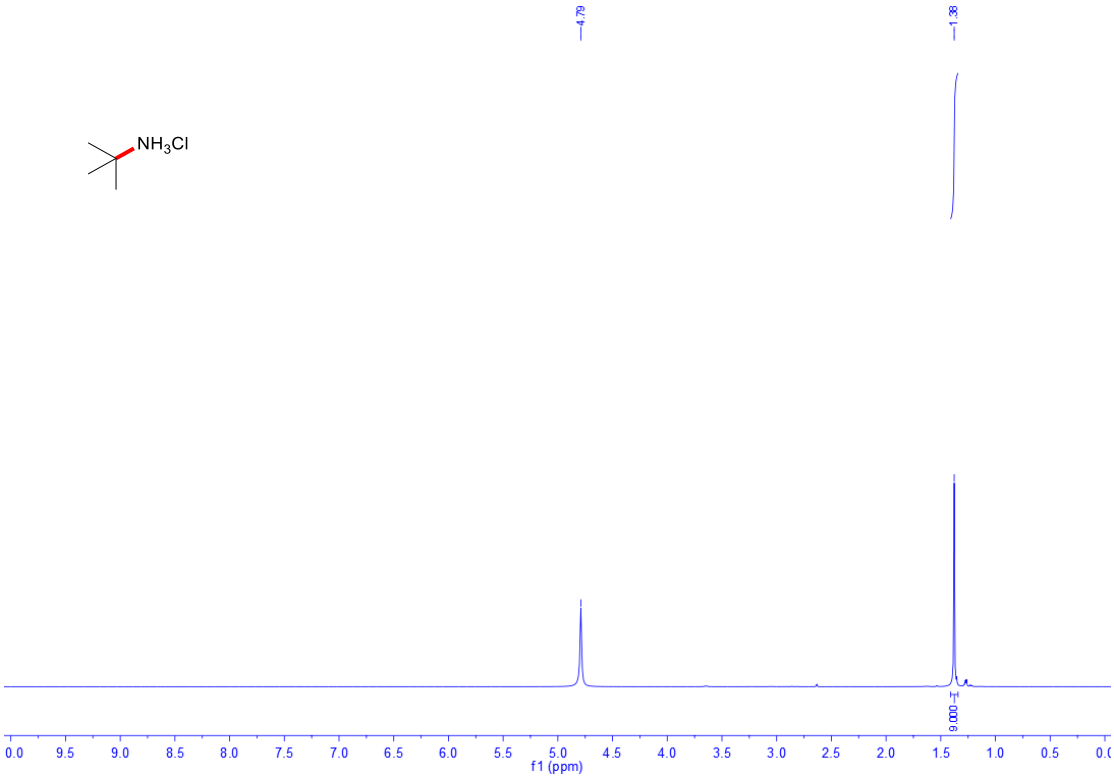

Figure S58. ^{1}H NMR (400 MHz, D_2O, 20 °C) of **5h**

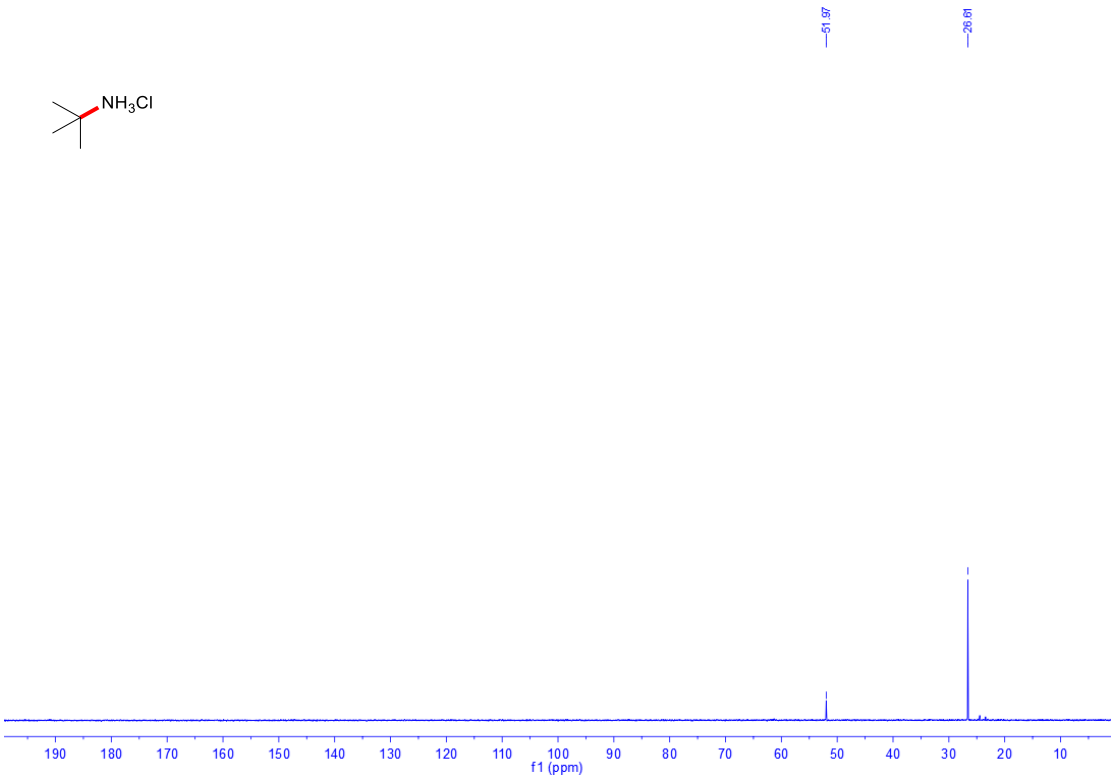

Figure S59. $^{13}C\{^{1}H\}$ (101 MHz, D_2O, 20 °C) of **5h**

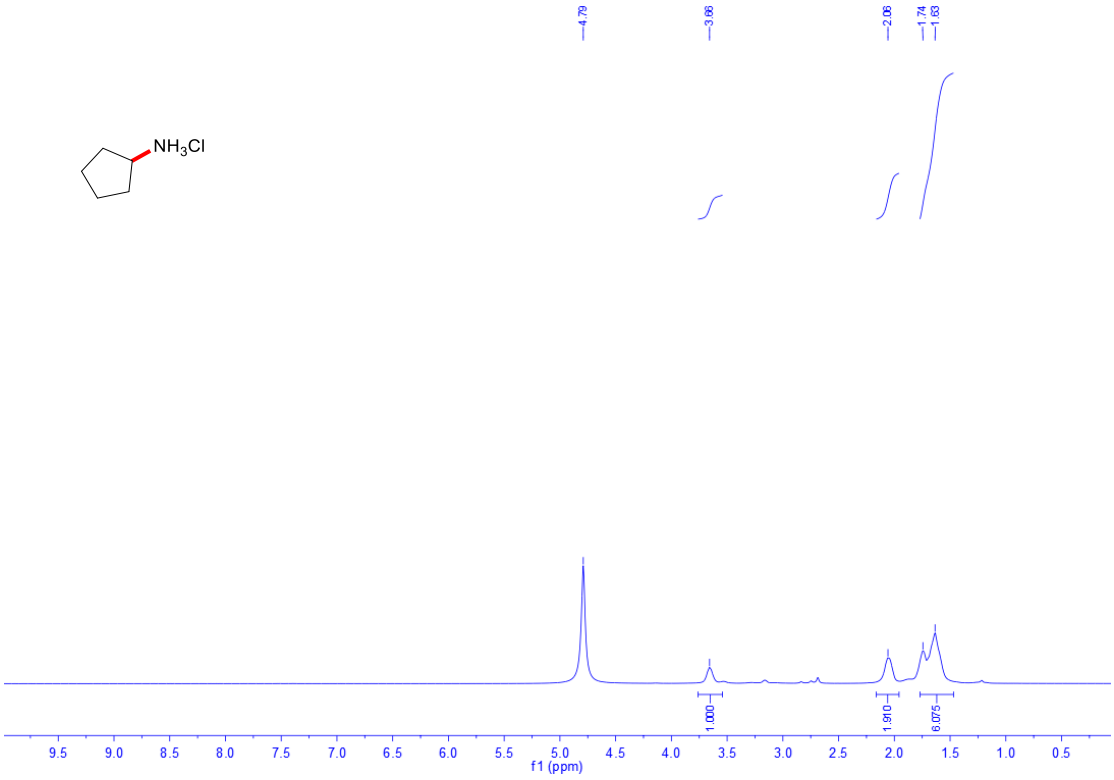

Figure S60. ^{1}H NMR (400 MHz, D_2O, 20 °C) of **5i**

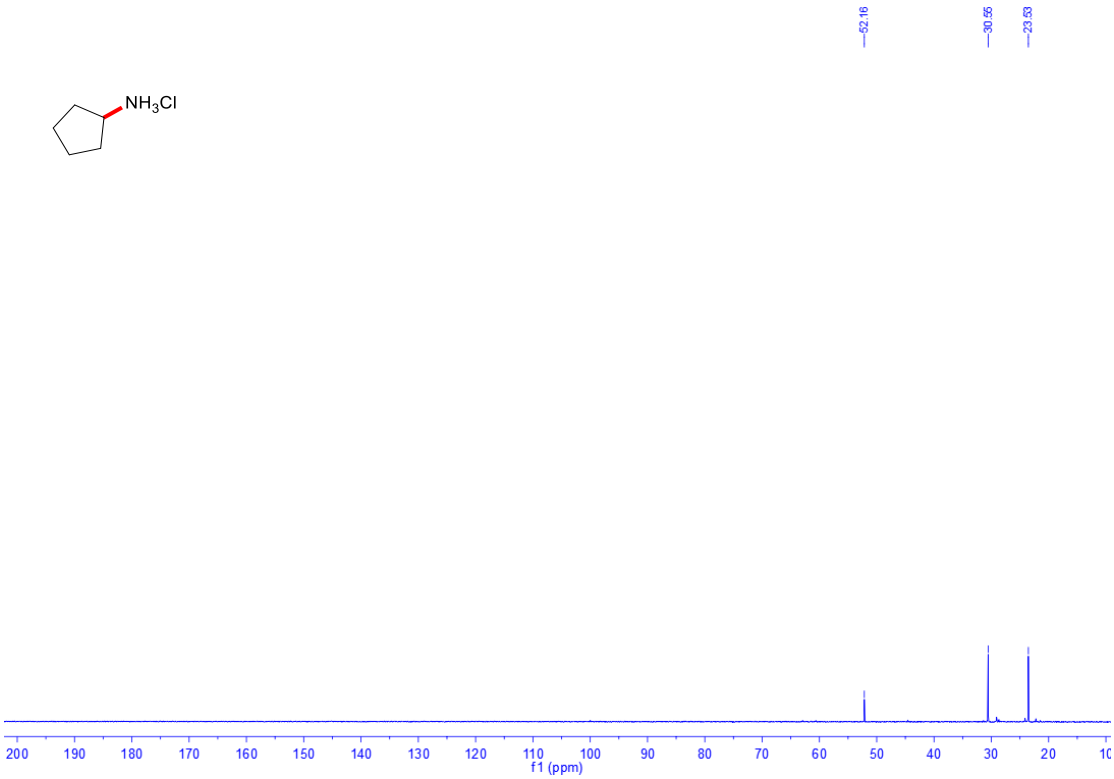

Figure S61. $^{13}C\{^{1}H\}$ (101 MHz, D_2O, 20 ºC) of **5i**

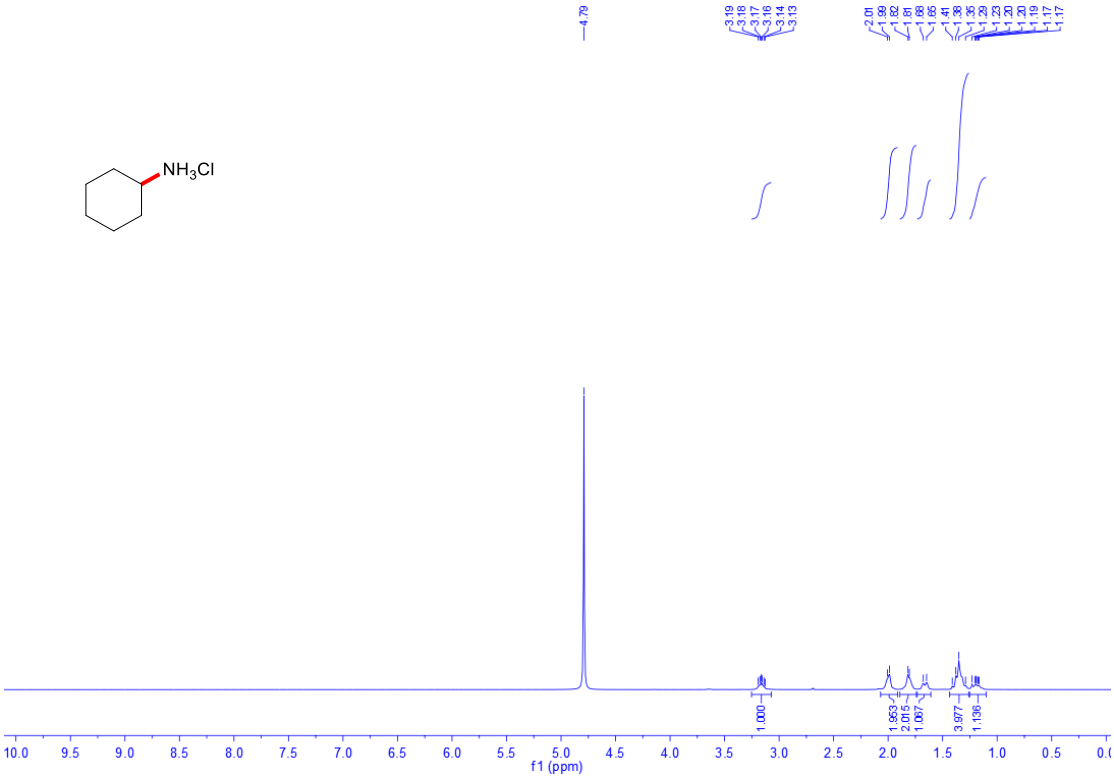

Figure S62. ^{1}H NMR (400 MHz, D_2O, 20 ºC) of **5j**

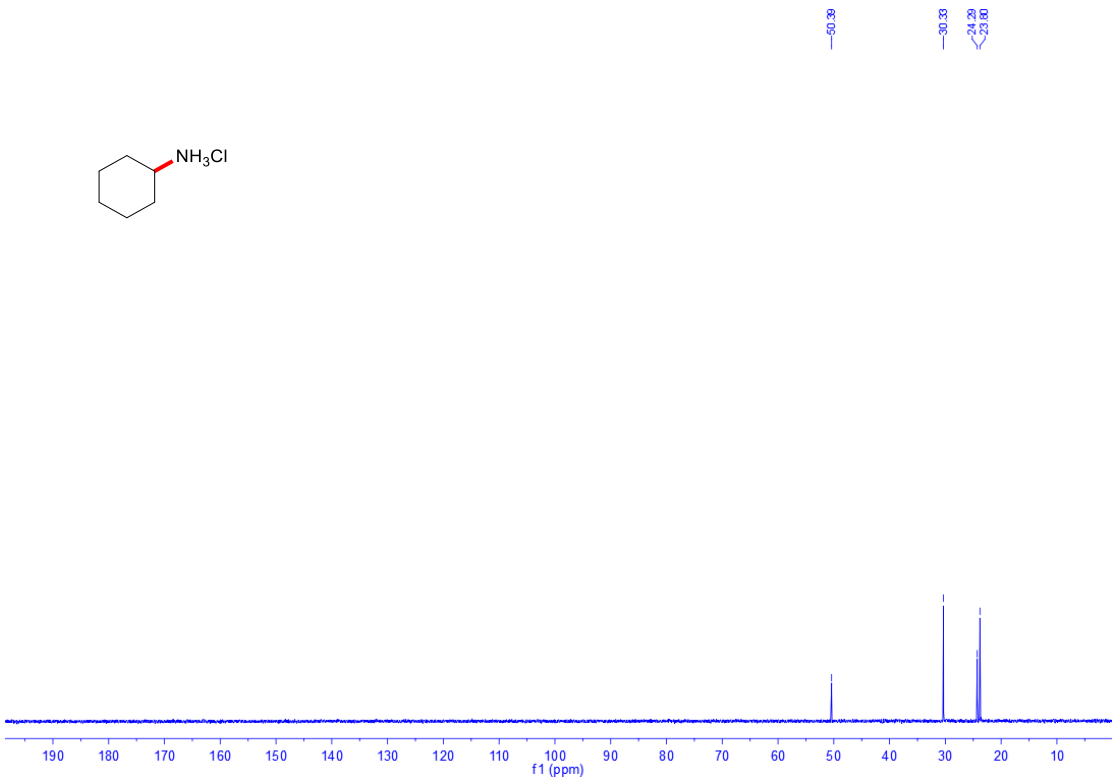

Figure S63. $^{13}C\{^{1}H\}$ (101 MHz, D_2O, 20 °C) of **5j**

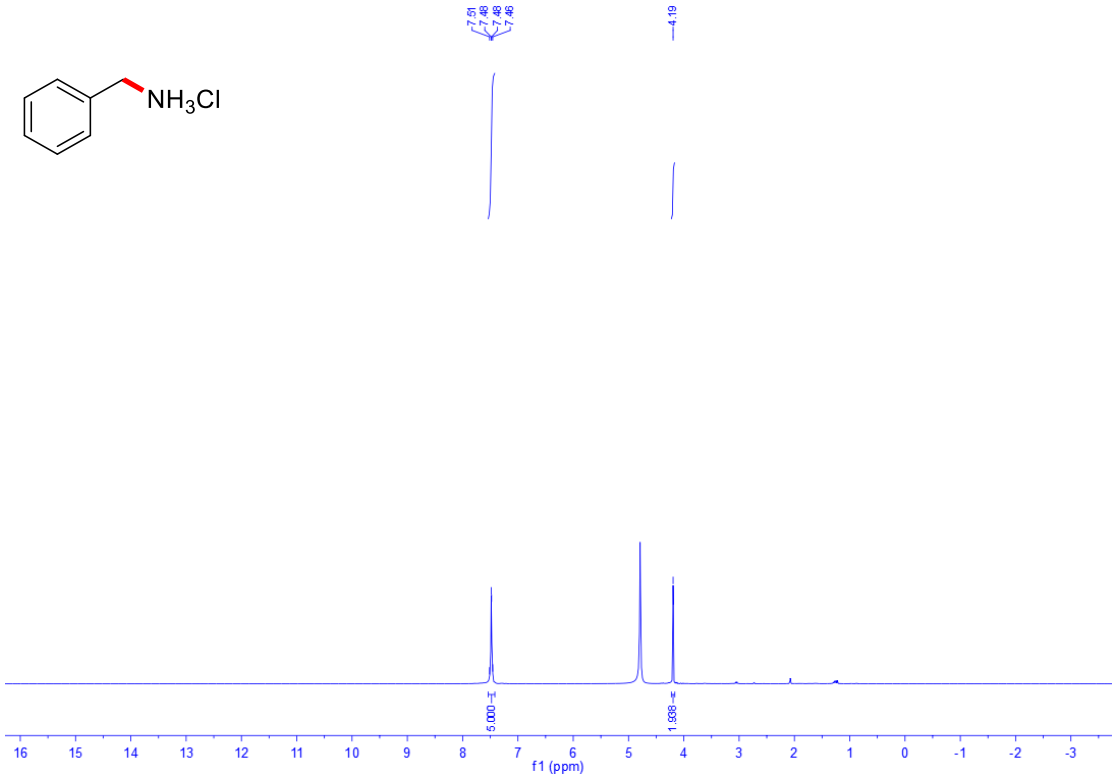

Figure S64. ^{1}H NMR (400 MHz, D_2O, 20 °C) of **5k**

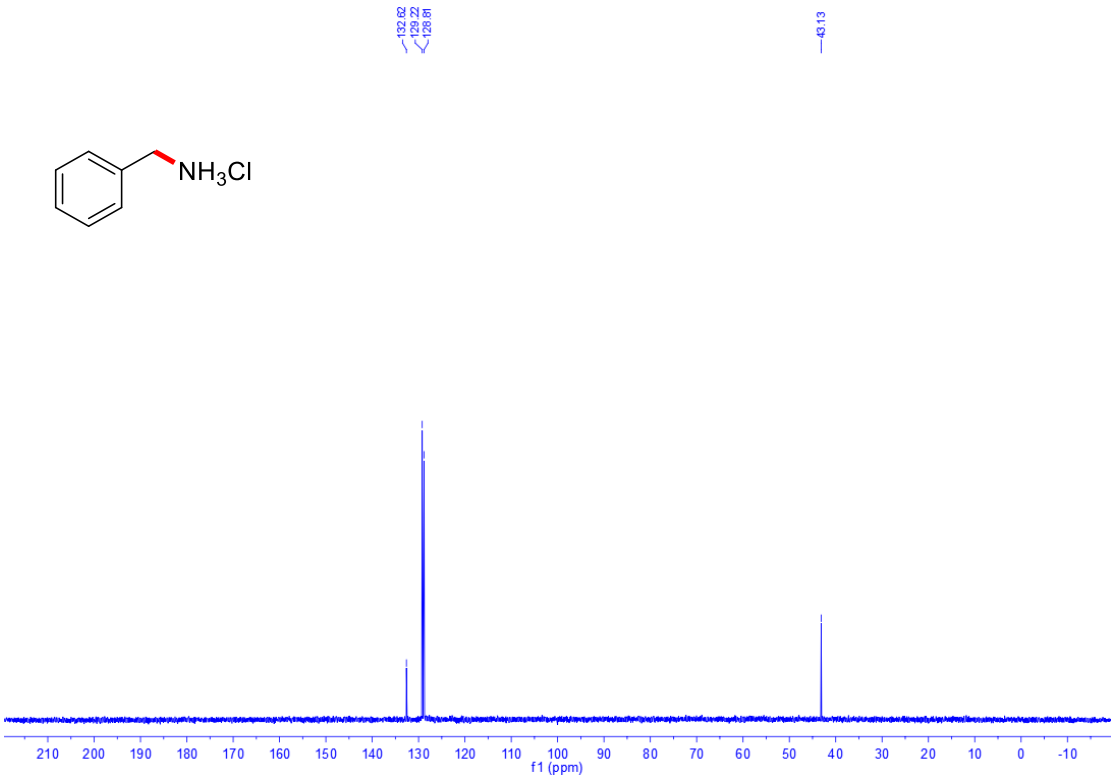

Figure S65. $^{13}C\{^{1}H\}$ (101 MHz, D_2O, 20 °C) of **5k**

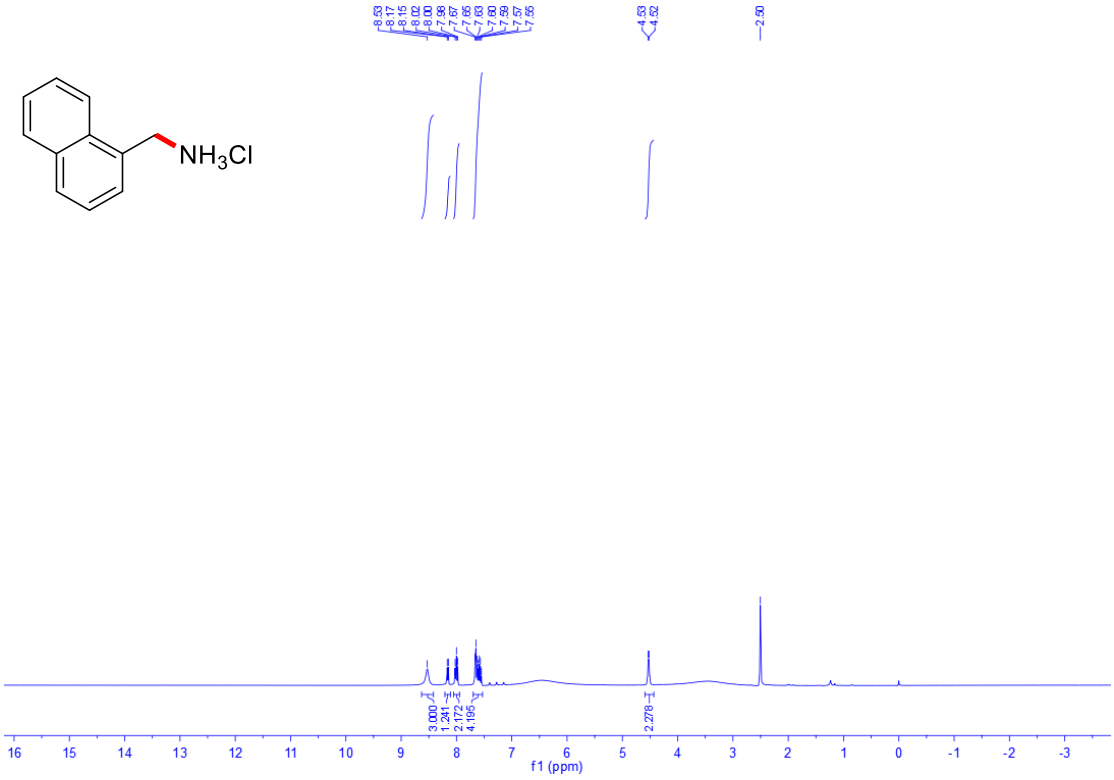

Figure S66. ^{1}H NMR (400 MHz, DMSO-d_6, 20 °C) of **5l**

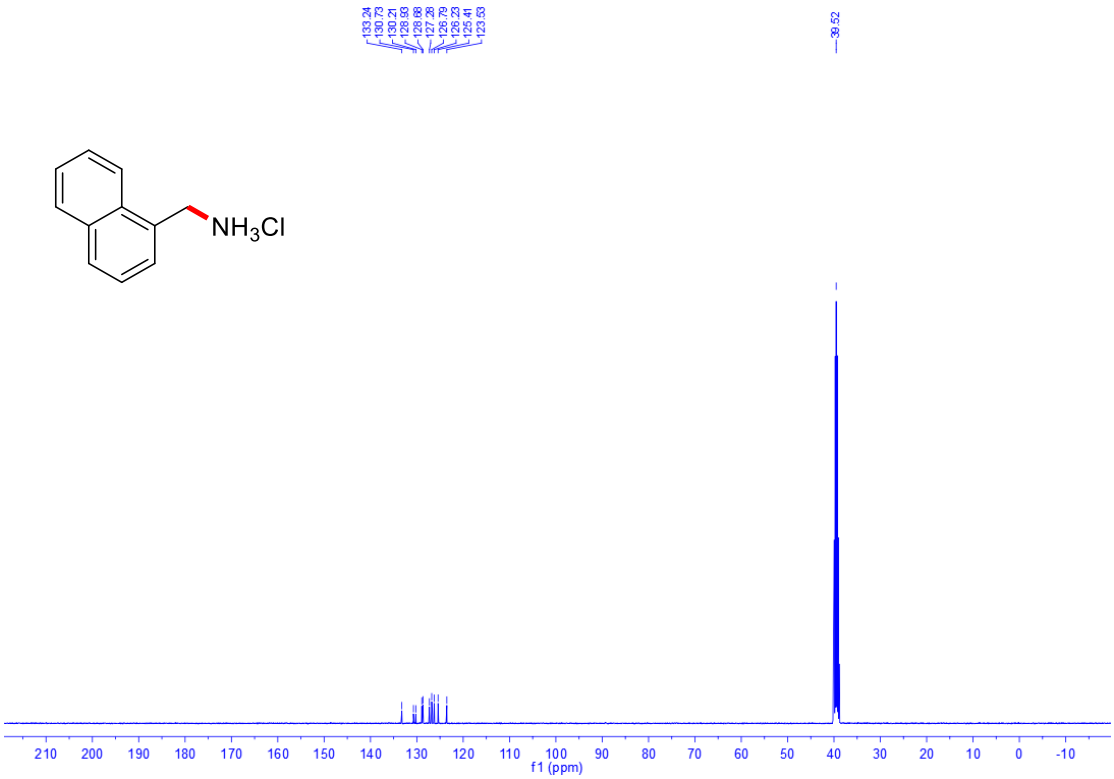

Figure S67. $^{13}C\{^{1}H\}$ (101 MHz, DMSO-d_6, 20 °C) of **5l**

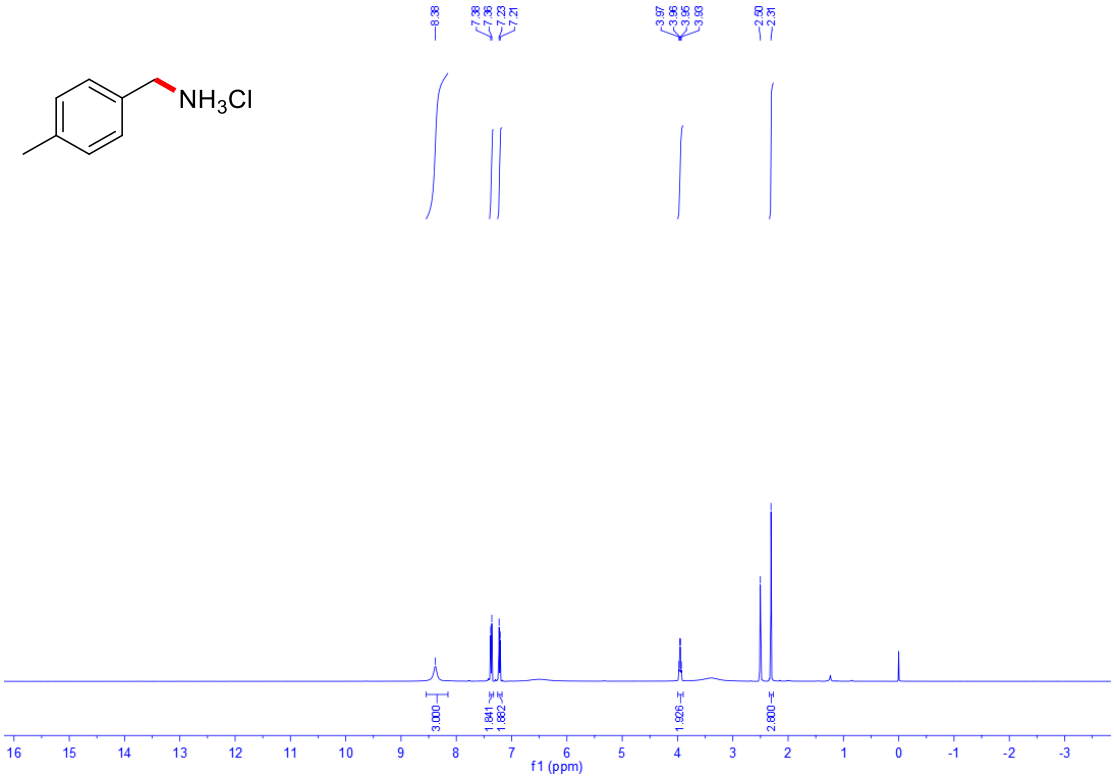

Figure S68. ^{1}H NMR (400 MHz, DMSO-d_6, 20 °C) of **5m**

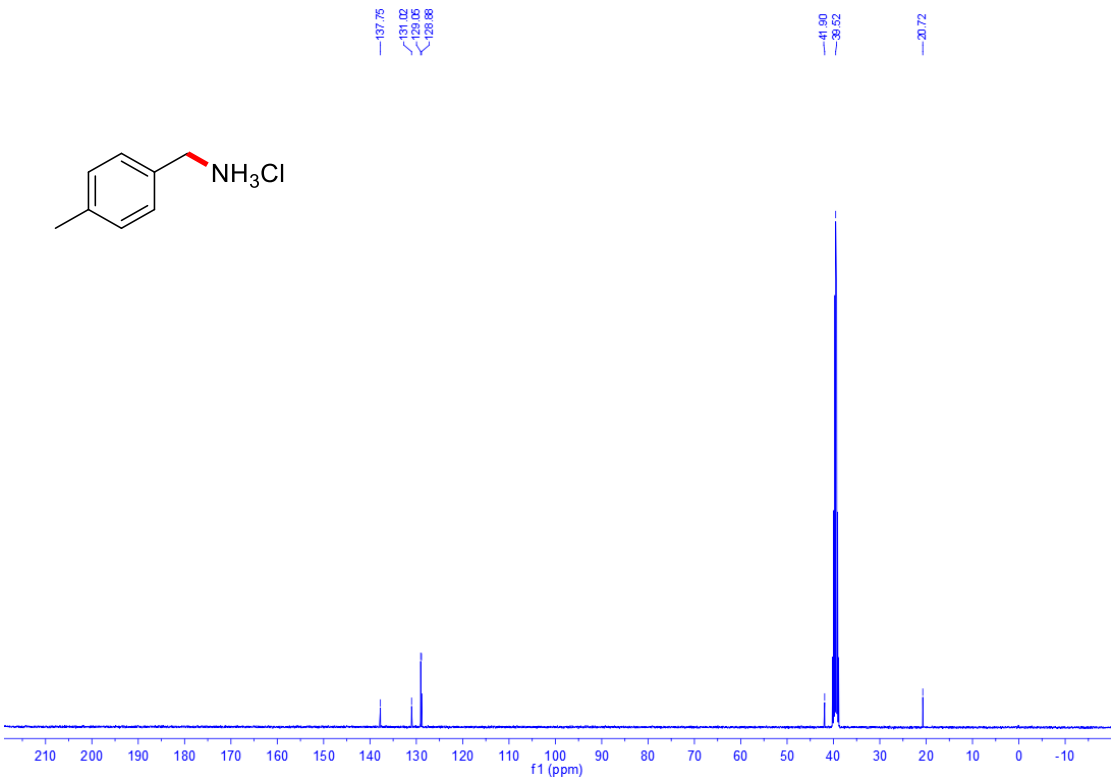

Figure S69. $^{13}C\{^{1}H\}$ (101 MHz, DMSO-d_6, 20 °C) of **5m**

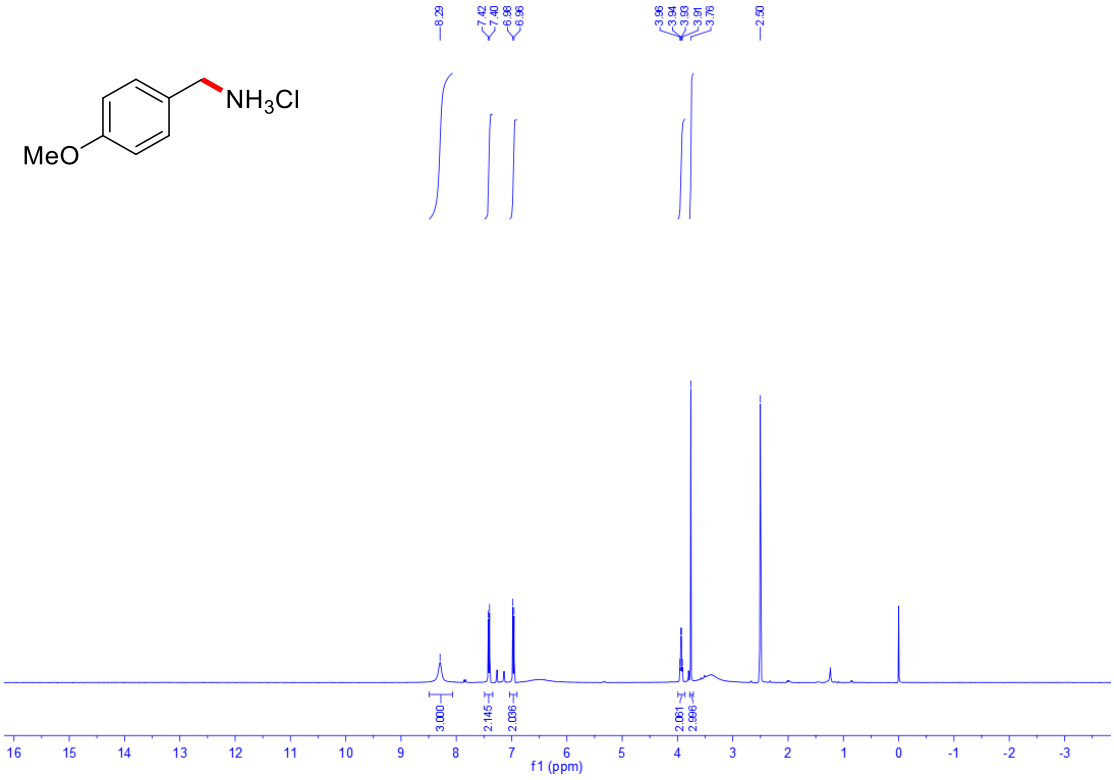

Figure S70. ^{1}H NMR (400 MHz, DMSO-d_6, 20 °C) of **5n**

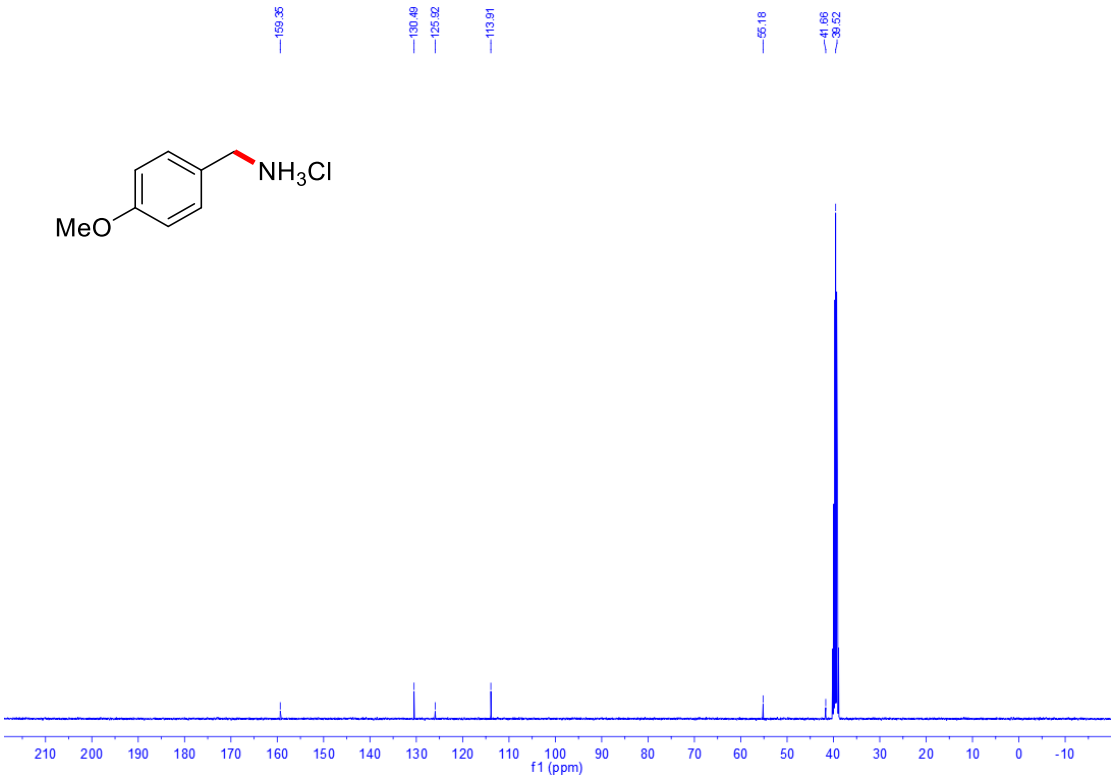

Figure S71. $^{13}C\{^{1}H\}$ (101 MHz, DMSO-d_6, 20 °C) of **5n**

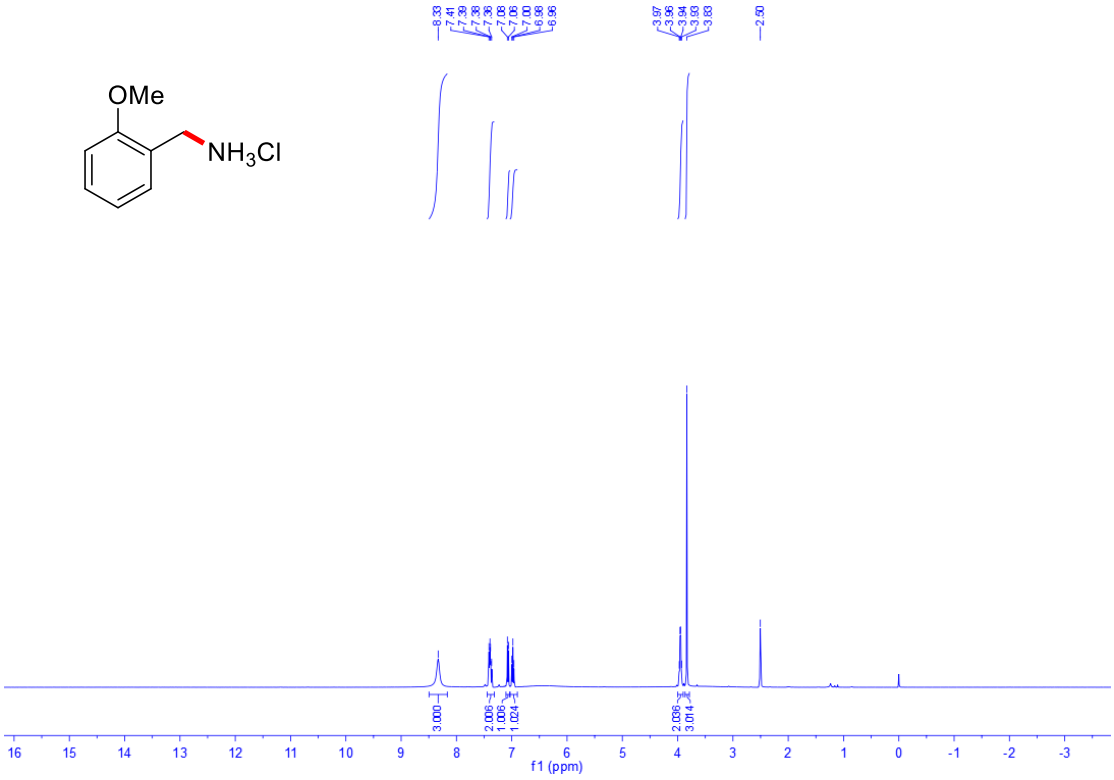

Figure S72. ^{1}H NMR (400 MHz, DMSO-d_6, 20 °C) of **5o**

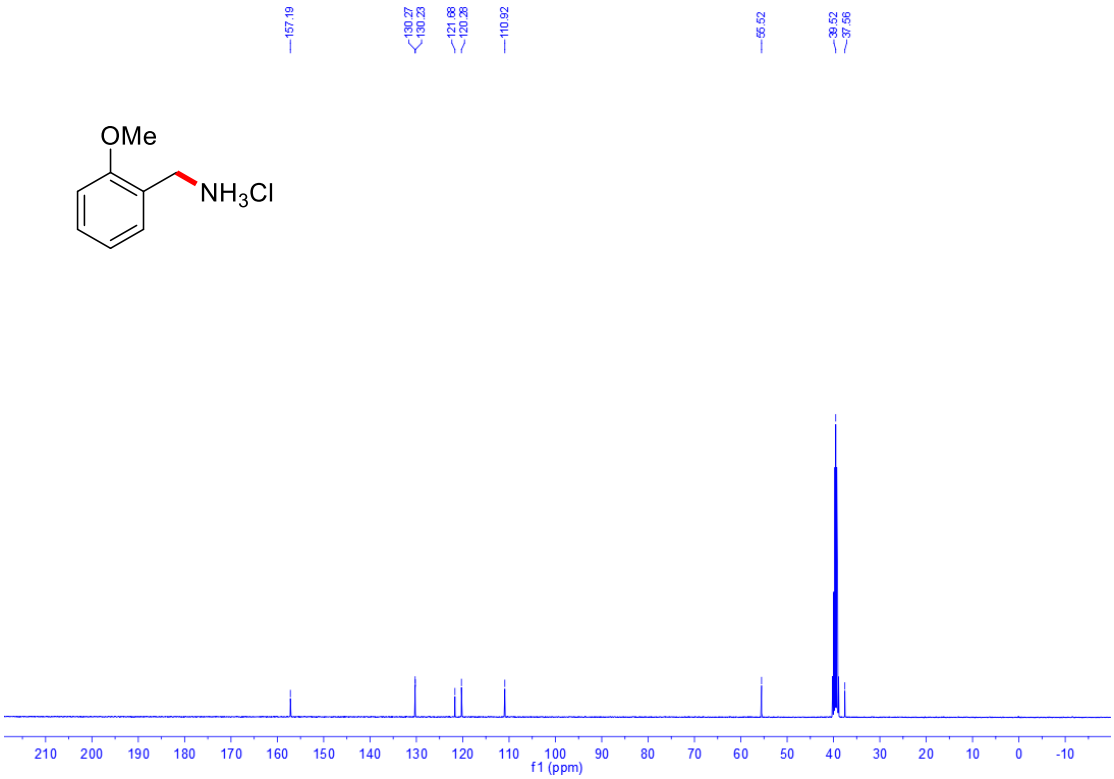

Figure S73. $^{13}C\{^{1}H\}$ (101 MHz, DMSO-d_6, 20 °C) of **5o**

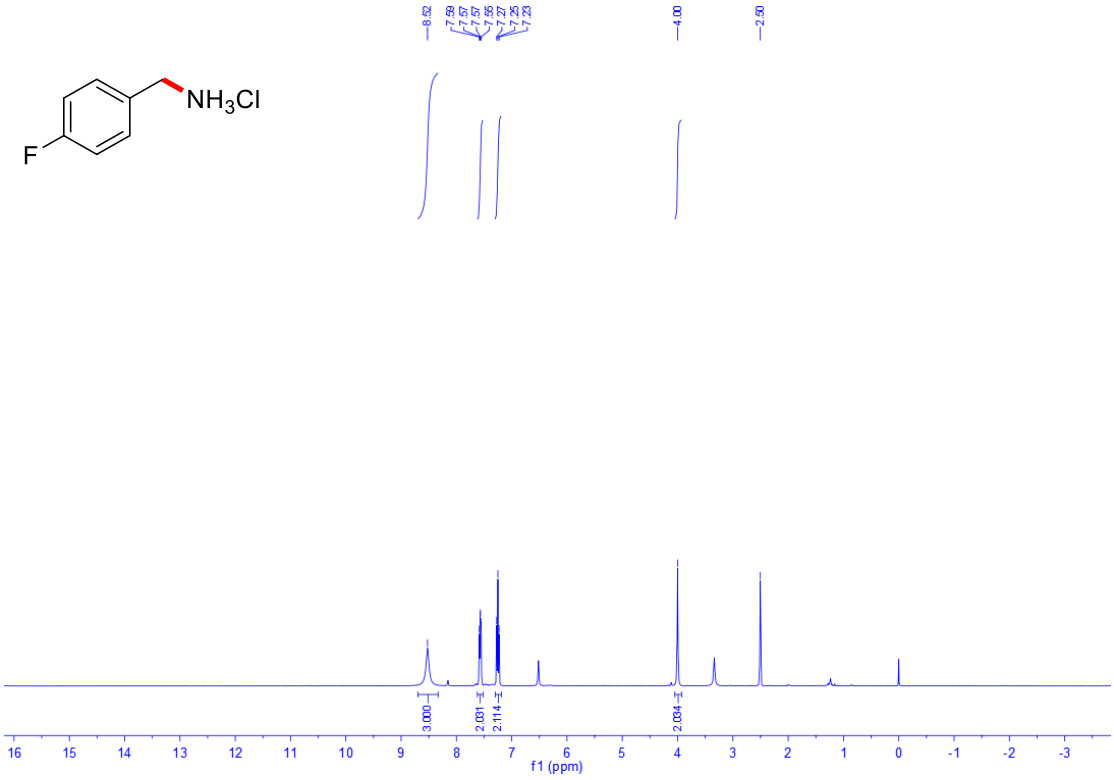

Figure S74. ^{1}H NMR (400 MHz, DMSO-d_6, 20 °C) of **5p**

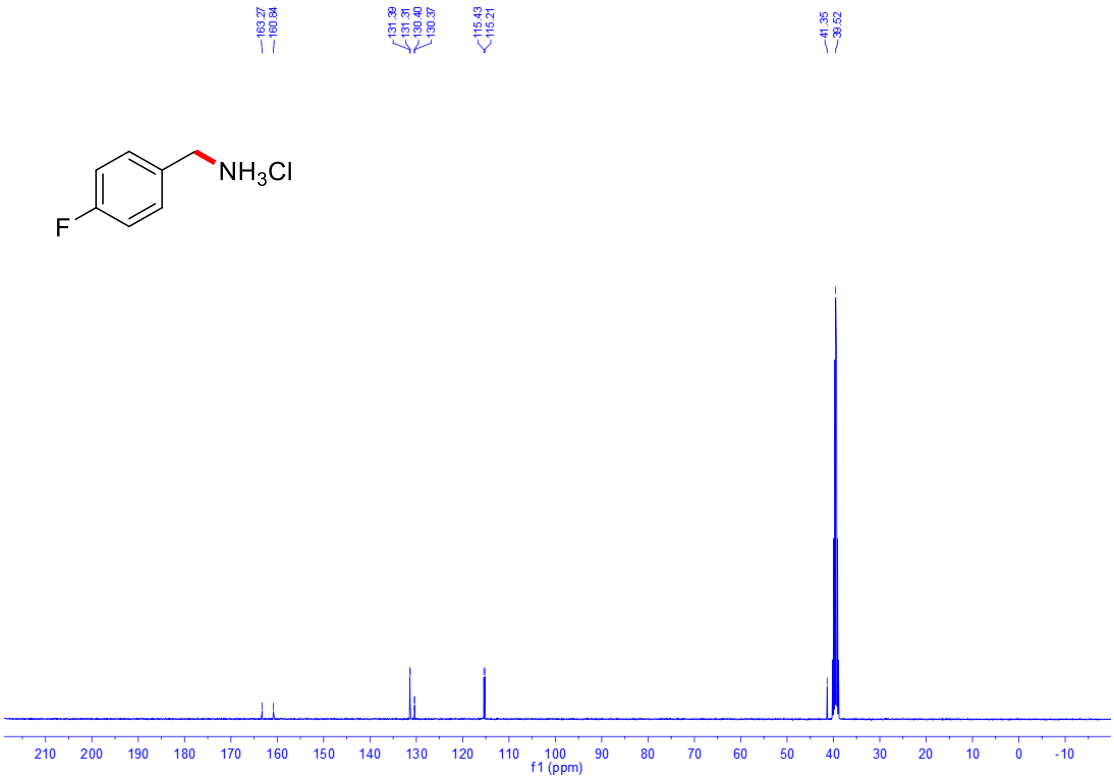

Figure S75. $^{13}C\{^{1}H\}$ (101 MHz, DMSO-d_6, 20 ºC) of **5p**

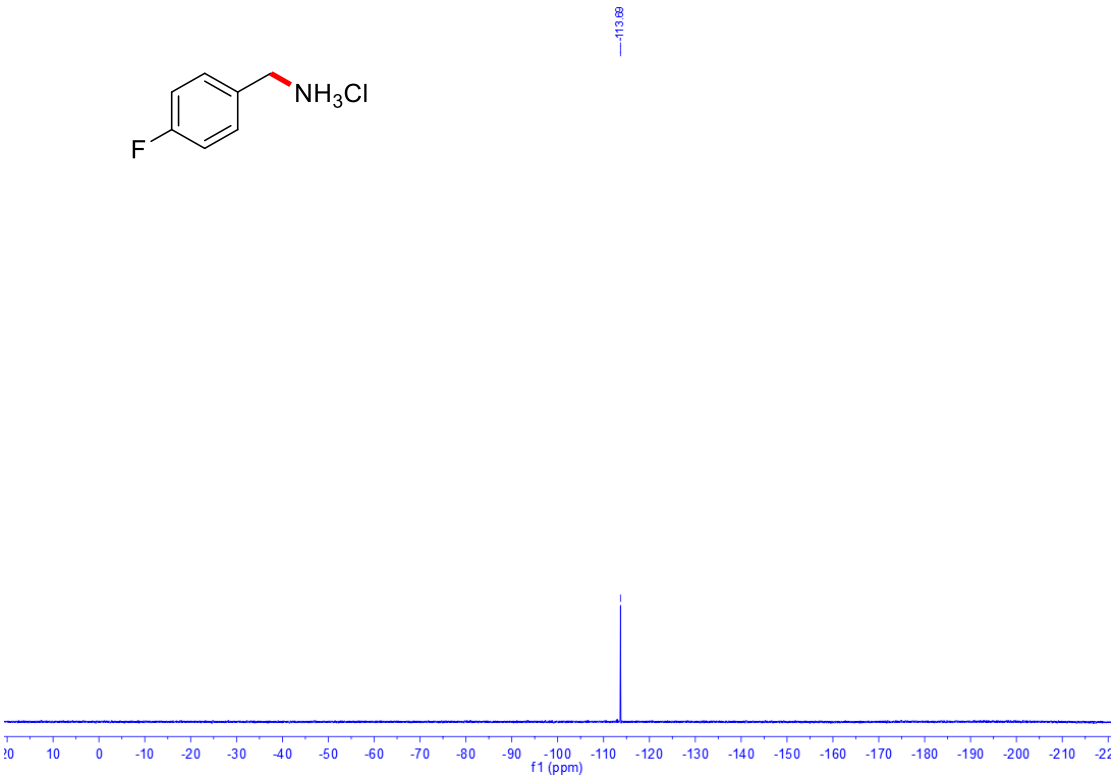

Figure S76. ^{19}F NMR (377 MHz, DMSO-d_6, 20 ºC) of **5p**

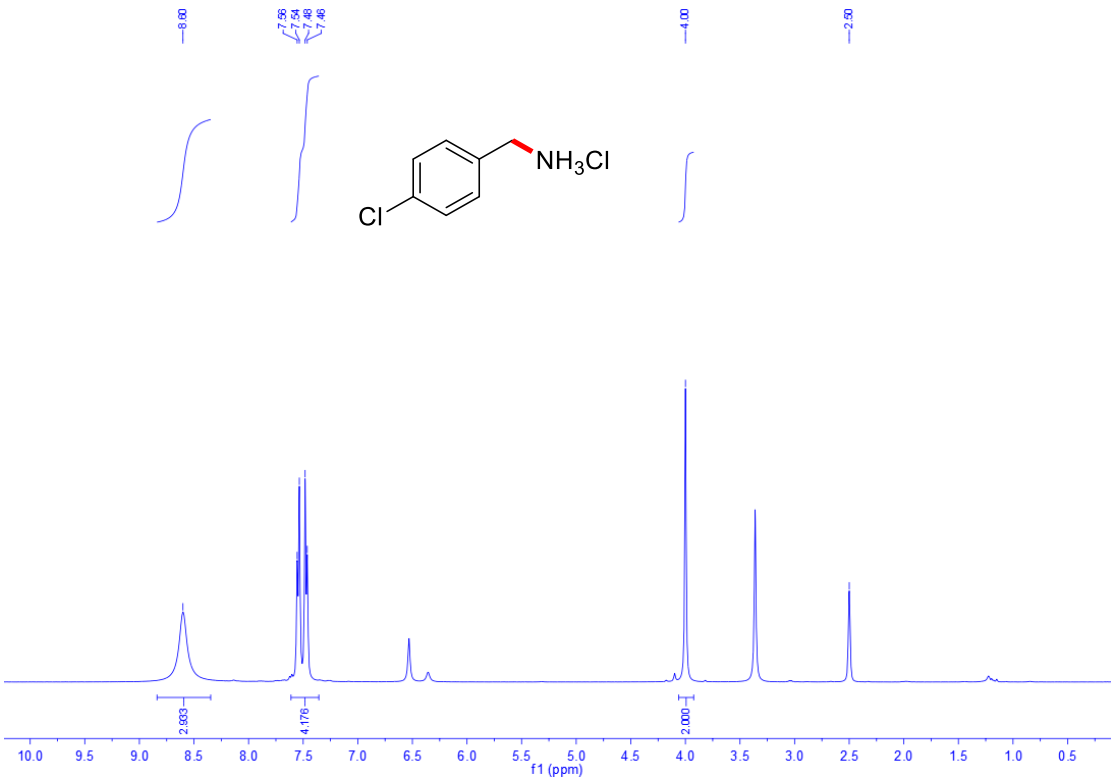

Figure S77. ^{1}H NMR (400 MHz, DMSO-d_6, 20 ^{o}C) of **5q**

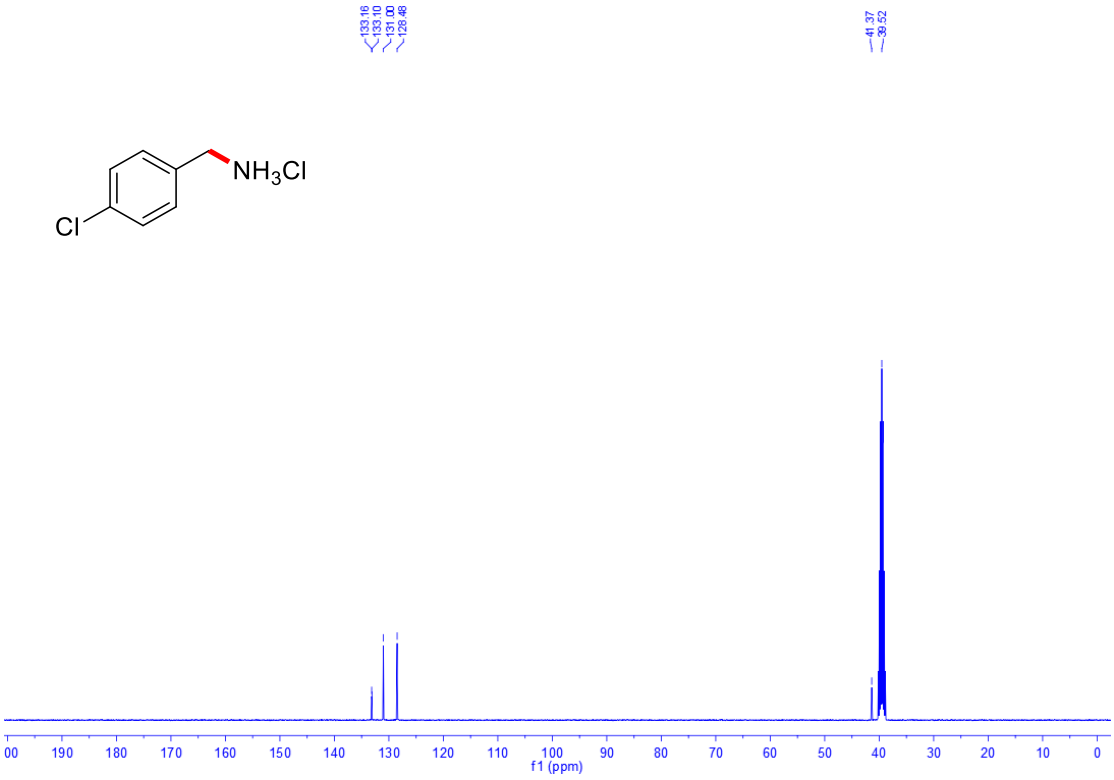

Figure S78. ^{13}C{^{1}H} (101 MHz, DMSO-d_6, 20 ^{o}C) of **5q**

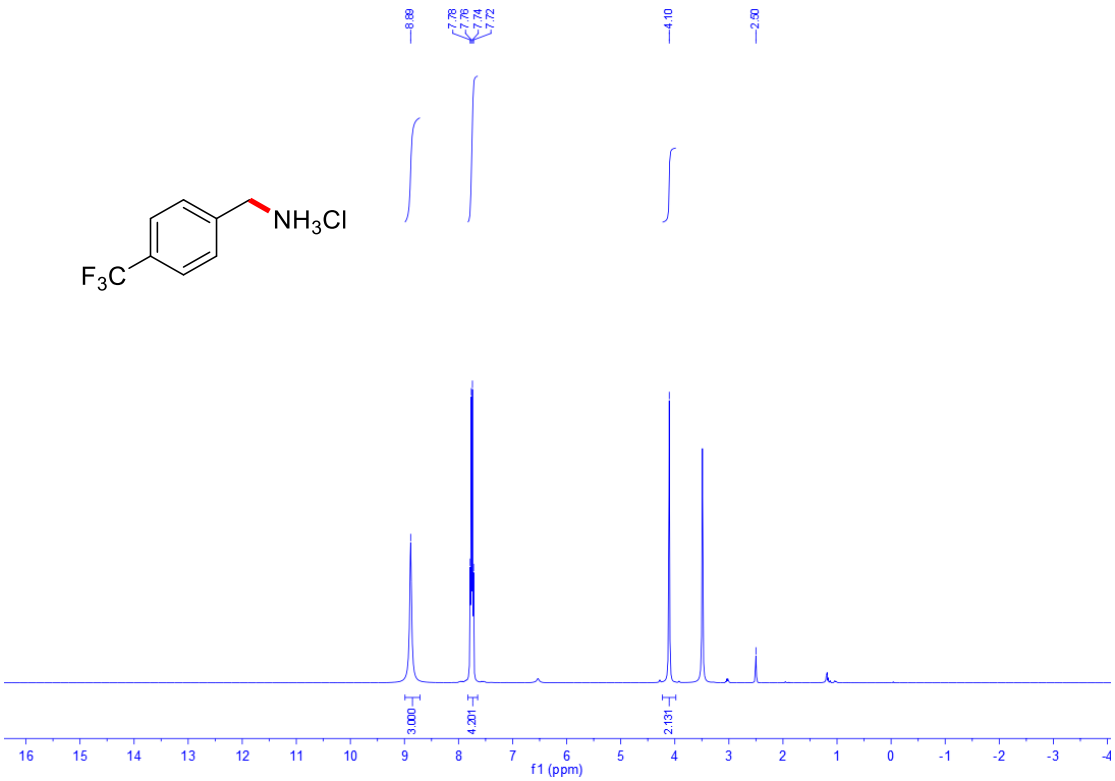

Figure S79. ^{1}H NMR (400 MHz, DMSO-d_6, 20 ^{o}C) of **5r**

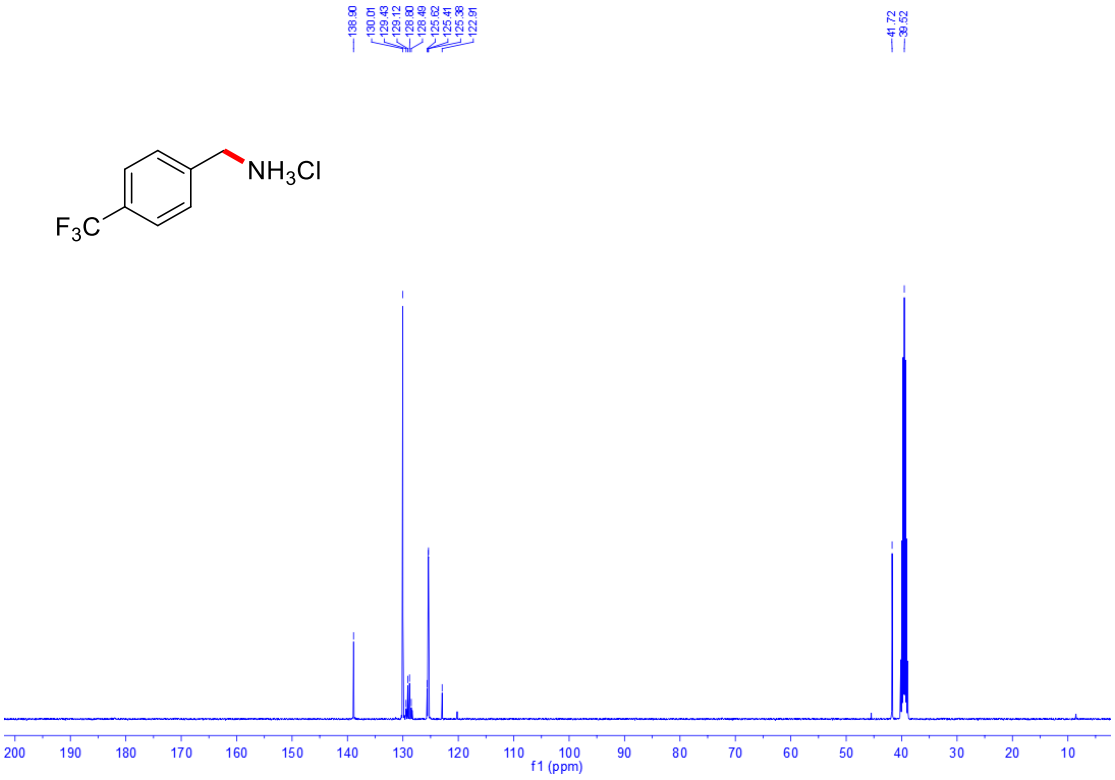

Figure S80. ^{13}C{^{1}H} (101 MHz, DMSO-d_6, 20 ^{o}C) of **5r**

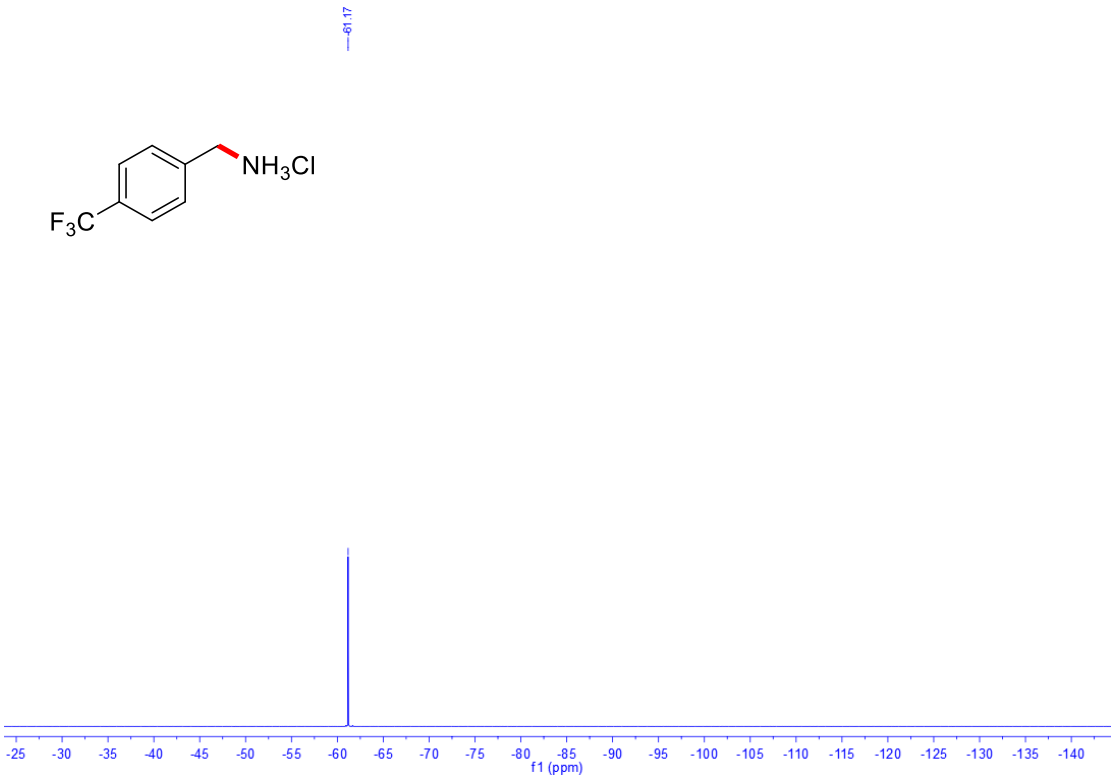

Figure S81. ^{19}F NMR (377 MHz, DMSO-d_6, 20 °C) of **5r**

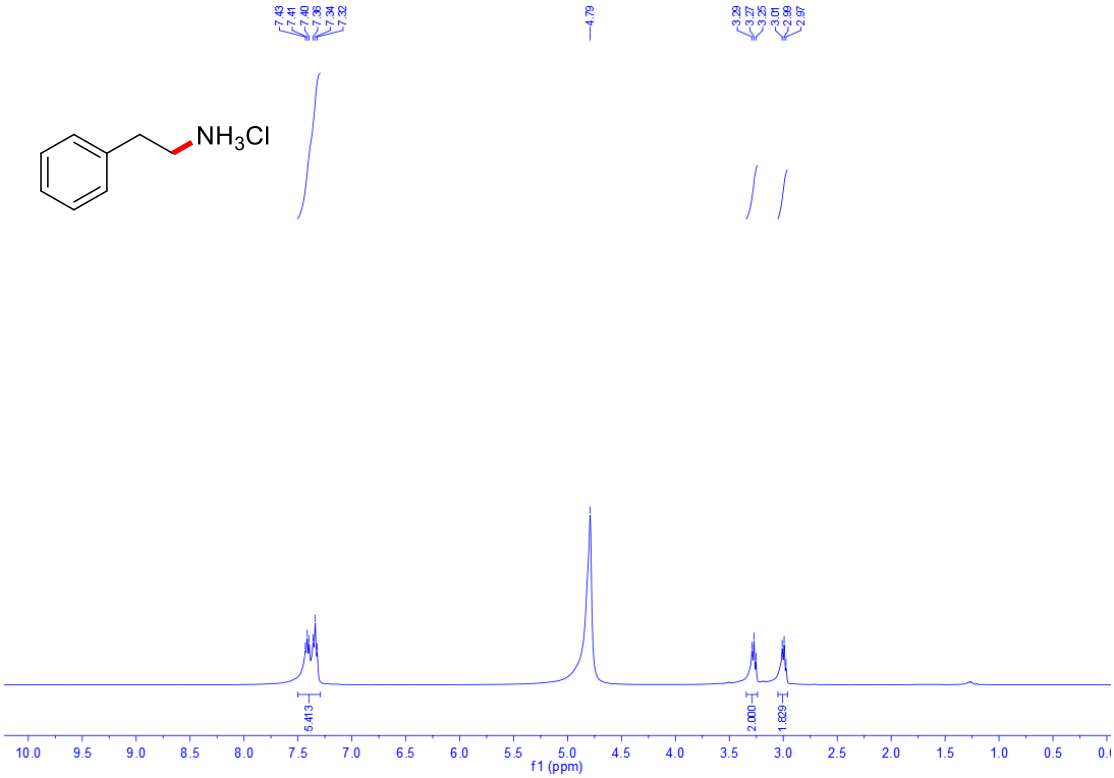

Figure S82. ^{1}H NMR (400 MHz, D_2O, 20 °C) of **5s**

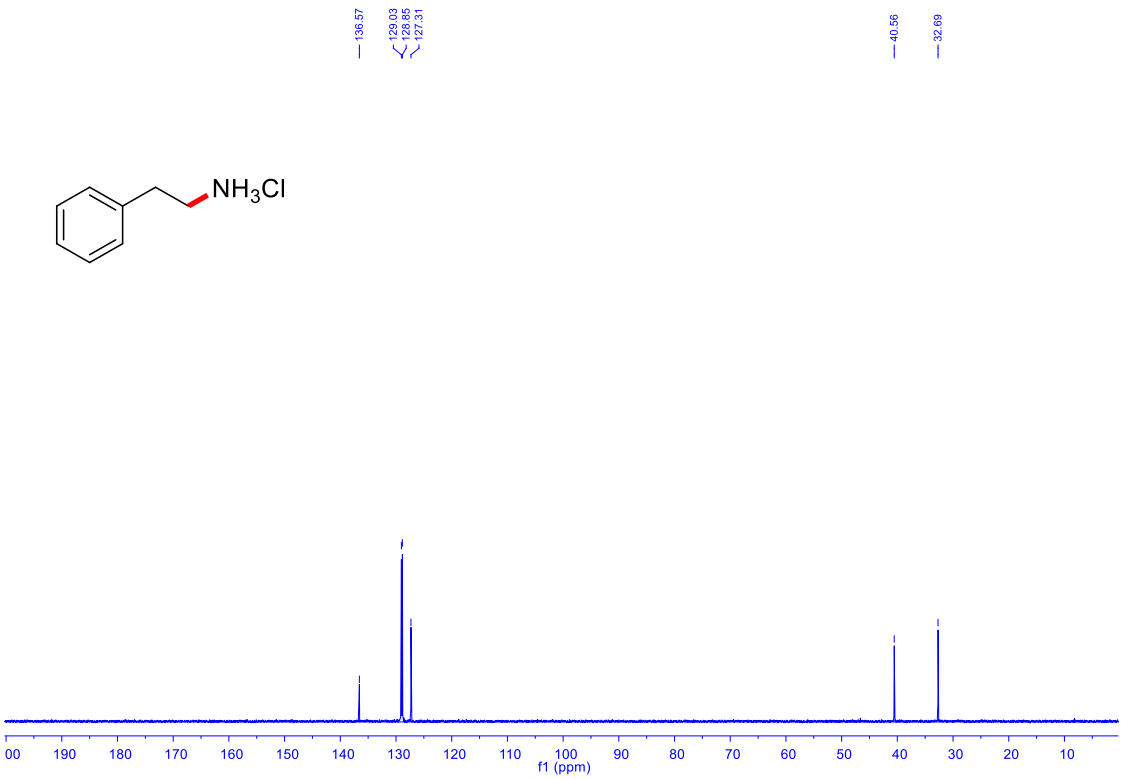

Figure S83. $^{13}C\{^{1}H\}$ (101 MHz, D_2O, 20 ºC) of **5s**

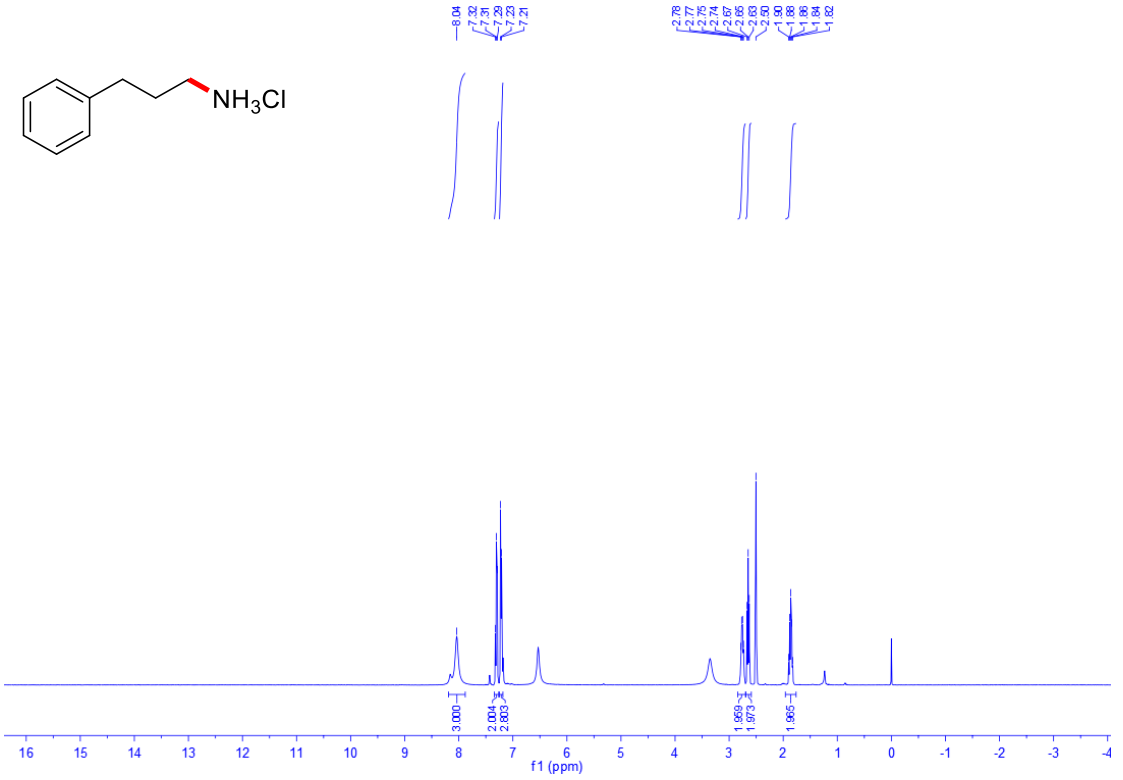

Figure S84. ^{1}H NMR (400 MHz, DMSO-d_6, 20 ºC) of **5t**

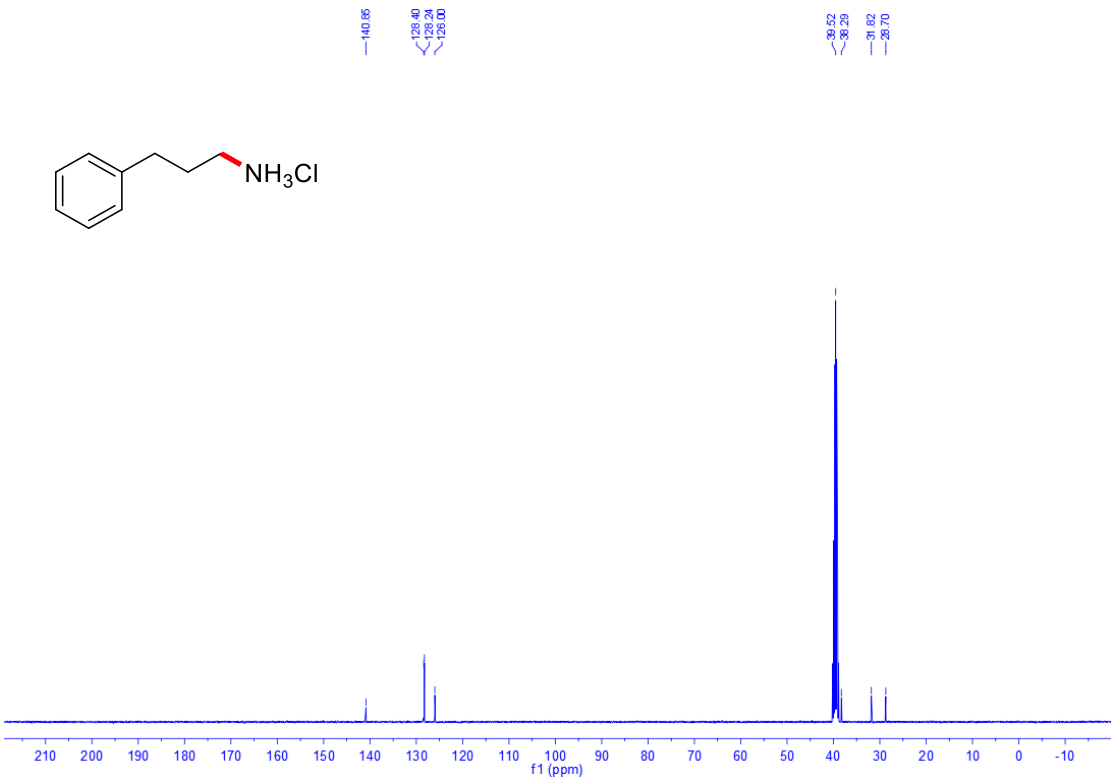

Figure S85. $^{13}C\{^{1}H\}$ (101 MHz, DMSO-d_6, 20 °C) of **5t**